Ca' Foscari
University
of Venice

Master's Degree programme

in Sustainable
Development

Final Thesis

Tracking the Evolution of Air Pollution Disparities in Mexico City: A Spatial and Statistical Analysis

Supervisor
Dr Prof. Carlo Gaetan

Co-supervisor
Prof. Josef Schöggl, Universität Graz

Graduand
María del Pilar Flores Vidriales
Matriculation Number: 890766

Academic Year
2022/ 2023

Abstract

This thesis aims to explore the intersection of environmental factors and social justice in the context of air pollution in Mexico City. Mexico City is a well-known hot spot for air pollution, with its high levels of pollutants being linked to a range of health issues. The problem of air pollution in the city is caused by several factors, such as its unique topography and meteorological conditions, rapid urbanisation, increasing vehicular traffic, and inadequate environmental policies and regulations. To understand the spatial and social distribution of air pollution, statistical and geospatial tools were used. The disparities in the distribution of air pollution based on neighbourhoods socioeconomic status were examined, while also analysing the changing relationship between socioeconomic factors and air pollution distribution over time. Furthermore, the study evaluated the effectiveness of policy and regulatory interventions in reducing air pollution.

Air pollutant concentrations were retrieved from the Atmospheric Monitoring System of Mexico City (SIMAT), while Poverty Rates and the Urban Marginalisation Index (UMI), which considers several indicators such as educational backwardness, access to health services, housing quality, and basic services were sourced from official data repositories.

The results of this study underscore the persistent socio-environmental disparities in Mexico City and emphasize the importance of comprehensive and integrated approaches for the development of air pollution control policies. The study consistently demonstrates positive associations between urban marginalisation, poverty percentages, and the concentrations of O_3, PM_{10}, and $PM_{2.5}$ across the studied years. It reveals that pollution sources in Mexico City, like in other parts of the world, are disproportionately located in low-income neighbourhoods mainly at the north and east of the city, consequently, the concentrations of pollutants tends to be higher in these areas. Moreover, as air pollution increases, housing prices go down, perpetuating the low-income status of these communities. It is worth noting that for O_3 concentrations, the wind patterns of the city cause higher levels in the southern region due to the transportation of precursors generated in the north.

Scientific studies indicate that current air quality policies have not effectively achieved objectives related to emissions prevention, environmental performance monitoring, and control of mobile source emissions in Mexico City. These findings have raised concerns about equity in air pollution management. Although progress has been made in reducing overall air pollutant concentrations, pollutants such as PM_{10}, $PM_{2.5}$, and O_3 still frequently exceed acceptable limits. Importantly, these concentrations are often higher in areas with lower socioeconomic status, where populations tend to be more vulnerable, highlighting the urgent need for further action.

This study provides crucial insights into effective policy and regulatory interventions that can help reduce air pollution and promote equity in both, social and environmental domains in the city.

Table of Contents

1. Introduction

1.1. Background and motivation

Mexico City, with a population of more than 9.2 million people, is one of the world's largest and most populous urban areas and is located within the Metropolitan Area of the Valley of Mexico (MAVM). This area comprises 16 municipalities within Mexico City and 60 municipalities within the States of Mexico and Hidalgo, with a combined population of 21.8 million people as of 2020 (INEGI, 2020c).

According to Molina and Molina (2004), "air pollution problems of megacities differ greatly and are influenced by several factors including topography, demography, meteorology, mobility and transportation patterns, fuel quality and usage, and the level and rate of industrialisation and socioeconomic development."

Most of the conditions that contribute to the build-up of atmospheric pollutants listed by Ahrens (2009) are often present in Mexico City. Its location in a valley surrounded by mountains plays a crucial role in the accumulation of pollutants, particularly in winter, when thermal inversions occur more frequently (Ezcurra, 1991; Olguín Lacunza, 2022). In addition, weather patterns during the dry season can produce circulation features that contribute to poor air quality in the city (Díaz-Esteban et al., 2022). The complex terrain in the Valley of Mexico further exacerbates air pollution by creating local wind patterns that trap pollutants and prevent their dispersion (Jazcilevich et al., 2005).

Moreover, emissions from the neighbouring Popocatepetl volcano contribute to the tropospheric gas and aerosol burden in the region (Pyle & Mather, 2005; Raga et al., 1999). However, while the city's location does play a significant role in its air quality, other factors contribute to its air pollution problems. Industrial activities, transportation emissions, open burning of waste and agricultural fires all contribute to poor air quality in the city (Bravo et al., 2002; CONAFOR, 2023; Hodzic et al., 2012; Legorreta, 1991).

Studies have shown that the spatial distribution of air pollutants in Mexico City is associated with socioeconomic status, with communities with lower income exposed to higher levels of air pollution than those with higher income (García-Burgos et al., 2022; Lome-Hurtado et al., 2020). Industrial activities are mostly concentrated in the northern and eastern parts of the city, where there is a high density of factories and transportation infrastructure. The emissions from these activities contribute to the formation of nitrogen dioxide (NO_2) and carbon monoxide (CO), which are also directly related to vehicle emissions. As a result, the annual averages of NO_2 and CO are highest in monitoring sites located in areas with abundant vehicular traffic, particularly in the centre and north of the city (SEDEMA et al., 2022).

Ozone (O_3), a secondary pollutant, is formed by the reaction of volatile organic compounds (VOCs) and NO_x in the presence of solar light. Its amount and accumulation in the Metropolitan Area of the Valley of Mexico depends on meteorological factors, and the highest concentrations of O_3 are typically observed downstream of emission sources of its precursors. These emission sources are concentrated in the northern and central areas of the Metropolitan Area, meaning that higher concentrations of O_3 are typically found in the south of the city.

In contrast, the highest concentrations of sulphur dioxide (SO_2) have been observed in the north of the city due to the influence of the Tula-Tepeji industrial corridor in the State of Hidalgo and, to a lesser extent, to local industrial emissions. The "Benito Juárez" International Airport, which is

one of the main emitters located within the city, also contribute to air pollution in the region (de Foy et al., 2009; SEDEMA et al., 2022).

Particulate matter (PM_{10} and $PM_{2.5}$) has anthropogenic and natural origins and originates from sources such as vehicular transit, industry, construction, eroded soil, bioaerosols, volcanic emissions, and forest fires. The main sources of PM_{10} in Mexico City include the resuspension of dust in paved streets, mobile sources, and area sources. $PM_{2.5}$, contribute to approximately half of PM_{10}, with mobile sources and area sources accounting for the majority of the total $PM_{2.5}$ (SEDEMA, Báez, et al., 2021). Weather patterns such as thermal inversions contribute to the accumulation of particulate matter (PM) by trapping pollutants close to the ground. In the east of the Metropolitan Area, local emissions from vehicular traffic significantly influence the high concentration of PM_{10}, while $PM_{2.5}$ shows homogeneity in most of the city except in the southwest, where there are lower concentrations (SEDEMA et al., 2022).

Social disparities in income and education have been linked to higher levels of exposure to environmental hazards and health risks from air pollution in low socioeconomic status areas in Mexico City (Islas-Camargo et al., 2022). The challenges of addressing environmental and health issues can be amplified in communities with greater levels of residential segregation and limited access to resources and support. Additionally, limited education can make it harder for individuals to acquire the knowledge and skills necessary to access resources and information that promote good health (Link & Phelan, 1995; Lynch & Kaplan, 2000; O'Neill et al., 2008).

Mexico City has been facing a severe air pollution crisis for decades, which has had a significant impact on the health and well-being of its residents. While the need for immediate action to address the issue has been emphasized before (Garza, 1996; Legorreta, 1991), the city's high population density and continuous exchange of people and vehicles between the boundaries of the MAVM and Mexico City, where the jobs are concentrated, have further contributed to the problem. As lower-income individuals are often displaced to the Metropolitan Area and have to spend a higher percentage of their income on transportation in order to commute to Mexico City for work, this situation has led to broad economic and social inequalities that exacerbate the effects of air pollution on disadvantaged populations (Damián, 2020; Leo et al., 2017).

Table 1.1 highlights that mobile sources are the primary contributor to $PM_{2.5}$, SO_2, CO, and NO_x emissions in the MAVM, accounting for more than 85% of NO_x and almost 95% of CO emissions. Area sources, including residential, commercial, and institutional buildings, are the second-largest contributor, while point sources such as factories and power plants account for a smaller portion of the total emissions. Natural sources contribute a small percentage of PM_{10} and $PM_{2.5}$ emissions.

Table 1.1 Percentual contribution of sources to the total emissions in the Metropolitan Area of the Valley of Mexico, 2018

Source	Percentual contribution to the total emissions in the MAVM, 2018				
	PM_{10}	$PM_{2.5}$	SO_2	CO	NO_x
Point sources[1]	12.02	19.25	33.19	0.77	6.58
Area sources[2]	44.24	35.79	32.29	4.65	7.35
Mobile sources[3]	39.56	43.01	34.52	94.57	85.82
Natural sources[4]	4.16	1.95	N/A	N/A	0.24

Source: (SEDEMA, Báez, et al., 2021)

(1) Point sources which are characterised as stationary or fixed point sources such as power plants, chemical industries, oil refineries and factories.
(2) Mobile sources encompassing all forms of transport and motor vehicles.
(3) Area sources. All those activities that together affect air quality, such as the use of wood, printing, dyeing, or agricultural activities, to name a few.
(4) Natural or biogenic sources. These are the result of animal and plant life phenomena, such as emissions from volcanoes, oceans and soil erosion.

The Metropolitan Area of the Valley of Mexico faces major sustainability challenges related to the transport sector that were summarised by Steurer & Bonilla (2016) among which are an increase in the carpool, constant local air pollution, high CO_2 emissions and a do-nothing policy of urban planning and growth. Some of these factors have led to an increasing occupation of public space that privileges predominantly private vehicular units, clogging up the roadways and increasing congestion (Chatziioannou et al., 2020). And, as it happens with other developing countries, public transportation in Mexico often faces economic limitations to provide good service and it usually gets congested, especially in the MAVM (Bautista-Hernández, 2021).

Given that mobile sources are the primary contributors to air pollution in the MAVM, the government has implemented a variety of environmental policies to address the issue. These policies include the "Hoy No Circula" program, which limits the circulation of vehicles based on their license plate numbers, and the "Programa de Verificación Vehicular Obligatoria" program, which requires all vehicles to undergo regular emissions testing. Additionally, the city has adopted strategies to improve public transportation and consolidate an Integrated Mobility System such as the expansion and rehabilitation of Metro Lines, the introduction of new lines of BRT Metrobus system, the construction of a Commuter Rail Line that connects the State of Mexico with Mexico City and the purchase of new and more efficient buses for the Trolleybus and Urban Bus systems (Gobierno de la Ciudad de México, 2020, 2022). In addition, the government has promoted the use of electric and hybrid vehicles to reduce emissions and established an air quality monitoring network to measure pollutant levels in the atmosphere.

In addition to these transportation-related policies, Mexico City has also implemented measures to boost the use of non-motorized mobility (NMM), such as bike-rental systems and the construction of bike lanes. However, even though the city has started a transition towards developing a more sustainable mobility, only 22% of investments made as a result of public policies in the mobility sector in Mexico are committed to public transport, 9% to cycling infrastructure and 4% to pedestrian one, while an amazing 65% is intended to be used for infrastructure for private cars (Chatziioannou et al., 2020). These percentages are contrasting with Mexico City's high multimodality since in 2020, 50.8% of the population used public transportation as the principal means to get to work, 38.8% used private cars and the rest used bikes or walked (Data México, 2020).

While transportation policies play a crucial role in reducing air pollution in Mexico City, other measures targeting high pollution events and industrial emissions are also in place. When the city

experiences high levels of pollution, environmental contingency plans are activated, which include measures such as restricting the circulation of vehicles but also industrial activities and limiting outdoor activities for vulnerable populations like children and the elderly. The city has also implemented regulations to control emissions from industrial sources, including the establishment of emissions standards for factories and power plants.

Despite these efforts, air pollution remains a significant public health concern in the city. Mexico City continues to struggle with high levels of air pollution and is considered one of the most polluted cities in Latin America (Alves, 2023).

This research seeks to explore the complex relationships between environmental factors and social justice, focusing on the spatial and social distribution of air pollution and the varying levels of exposure based on individuals' socioeconomic circumstances. By utilising statistical and geospatial tools, this study aims to provide a comprehensive understanding of the environmental burdens related to air quality faced by different socioeconomic groups in Mexico City. The findings of this research will provide insights into the pressing need for equitable policies and interventions to alleviate the detrimental effects of air pollution on public health and the environment.

1.2. Research questions and objectives

- How has the relationship between socioeconomic factors and air pollution distribution in Mexico City changed over time?
- To what extent have policy and regulatory interventions aimed at reducing air pollution in Mexico City been effective, and how have they impacted disparities in air pollution distribution over time?

2. Literature Review

2.1. Air pollution and health effects

Air pollution has been identified as a major public health concern globally, the World Health Organisation estimates that outdoor air pollution causes about 4.2 million premature deaths each year, while indoor air pollution causes about 3.8 million deaths annually (WHO, 2022). The most common air pollutants that pose a threat to human health include particulate matter (PM), nitrogen oxides (NO_x), sulphur oxides (SO_x), and ozone (O_3). Exposure to these pollutants has been extensively studied and has been linked to a wide range of health effects, including lung cancer, stroke, asthma, and heart disease (Cohen et al., 2017; De Matteis et al., 2022; Manisalidis et al., 2020). Vulnerable populations, such as children, the elderly, and individuals with pre-existing health conditions, are particularly at risk.

As in other countries, exposure to air pollution in Mexico City has been associated with an increased risk of cardiovascular disease and stroke (Borja-Aburto et al., 1997), and short-term exposure has been estimated to be responsible for at least 10% of Cardiovascular Emergency Department Visits in the city (Ugalde-Resano et al., 2022). In addition, particulate air pollution exposure has been linked to damage to the body's cells and DNA, leading to cell death (Alfaro-Moreno et al., 2002), while exposure during pregnancy has been found to be related to an increased risk of post-partum depression (Niedzwiecki et al., 2020). Furthermore, long-term exposure to O_3, PM_{10} and NO_2 has been linked to a decrease in the growth of lung function among children, which could increase the likelihood of developing chronic obstructive lung disease over time, as well as increased cardiovascular morbidity and general mortality (Rojas-Martinez et al., 2007). Air pollution, measured by PM_{10} concentrations, has been found to be one of the most significant environmental risks for mortality in Mexico (Stevens et al., 2008).

2.2. Environmental justice and environmental inequalities

In recent decades, there has been a growing concern about the unequal distribution of environmental hazards and risks, leading to the emergence of two related but distinct fields of study: environmental justice and environmental inequalities. Environmental justice is concerned with the fair distribution of environmental benefits and burdens, while environmental inequalities focus on the unequal distribution of environmental risks and hazards based on social and demographic factors (Brulle & Pellow, 2006; Bullard, 2000). While these two fields share similar concerns, they approach the issue from different perspectives and use different theoretical frameworks. In this section, I will first explore the concept of environmental justice, then discuss environmental inequalities, and finally, compare and contrast the two fields.

Environmental justice is a movement and a policy approach that seeks to address the disproportionate distribution of environmental burdens and benefits across society, with a focus on marginalized and vulnerable communities (Bullard, 2000; Pastor et al., 2001). It aims to ensure that all people, regardless of race, ethnicity, or socioeconomic status, have equal access to healthy and safe environments (US EPA, 2022).

The environmental justice movement emerged in the United States in the 1980s as a response to the disproportionate exposure of marginalised communities, particularly low-income communities and communities of colour, to environmental hazards and pollution. The movement sought to address the unequal distribution of environmental burdens and promote the equitable distribution of environmental benefits. The landmark report "Toxic Wastes and Race in the United

States" by the United Church of Christ Commission for Racial Justice (1987) was instrumental in bringing attention to the issue of environmental injustice, it was the first one to demonstrate the correlation between race, socioeconomic status, and exposure to toxic waste sites in the United States, providing evidence for the unequal distribution of environmental burdens across communities. It brought national attention to the issue of environmental racism and catalysed the movement. Since then, the environmental justice movement has grown and spread to other countries and has influenced policies and regulations aimed at addressing environmental disparities.

Schlosberg (2007) argued that the environmental justice movement has a distributive justice component, which recognizes that low-income neighbourhoods and communities of colour are often subjected to a disproportionate burden of environmental hazards. Distributive justice refers to the fair distribution of benefits and burdens within a society, and in the context of environmental justice, it seeks to ensure that the benefits of effective environmental policies are shared equally across different demographics and locations, while also ensuring that certain groups do not bear the majority of environmental risks and costs. This idea of distributive justice is influenced by the work of Rawls (1999), who proposed the concept of the "veil of ignorance" as a way to ensure fairness in the distribution of resources and opportunities in society. The veil of ignorance is a hypothetical scenario where individuals must make decisions about societal institutions and policies without knowing their position in society, ensuring impartiality and fairness. In the context of environmental justice, the veil of ignorance emphasizes the importance of ensuring that all individuals have equal access to healthy and safe environments, regardless of their race, ethnicity, or socioeconomic status.

This view is reinforced by the work of Bullard (2000) who argued that the spatial distribution of environmental hazards is closely linked to issues of race and socioeconomic conditions. In his research, Bullard found that toxic waste sites, hazardous waste facilities, and other environmental hazards were often located close to low-income neighbourhoods and communities of colour.

The concept of environmental justice has evolved to include not only distributive issues but also social, economic, and political factors that shape environmental outcomes. This broader perspective is reflected in the emerging discourse of "just sustainability" in environmental justice scholarship (Agyeman & Evans, 2004). This discourse highlights the need to address underlying social and economic inequalities that create environmental disparities in the first place and to ensure that marginalised communities have a voice in decisions affecting their environments.

In recent years, the concept of environmental justice has continued to evolve, with a growing focus on the importance of environmental justice in the global South. Overall, the evolution of environmental justice scholarship reflects a growing recognition of the complex and intersectional nature of environmental issues and the need for more inclusive and equitable approaches to environmental decision-making.

Environmental inequalities, on the other hand, refer to disparities in exposure to environmental hazards and pollutants across different socio-demographic groups (Brulle & Pellow, 2006). This can include differences in exposure based on factors such as income, race/ethnicity, and education. Numerous studies have documented the existence of environmental inequities in various contexts, including air pollution, toxic waste sites, and access to clean water and green spaces.

For example, research in the United States has consistently demonstrated that low-income communities and neighbourhoods with a high proportion of ethnic minorities tend to be exposed to higher levels of various environmental pollutants (Clark et al., 2014; Jerrett et al., 2005). Similar findings have been reported in other countries around the world, such as Brazil, where low-income people who belong to non-white racial groups are often the most vulnerable to environmental hazards such as flooding or landslides (Carvalho et al., 2022) or India, where air pollution from coal-fired power plants disproportionately affects poor and low-caste communities compared to their wealthier and high-caste counterparts (Kopas et al., 2020).

In summary, environmental justice focuses on achieving fairness in the distribution of environmental benefits and burdens, while environmental inequalities highlight the unequal exposure to environmental risks and hazards experienced by different social and demographic groups.

2.3. Socioeconomic status and air pollution exposure

The evolution of environmental justice scholarship has brought attention to the intersections of socioeconomic conditions and environmental issues. Specifically, research has shown that low-income communities tend to be exposed to higher levels of environmental pollutants (Hajat et al., 2015; Rentschler & Leonova, 2022). Numerous studies have demonstrated that socioeconomic status is a significant predictor of air pollution exposure. In this section, I will explore the literature on the relationship between socioeconomic status and air pollution exposure in more detail.

In the United States, research on environmental justice and air pollution consistently demonstrates that low-income communities and neighbourhoods with a high proportion of ethnic minorities tend to be exposed to higher levels of various environmental pollutants. For instance, Clark et al. (2014) discovered that outdoor NO_2 air pollution is more concentrated in neighbourhoods with higher percentages of low-income and minority residents, while Jerret et al. (2005) found that residents of low-income communities, particularly those of colour, were more likely to experience higher levels of air pollution and a greater risk of premature death due to long-term exposure to fine particulate matter ($PM_{2.5}$).

In the United Kingdom, McLeod et al. (2000), found that people residing in deprived areas in England and Wales experience higher levels of air pollution (NO_2, SO_2 and PM_{10}) compared to those in affluent areas, while Fairburn et al. (2005) results revealed that areas of high social deprivation in Scotland tend to have higher levels of NO_2, PM_{10} CO and Benzene.

The associations between air pollution and socioeconomic characteristics, ethnicity, and age profile of neighbourhoods were investigated in England and the Netherlands by Fecht et al. (2015). The study found that in both countries, the highest air pollution levels were observed in neighbourhoods with lower socioeconomic status and higher levels of ethnic diversity.

Samoli et al. (2019) identified that people with lower socioeconomic status in metropolitan areas of Europe are generally more exposed to higher levels of NO_2 air pollution. Additionally, their study revealed that different socioeconomic indicators, such as population density, the population born outside the European Union and unemployment, may play different roles in determining air pollution exposure across the cities. Similarly, Moreno-Jiménez et al. (2016) found that areas with higher levels of poverty and unemployment in Barcelona and Madrid in Spain tended to have higher levels of NO_2 air pollution. They also found that immigrant populations were more likely to be more exposed to air pollution.

Venter et al. (2023) found that socioeconomically disadvantaged sub-districts in the city of Oslo in Norway are more exposed to environmental hazards such as higher NO_2 concentrations, even beyond the WHO recommendations.

While many studies have found that people with lower socioeconomic status are generally more exposed to higher levels of NO_2 air pollution in metropolitan areas of Europe, there are some contrasting findings. For instance, Branis and Linhartova (2012) documented that low educational attainment and high unemployment rate in the Czech Republic are inversely associated with increasing SO_2 and PM_{10} but not with NO_2 concentration, residents of larger cities in the Czech Republic with higher socioeconomic status are potentially exposed to higher levels of NO_2 air pollution.

In India, Kopas et al. (2020) results revealed that low-caste and marginalised communities are disproportionately exposed to air pollution from coal-fired power plants, with higher concentrations of air pollutants observed in areas with higher percentages of low-caste residents.

The studies by Pearce and Kingham (2008) in New Zealand and Knibbs and Barnett (2015) in Australia both reveal a strong link between lower socioeconomic status and higher exposure to air pollution. In New Zealand, individuals living in areas with lower socioeconomic status experienced higher levels of air pollution, while in Australia, those living in socioeconomically disadvantaged areas and near major roads were exposed to higher levels of NO_2 air pollution.

The findings of these articles indicate that air pollution has evolved into an environmental inequality concern, with a disproportionate impact on the most vulnerable groups in society.

2.3.1. Latin America and Mexico

As the previous section highlights, studies around the world have shown that air pollution exposure is often unequally distributed along lines of socioeconomic conditions. However, the effects of environmental inequalities are not limited to these regions, and scholars have increasingly turned their attention to the experiences of communities in other parts of the world, such as Latin America (Fernández et al., 2023). Despite this, there is still a lack of research on the intersection of air pollution and environmental inequalities in the region. This section will review some of the key findings and trends in this area.

The Multicity Study of Air Pollution and Mortality in Latin America, also known as the ESCALA study (Romieu et al., 2012), was a large-scale epidemiological study conducted in eight Latin American cities to investigate the relationship between air pollution and mortality. The study analysed data from 12 years of mortality records and air pollution monitoring in Monterrey, Toluca, and Mexico City in Mexico; Rio de Janeiro, São Paulo, and Porto Alegre in Brazil; and Santiago, Concepción, and Temuco in Chile. The study found a significant association between air pollution and increased mortality risk, particularly concerning cardiovascular and respiratory diseases. The results of the study also indicated that people with the lowest socioeconomic status were at greater risk of mortality, particularly related to respiratory causes.

O'Neil et al. (2008) found a consistent association between exposure to air pollution and increased mortality in Mexico City, Mexico; Santiago, Chile; and São Paulo, Brazil, with PM_{10} linked to increases in mortality, with a stronger association observed for cardiovascular diseases compared to respiratory diseases. However, this study did not observe gradients of increasing associations between particles and mortality with decreasing levels of education. The authors suggest that this could be attributed to the higher and more widespread air pollution levels in Latin

America, which lead to a more universal exposure and less variation in exposure based on socio-economic factors.

Romero-Lankao et al. (2013) found that at high concentrations of criteria pollutants in Mexico City, Mexico; Bogotá, Colombia; and Santiago, Chile, populations in the municipalities that are both the least and the most socioeconomically vulnerable face comparable risks when exposed to air pollution and temperature extremes. This finding contrasts with the predictions made by environmental inequalities literature, which typically expects disadvantaged communities to be more severely impacted by pollution. However, their study focused on vulnerability factors rather than the spatial distribution of exposure to explain the health risks related to air pollution.

Spatial distribution of exposure refers to the geographic location of a community concerning pollution sources and the concentration of pollutants in the area. Disadvantaged communities, such as low-income neighbourhoods are often located near industrial zones and transportation infrastructure, which exposes them to higher levels of air pollution (US EPA, 2021).

On the other hand, vulnerability factors refer to the physical or social characteristics of a community that make them more susceptible to the adverse health effects of air pollution. For example, individuals with pre-existing health conditions, such as asthma or heart disease, may be more vulnerable to the effects of air pollution. Similarly, individuals with limited access to healthcare, social networks, and education may be less equipped to mitigate the health risks associated with air pollution exposure.

Romero Lankao et al.'s study focused on vulnerability factors rather than the spatial distribution of exposure to explain the health risks related to air pollution. Their findings suggest that vulnerability factors may play a larger role in determining the health risks of air pollution exposure than spatial distribution of exposure. This may explain why their results contradict the environmental justice literature, which typically focuses on the spatial distribution of exposure.

The issue of air pollution and environmental justice is particularly relevant in the case of Mexico City, which has long been affected by severe air pollution problems. The intersection of environmental inequalities and air pollution in Mexico City provides a compelling case study for examining the complex social, economic, and political factors that contribute to environmental inequalities and the challenges of implementing effective environmental policies in a rapidly urbanising region of the world.

A large body of published studies links air pollution exposure in the Mexico City Metropolitan Area to various adverse health outcomes. For instance, Carbajal-Arroyo et al. (2011) found that in the Mexico City Metropolitan Area, exposure to both PM_{10} and O_3 was associated with an increased risk of infant mortality, with a stronger association for O_3. Infants from lower to medium socioeconomic status were at a higher risk of mortality due to air pollution.

García-Burgos et al. (2022) studied the spatial association between air pollutants (NO_2, CO, O_3, PM_{10} and $PM_{2.5}$) and socioeconomic status in Mexico City from 2017 to 2019. The study used a spatial autocorrelation approach to evaluate the association between air pollutants and socioeconomic indicators. The study findings revealed that the population with lower socioeconomic status residing in the southern periphery of the city had greater exposure to O_3, whereas the highest exposure to NO_2 and CO_2 was observed in the wealthy city centre. The pollutants PM_{10} and $PM_{2.5}$ were weakly associated with the socioeconomic indicators the study evaluated

Lome-Hurtado et al. (2020) aimed to identify environmental justice concerns in Mexico City by analysing the spatial distribution of air pollution and socio-economic indicators. The study used a spatial quantile regression approach to estimate the relationship between exposure to air pollutants and socio-economic vulnerability at different levels of air pollution. The results showed that the populations in the most socio-economically vulnerable neighbourhoods are exposed to higher levels of PM_{10}, and these neighbourhoods are not randomly distributed throughout the city but are concentrated in certain areas. The study also found a negative association between lower socioeconomic conditions and O_3.

3. Data

3.1. Air Quality Data

The Atmospheric Monitoring System (SIMAT) is responsible for the continuous measurement of the main air pollutants in Mexico City. This system consists of 44 monitoring stations located throughout the metropolitan area, covering areas in both Mexico City and the conurbation zone of the State of Mexico. These monitoring stations use continuous equipment to measure the required criteria pollutants mandated by federal regulations, including sulphur dioxide (SO_2), carbon monoxide (CO), nitrogen dioxide (NO_2), ozone (O_3), and suspended particles (PM_{10} and $PM_{2.5}$). Some stations also measure the main surface meteorological variables, including solar ultraviolet radiation, while in others manual samples of suspended particles and atmospheric deposition information are collected. The information collected by SIMAT is used to generate air quality indexes and alerts for the population, as well as to inform decision-makers and guide policy aimed at reducing air pollution in the region. The location of the monitoring stations is presented in Figure 3.1.

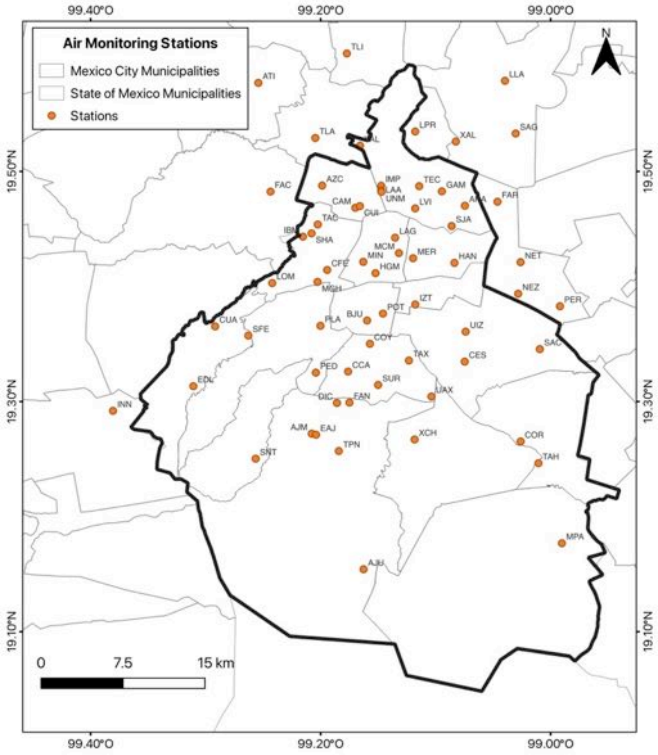

Figure 3.1 Location of air quality monitoring stations
Source: Self-made with data from SEDEMA (n.d.)

The list of the air quality monitoring stations that have made a part of the Atmospheric Monitoring System of Mexico City is shown in Annex I. Air Quality Monitoring Stations. Out of the total 44 stations, 28 are located in Mexico City while the remaining 16 are situated in the State of Mexico.

3.1.1. Datasets

Air quality data were retrieved in .csv files for the years 2000, 2005, 2010, 2015 and 2020. Table 3.1 presents a sample of the air quality datasets.

Table 3.1 Sample table from the air quality datasets

date	id_station	id_parameter	value	unit
01/01/19 1:00	CAM	PM10	122	15
01/01/19 1:00	CAM	PM2.5	90	1
01/01/19 1:00	CAM	PMCO	32	1

Source: (SEDEMA, 2023)

3.1.2. *Pre-processing*

The hourly registers of the following variables were considered for the analysis:

- Date: continuous numerical variable [format: datetime]
- Station: categorical variable.
- Ozone (O_3): continuous numerical variable [unit: ppb]
- Carbon Monoxide (CO): continuous numerical variable [unit: ppm]
- Sulphur Dioxide (SO_2): continuous numerical variable [unit: ppb]
- Nitrogen Oxides (NO_x): continuous numerical variable [unit: ppb]
- Particulate Matter (PM_{10}): continuous numerical variable [unit:µg/m³]
- Particulate Matter ($PM_{2.5}$): continuous numerical variable [unit:µg/m³]

The location of all the monitoring stations was retrieved from the official air quality website of Mexico City and the coordinates and altitude were added as additional columns:

- Latitude: continuous numerical variable [unit: degrees north]
- Longitude: continuous numerical variable [unit: degrees west]
- Altitude: continuous numerical variable [unit: m]

Pre-processing of the data was conducted with R Studio Version 2023.03.0+386 for Mac OS and QGIS 3.30.1-'s-Hertogenbosch software for Mac OS was used to perform the spatial analyses, both are widely used open-source software packages.

3.2. Socioeconomic Indicators

The socioeconomic indicators for this study are mainly measured at the AGEB level, which is a territorial subdivision of municipal geostatistical areas in Mexico. AGEBs are considered the fundamental unit of the National Geostatistical Framework and are classified into rural or urban areas depending on their characteristics. The use of AGEBs as the unit of analysis allows for more precise spatial analysis and comparison of socioeconomic indicators. AGEBs of Mexico City are shown in Figure 3.2. It is to be noted that the AGEBs have changed slightly over the years because the Geostatistical Framework has gone through updates. For this study, only the Urban AGEBs were considered, since there is no data available for the rural ones.

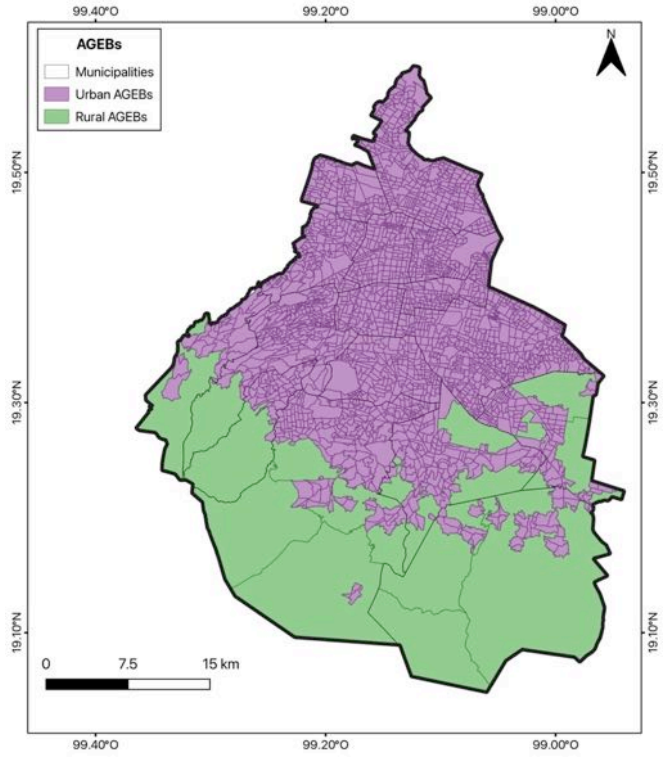

Figure 3.2 2020 AGEBs
Source: Self-made with data from INEGI (2020a, 2020b)

3.2.1. Datasets and/or layers

3.2.1.1. Index of Urban Marginalisation

The Urban Marginalisation Index (UMI) is a measure that summarises indicators of social deficiencies and household assets in urban AGEBs in Mexico. It uses four dimensions: educational backwardness, access to health services, quality and spaces of housing, and basic services in housing. Additionally, it incorporates indicators related to household assets. The UMI aims to identify the intensity of these dimensions in the urban AGEBs of the country and assign them a degree of social marginalisation: very low, low, medium, high, or very high. It is worth noting that the UMI is not a poverty measurement tool, as it does not take into account indicators such as income, social security, and food. Rather, it serves as a means of comprehending and analysing the uneven distribution of development and its advantages within urban areas, cities, and metropolitan zones. By using this index, areas that might be left out or at a disadvantage during the process of urban development can be identified (CONAPO, 2021a).

Pre-processing

2000 Urban Marginalisation Index

To generate an Urban Marginalisation Index layer for the year 2000, the available data had to be processed as an official layer has not been issued to date The starting point was the SHP layer of the 2000 National Geostatistical Framework, obtained from INEGI (2000). This layer contained multiple individual layers of AGEBs, which were combined into a single layer covering Mexico City.

Then, the dataset of the Urban Marginalisation Index per AGEB from 2000 to 2010 was retrieved from the official Open Data portal of Mexico (CONAPO, 2023) and was separated per year. Table 3.2 provides an overview of the relevant columns for the study.

Table 3.2 Overview of the dataset of the Urban Marginalisation Index from 2000 to 2010

NOM_ENT	CVE_AGEB	GMU	AÑO
Distrito Federal	900200010010	Bajo	2000
Distrito Federal	900200010010	Muy bajo	2005
Distrito Federal	900200010010	Muy bajo	2010

Source: (CONAPO, 2023)

To create the layer of Urban Marginalisation Index per AGEB, a union was performed in QGIS by importing the CSV file of the UMI for the year 2000 and joining it with the 2000 Geostatistical Framework layer using a join operation, at the end of the processing, it was found that the Urban Marginalisation Index dataset did not include 61 AGEBs that were included in the Geostatistical Framework layer. These AGEBs were removed from the analysis.

2005 Urban Marginalisation Index

To generate an Urban Marginalisation Index layer for the year 2005, the available data had to be processed as an official layer has not been issued to date The starting point was the SHP layer of the 2004 National Geostatistical Framework, obtained from INEGI (2004). Then, the dataset of the Urban Marginalisation Index per AGEB from 2000 to 2010 was used and the same procedure of 2000 was followed. At the end of the processing, it was found that the Urban Marginalisation Index dataset did not include 62 AGEBs that were included in the Geostatistical Framework layer. These AGEBs were removed from the analysis.

2010 Urban Marginalisation Index

To generate an Urban Marginalisation Index layer for the year 2010, the available data had to be processed as an official layer has not been issued to date The starting point was the SHP layer of the 2010 National Geostatistical Framework, obtained from INEGI (2010). Then, the dataset of the Urban Marginalisation Index per AGEB from 2000 to 2010 was used and the same procedure of 2000 was followed. At the end of the processing, it was found that the Urban Marginalisation Index dataset did not include 66 AGEBs that were included in the Geostatistical Framework layer. These AGEBs were removed from the analysis.

Normalisation of the Urban Marginalisation Indexes

To facilitate the comparison of the Urban Marginalisation Index values across different years and spatial units, the Min-Max scaling method was used to normalise the index to a 0-1 range. This method rescales the values of a variable to a range between 0 and 1 by subtracting the minimum value from each observation and then dividing the result by the range of the variable (i.e., the difference between the maximum and minimum values).

However, since the minimum and maximum values of the Urban Marginalisation Index vary across different years (2000, 2005, 2010, and 2020), the rescaling procedure was performed separately for each year. By using this method, the Urban Marginalisation Index values were transformed into a common range of 0-1, which allowed for the comparison of the relative levels of marginalisation across different years and spatial units. Normalised values were used for Local Bivariate Moran's I Index.

Annex II. Urban Marginalisation Index, shows the maps of the Index of Social Marginalisation for Mexico City over the years 2000, 2005, 2010 and 2020.

3.2.1.2. Urban Poverty

The urban poverty layers provide information on the percentage of poverty by AGEB. They allow for the identification of urban areas where a majority of the population lives under conditions of poverty.

Pre-processing

2015 Poverty Percentages

The layer was retrieved from the National Council for the Evaluation of Social Development Policy (CONEVAL, 2018). It classifies AGEBs into five categories based on poverty percentages. Table 3.3 presents a sample of the attribute table for the urban poverty layer.

Table 3.3 Sample attribute table for Urban Poverty

CVEGEO	POBREZA	POBREZAEX	ID
0900200010010	(18,34]	[0,20]	1
0900200010025	[0,18]	[0,20]	2
090020001003A	[0,18]	[0,20]	3

Source: CONEVAL (2018)

To facilitate the comparison of the 2015 poverty indicator with the air pollutants concentrations, an index was created for each poverty category. The index ranged from 1, representing the lowest range of poverty percentages, to 5, representing the highest range of poverty percentages. This allowed for the poverty indicator to be incorporated as a numerical variable in the statistical analysis alongside the air pollutant concentrations.

2020 Poverty Percentages

To generate a Poverty Percentages layer for the year 2020, the available data had to be processed as an official layer has not been issued to date. The poverty information for 2020 was obtained from the dataset of the Social Development Index (EVALUA, 2020). The percentages of people living in poverty were calculated by dividing the number of people living in poverty by the population of each AGEB. Finally, a union was performed in QGIS by importing the CSV file of the Social Development Index for the year 2020 and joining it with the 2020 Geostatistical Framework to create the layer of poverty percentages per AGEB.

Annex III. Poverty Percentage shows the maps of poverty percentages for Mexico City for the years 2015 and 2020.

4. Methodology

4.1. IDW interpolation of air pollutants

Inverse Distance Weighting Interpolation was used to estimate the concentration of air pollutants across Mexico City for each of the studied years. IDW predicts the value of a target location based on the values of surrounding known locations, weighted by their distance to the target location. The closer the known locations, the more weight they are given in the interpolation process. IDW assumes that the variable being interpolated varies smoothly in space and that nearby points are more similar than distant points. In air pollution modelling, IDW is a popular alternative to the Kriging methodology on various scales (Deligiorgi & Philippopoulos, 2011; Goutham Priya & Jayalakshmi, 2018).

Deterministic methods like IDW use a fixed mathematical relationship to estimate the values at unobserved locations based on the distances to the observed data points. These methods assume that the influence of the observed data decreases as the distance between the data point and the unobserved location increases. IDW uses a power function to weight the contribution of the data points, with the exponent determined by a user-specified distance coefficient. It is to be noted that while deterministic methods are simple and computationally efficient, they do not incorporate any uncertainty in the predictions and may not account for complex spatial relationships between the variables.

The IDW equation (Equation 1). is as follows. The estimation of the value $\boldsymbol{Z_i}$ at location $\mathbf{x}$ is a weighted mean of nearby observations:

$$\hat{z}(x) = \frac{\Sigma_i^n w_i z_i}{\Sigma_i^n w_i} \text{ , where } w_i = |x - x_i|^{-\beta}$$

And where $\beta \geq 0$ and $|\cdot|$ corresponds to the Euclidean distance.

Equation 1: IDW Interpolation

The parameter β in the IDW method indicates how much preference is given to nearby points compared to distant points. β can take values of 1 or 2, corresponding to an inverse or inverse squared relationship, respectively. In this study, it was set to 2, based on previous studies (Kamboj et al., 2022; Shukla et al., 2020). The number of surrounding points, n, determines whether a global or local weighting is applied. If the point x coincides with an observation location $(x=xi)$, the observed value, x, is returned to avoid infinite weights (Hartmann et al., 2018).

To ensure that the results of the interpolation were as accurate as possible, only the stations that had 75% of hourly data or above were considered for the analysis. Yearly averages were calculated for these stations. The list of stations is included in Annex IV. Air Quality Stations Used for the Interpolations.

4.2. Zonal statistics

Once the layers of the interpolated pollutants were ready, the zonal statistics function in QGIS was used to calculate the average of each pollutant at each AGEB. Zonal statistics is a spatial analysis technique that summarises the values of a raster layer (in this case, the interpolated pollutant layers) within the boundaries of a vector layer (Urban Marginalisation Index by AGEBs).

In other words, it calculates the average value of each pollutant for each AGEB. The outcome of this process was layers of AGEBs with the Urban Marginalisation Index and the averages of pollutants.

4.3. Weighted Cohen's Kappa (Interrater reliability)

Weighted Cohen's Kappa is a statistical measure used to assess the agreement between two raters or measurements for categorical variables with an inherent order. It takes into account the ordinal nature of the categories and assigns weights to reflect the level of disagreement between different pairs of categories. In this study, Weighted Cohen's Kappa was applied to the Urban Marginalisation Index (UMI) data. The weighted Cohen's Kappa can be calculated with the following equation (Equation 2):

$$K_W = 1 - \frac{\Sigma w_{ij} \times f_{oij}}{\Sigma w_{ij} \times f_{eij}}$$

Equation 2: Weighted Cohen's Kappa

Where W are the weighting factors, f_o are the observed frequencies, and f_e are the expected frequencies.

To calculate Weighted Cohen's Kappa, the `vcd` package in R was utilised. The dataset was prepared by excluding AGEBs that did not have values for all four studied years, resulting in a total of 2,051 AGEBs.

To perform this analysis, the data was first subsetted for each pair of consecutive years by selecting the corresponding columns. This resulted in a subsetted dataset representing the UMI values for those specific years.

The subsetted data was then transformed into a contingency table, a statistical tool frequently employed to display categorical data in the form of frequency counts arranged in a table format. In this case, the contingency table represented the observed agreement between the two years, capturing the frequency of each category combination.

It is noteworthy that the contingency table was created in the order from "Very High" to "Very Low." This ordering aligns with the expected logical progression of marginality in Mexico City, where areas with higher marginality are categorized as "Very High" and areas with lower marginality are categorized as "Very Low."

The Weighted Cohen's Kappa was then calculated using the contingency table for each pair of years. The resulting kappa value provides an indication of the agreement level between the consecutive years in terms of UMI. Table 4.1 was used to interpret the Kappa values.

Table 4.1 Agreement measures for categorical data

Kappa statistic	Strength of agreement
< 0.0	Poor
0.0 – 0.20	Slight
0.21 – 0.40	Fair
0.41 – 0.60	Moderate
0.61 – 0.80	Substantial
0.81 – 1.00	Almost Perfect

Source: Landis & Koch (1977)

4.4. Bivariate Moran's I Index

Moran's I is a common measure used to assess spatial autocorrelation, which refers to the similarity in spatial patterns between neighbouring locations. The Moran's I test statistic ranges between -1 and 1, with values closer to 1 indicating strong positive spatial autocorrelation (i.e., similar values tend to cluster together), values closer to -1 indicating strong negative spatial autocorrelation (i.e., dissimilar values tend to cluster together), and values close to 0 indicating no spatial autocorrelation.

On the other hand, bivariate Local Moran's I is a statistical measure used to assess the spatial autocorrelation between two variables in a geographic area. It measures the degree of spatial association between two variables, indicating whether high or low values of one variable are clustered near high or low values of the other variable, or whether there is no spatial association between the two variables. Bivariate Local Moran's I was employed with the open-source software GeoDa 1.20.0.36 for Mac OS to investigate the spatial association between two variables at the local level.

Specifically, it measures the correlation between the values of the two variables at different locations and their spatial arrangement, taking into account the values of the neighbouring locations. If high values of one variable tend to be close to high values of the other variable, the Bivariate Moran's I will have a positive value, indicating positive spatial association. If the high values of one variable tend to be close to the low values of the other variable, or vice versa, the Bivariate Moran's I will have a negative value, indicating negative spatial association.

As a first step, a spatial weights matrix was constructed using queen contiguity weights with an order of contiguity 1. This approach takes into account the geographic proximity between neighbouring locations, including those that are adjacent and diagonal to each other. Queen contiguity is often appropriate for analysing spatial data where the features have irregular shapes.

Isolated observations without neighbours were removed for all years. This step was taken to ensure that the spatial relationships and associations examined in the subsequent analyses are based on meaningful spatial connections. The removed observations ranged from 1 to 3.

Once the spatial weights matrix is constructed, the spatial lags for each variable are calculated. The spatial lag for a variable is defined as the weighted average of that variable's values for all of its neighbouring units, using the spatial weights matrix. This produces two new variables, one for each of the original variables, that reflect the spatial context of each unit's value.

Then, the variables used in the analysis are standardised, meaning that they are transformed so that their means are zero and their variances are one. This ensures that all variables are on the same scale and have equal weight in the analysis. Additionally, the spatial weights used in the analysis are row-standardized to ensure that the weights sum one for each observation.

Next, the program calculates the cross-product of the two standardised variables for each pair of neighbouring units, using the spatial weights matrix. This results in a new matrix of cross-products that captures the spatial covariation between the two variables.

Then, the bivariate Moran's I statistic is calculated, which is defined as the ratio of the sum of the cross-product terms to the sum of the product of the spatial lags for each variable. In the Bivariate Moran Scatter Plot, one variable is represented on the x-axis and the spatial lag of another variable on the y-axis. Specifically, the plot measures the degree to which the value of one variable at a location is correlated with its neighbours for a different variable. The focus of interest

is on the slope of the linear fit of the points on the plot, which yields a bivariate Moran's I-like statistic (IB). The slope of the regression line is calculated using the formula (Equation 3):

$$I_B = \frac{\Sigma_i(\Sigma_j w_{ij} y_j \times x_i)}{\Sigma_i x_i^2}, \text{ or the slope of a regression of } W_y \text{ on } x.$$

Equation 3: Bivariate Moran's I Statistic

Along with the scatterplot, a LISA Cluster Map is generated to display the spatial pattern of the bivariate relationship. LISA Cluster Map refers to a graphical representation of Local Indicators of Spatial Association (LISA), which is a local spatial statistic calculated for each location within a given study area. LISA measures are used to analyse spatial patterns and identify clusters or spatial autocorrelation at the local level. The plot distinguishes between four types of local spatial association: high-high, low-low, high-low, and low-high.

Spatial Clusters

- A high-high relationship occurs when neighbouring observations have high values for both variables, indicating a cluster of high values for both variables in a particular area, which suggests a positive association between the two variables.
- A low-low relationship occurs when neighbouring observations have low values for both variables, indicating a cluster of low values for both variables in a particular area, which suggests a negative association between the two variables.

Spatial Outliers

- A high-low relationship occurs when neighbouring observations have high values for one variable and low values for the other variable.
- Finally, a low-high relationship occurs when neighbouring observations have low values for one variable and high values for the other variable.

4.5. Spatial Lag Model – Maximum Likelihood Estimation

Spatial data, such as air pollutant concentrations and socioeconomic factors, often exhibit spatial autocorrelation, wherein nearby areas tend to have more similar values than those that are farther apart. Therefore, it is important to use statistical methods that account for this autocorrelation, rather than assuming independence between observations (Gouveia et al., 2022).

In this study, the relationship between the socioeconomic factors and various pollutants (O_3, CO, NO_x, SO_2, PM_{10} and $PM_{2.5}$) was analysed considering their spatial distribution. To account for spatial autocorrelation, the spatial regression decision tree proposed by Anselin (2005) was employed. The preliminary analysis to choose the model focused on the year 2000 and GeoDa was utilised for the analysis.

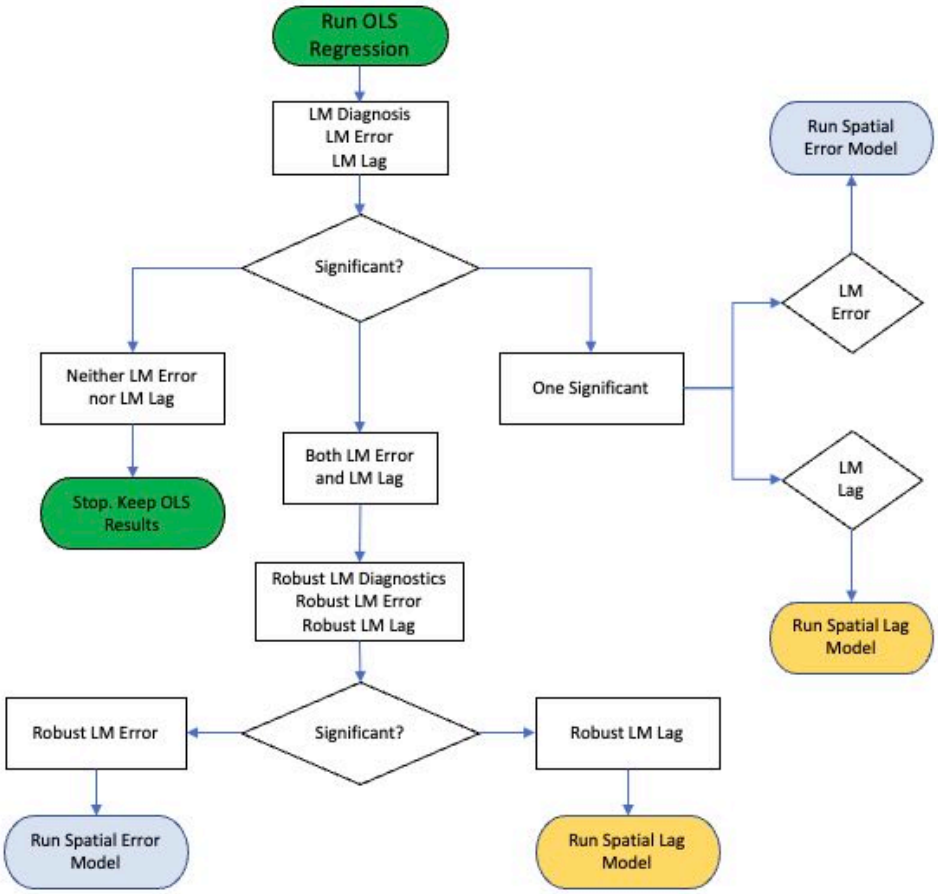

Figure 4.1 Spatial Regression Decision Tree
Source: Anselin (2005)

As a first step, an Ordinary Least Squares Estimation (OLS) Regression was conducted considering the same spatial weights matrix created before. The diagnostics for spatial dependence revealed evidence of spatial clustering or patterns in the data that cannot be explained by chance alone (see Table 4.2). Hence, spatial regression techniques were deemed more appropriate for modelling the data compared to non-spatial techniques. Furthermore, both the Lagrange Multiplier (LM) Lag and LM Error tests yielded significant p-values. Subsequently, Robust LM diagnostics were considered, and only the Robust LM lag was found to be significant, suggesting the estimation of a spatial lag model.

Anselin (1988) introduced the Lagrange Multiplier (LM) test to detect spatial autocorrelation, which is the presence of residual spatial dependence in a spatial regression model. This test examines whether residual spatial dependence exists after accounting for the spatial structure captured by the model. It helps identify whether there are unexplained spatial patterns or correlations in the residuals that are not adequately captured by the spatial regression model.

In addition, the Robust LM test was proposed by Anselin et al. (1996) as an alternative to the traditional LM test. The Robust LM test addresses potential model misspecification and heteroscedasticity, which can impact the accuracy of the results.

The LM Lag test focuses on the spatial lag component of the model. It helps determine whether there is spatial autocorrelation in the dependent variable itself, considering the influence of neighboring observations. On the other hand, the LM Error test examines spatial dependence in

the model residuals. It assesses whether there are spatial patterns or correlations remaining in the residuals after accounting for the spatial lag component and other covariates. capture all the spatial effects. More information on these tests can be found in Anselin (2017).

Table 4.2 OLS Diagnostics for spatial dependence for 2000 data

Test	MI/DF	Value	Prob
Moran's I (error)	0.6487	51.13	0.00
Lagrange Multiplier (lag)	1	2573.32	0.00
Robust LM (lag)	1	5.75	0.02
Lagrange Multiplier (error)	1	2567.58	0.00
Robust LM (error)	1	0.01	0.92
Lagrange Multiplier (SARMA)	2	2573.33	0.00

The complete results of the OLS Regression are presented in Annex VI. Spatial Lag Model – Maximum Likelihood Estimation.

Although the spatial lag model was initially suggested, both a spatial lag model and a spatial error model were evaluated to assess their goodness of fit. The Alkaike Information Criterion (AIC), which is based on the likelihood function, was employed as a measure of goodness-of-fit. The model with the lowest AIC was considered the best. In this case, the spatial lag model exhibited the lowest AIC, confirming its suitability as the best fit for the data.

Finally, Moran scatterplots were constructed to analyse the model residuals (Figure 4.2) and the model-predicted errors (Figure 4.3). The Moran's I test statistic for the spatially autoregressive error term in the model was -0.056, indicating the elimination of spatial autocorrelation as intended. In contrast, Moran's I statistic for the predicted errors remained similar to the original OLS residuals.

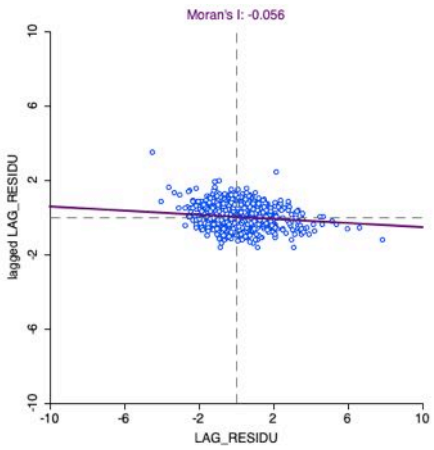

Figure 4.2 Moran's I for spatial lag model residuals

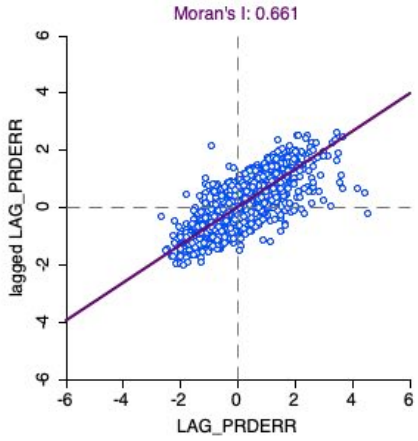

Figure 4.3 Moran's I for spatial lag model predicted errors

In a spatial lag models, explanatory variables and a response variable are related similarly to a standard linear regression model, with the distinction that the response variable is also influenced by spatially lagged response variables (Chi & Zhu, 2019). Spatial lag models are appropriate when the focus of interest is the assessment of the existence and strength of spatial interaction (Anselin, 1999). The spatial lag regression model can be expressed as in Equation 4:

$$y = \rho W y + X_\beta + \varepsilon$$

Equation 4 Spatial Lag Model

Where y is a vector of observations on the dependent variable, X is a matrix of observations on the explanatory variables, W_y is a spatially lagged dependent variable for weights matrix W, ε is a vector of independent and identically distributed error terms and ρ and β are parameters. This model is an estimation using the maximum likelihood of a spatial regression model that includes a spatially lagged dependent variable. (Anselin, 2005).

Once the models were conducted, the statistical significance of coefficients was assessed following Chi & Zhu's (2019) approach. Coefficients with $p < 0.001$ were considered to provide very strong evidence against the null hypothesis, those marked with ** at $p < 0.01$ were considered to provide strong evidence, and coefficients with * at $p < 0.05$ were considered to provide moderate evidence against the null hypothesis.

5. Results

5.1. Descriptive statistics

Table 5.1 provides an overview of the descriptive statistics of the air pollutants and socioeconomic variables considered over the studied period.

Table 5.1 Descriptive statistics

Statistic	2000	2005	2010	2015	2020
O_3 (ppb)					
Mean	37.09	31.01	27.04	27.98	31.92
SD	39.87	31.67	27.93	26.18	25.78
Min	22.24	20.76	22.24	23.72	25.20
Max	282.00	222.00	208.00	179.00	159.00
CO (ppm)					
Mean	2.28	1.32	1.02	0.72	0.32
SD	1.60	1.04	0.80	0.50	0.30
Min	1.19	0.74	0.59	0.30	0.15
Max	19.60	12.20	11.30	7.80	4.60
NOx (ppb)					
Mean	58.19	60.47	54.54	44.82	29.63
SD	55.60	53.85	49.54	39.34	29.94
Min	32.62	34.10	29.65	23.72	14.83
Max	500.00	615.00	716.00	717.00	509.00
SO_2 (ppb)					
Mean	17.38	11.13	5.81	4.39	3.29
SD	15.93	18.98	10.96	7.85	6.28
Min	8.90	5.93	2.97	1.48	1.48
Max	422.00	450.00	344.00	299.00	170.00
PM_{10} ($\mu g/m^3$)					
Mean	53.49	55.71	50.88	43.24	38.26
SD	46.84	39.38	38.25	29.38	25.76
Min	34.10	32.62	29.65	22.24	20.76
Max	998.00	683.00	830.00	742.00	615.00
$PM_{2.5}$ ($\mu g/m^3$)					
Mean	ND	29.05	22.72	23.67	19.05
SD	ND	20.95	16.56	16.59	11.81
Min	ND	17.79	13.34	13.34	10.38
Max	ND	541.00	378.00	690.00	189.00
Urban Marginalisation Index (Original and Normalised)					
Mean	-1.94 (0.29)	-0.69 (0.22)	-0.63 (0.29)	ND	0.05 (0.29)
SD	1.48 (0.16)	0.49 (0.14)	0.55 (0.16)	ND	0.02 (0.12)
Min	-4.72 (0)	0.45 (0)	-1.61 (0)	ND	0 (0)
Max	4.74 (1)	-1.47 (1)	1.75 (1)	ND	0.15 (1)
Poverty Rates (%)					
Mean	ND	ND	ND	ND	64.29
SD	ND	ND	ND	ND	17.34
Min	ND	ND	ND	ND	17.5
Max	ND	ND	ND	ND	98.86

5.2. Spearman Correlation

The Spearman correlations of the Urban Marginalisation Index (UMI) and Poverty Percentages (P %) were analysed over the studied years to get an overview of the data before the spatial analyses. It was observed that significant positive correlations were constantly observed between UMI and air pollutants O_3, PM_{10}, and $PM_{2.5}$, while negative correlations were found between UMI and CO, NOx, and SO_2. The strength of these correlations varied over time, with the highest correlation coefficient observed in 2010 for $PM_{2.5}$ and in 2005 for PM_{10}. As for Poverty Percentages, significant positive correlations were found with all pollutants except NOx and SO_2 in 2020.

Table 5.2 Summary of Spearman Correlations

Year	O_3	CO	NOx	SO_2	PM_{10}	$PM_{2.5}$
2000 UMI	0.142**	0.059**	-0.116**	-0.098**	0.236**	ND
2005 UMI	0.211**	-0.226**	-0.092**	-0.321**	0.339**	-0.321
2010 UMI	0.214**	-0.124**	-0.099**	-0.294**	-8.454**	0.381
2020 UMI	0.159**	0.105**	-0.144**	-0.207**	0.220**	0.293**
2015 P %	0.234**	-0.155**	-0.221**	-0.264**	-0.011	-0.177**
2020 P %	0.186**	0.115**	-0.170**	-0.233**	0.235**	0.318**

*Note: The coefficients with *** are statistically significant at $p < 0.001$*

5.3. Temporal Evolution and Spatial Distribution of Variables

5.3.1. Air pollutants

To provide a general overview of the temporal evolution of air pollutants in Mexico City, a yearly average time series plot based on monthly averages was created using data from 1986 to 2021 (See Figure 5.1). The `openair` package in R Studio was utilised for this purpose. To compare all pollutants, the time series were normalised by dividing each one by its mean value. The plot includes data from all stations in Mexico City since their establishment and for the entire duration that each station was operational until 2021. Overall, the plot shows that the concentration of pollutants has decreased in Mexico City over time. There was a particularly marked decrease in 2020 for most of the pollutants, which is probably related to the lockdown restrictions imposed during the COVID-19 pandemic.

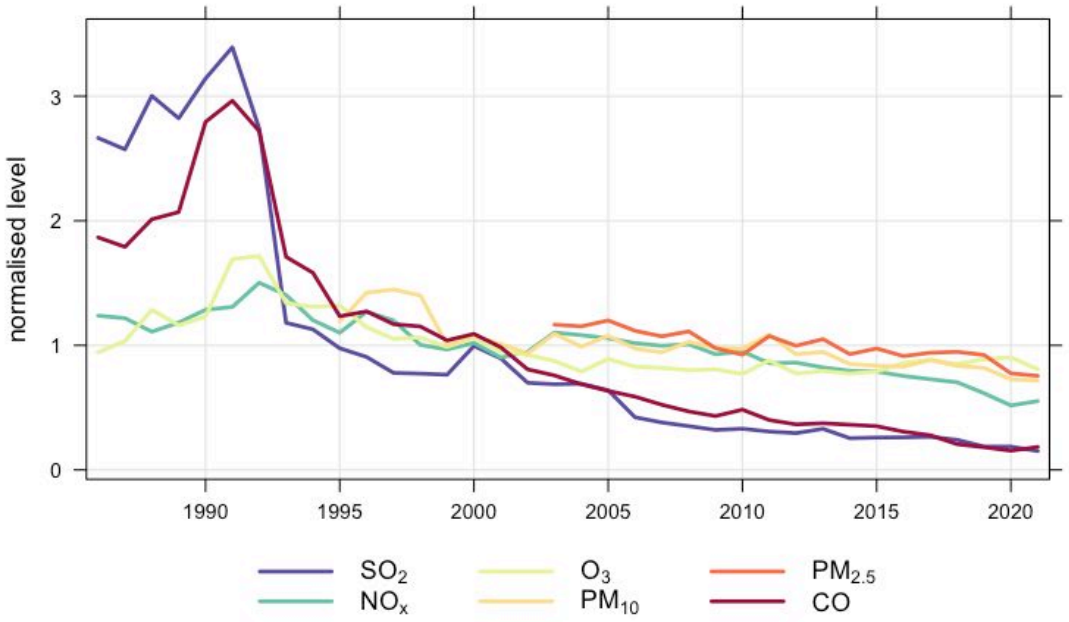

Figure 5.1 Normalised yearly average time plot of pollutants in Mexico City from 1986 to 2021

Regarding the spatial distribution of pollutants, for Ozone (O_3), concentrations have been consistently higher in the southern region of the city throughout the study period. For Carbon Monoxide (CO), higher concentrations have increasingly clustered in the northern part of the city, with high concentrations observed throughout most of the city, except for the western area, in 2020.

For Nitrogen Oxides (NO_x), a cluster of higher concentrations was present in the central and northeastern parts of the city in 2000, which expanded to cover most of the north by 2010, a trend that has continued until 2020. For Sulphur Dioxide (SO_2), higher concentrations have been consistently observed in the northern regions of the city, especially in the northwest.

The spatial distribution of higher concentrations of Particulate Matter PM_{10} and $PM_{2.5}$ have fluctuated over the years, but since 2015, the highest concentrations have been consistently located in the north and east of the city.

See Figure 5.2 and Figure 5.3 for O_3 overall trends and Annex IV. Air Pollutant Interpolations for full-size maps of the pollutants across the studied years.

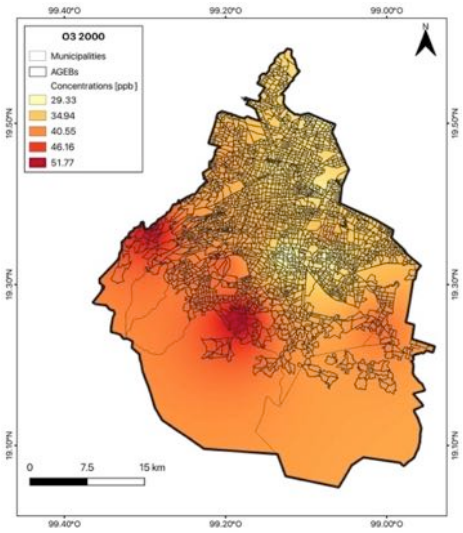

Figure 5.2 Average O_3 concentrations in 2000

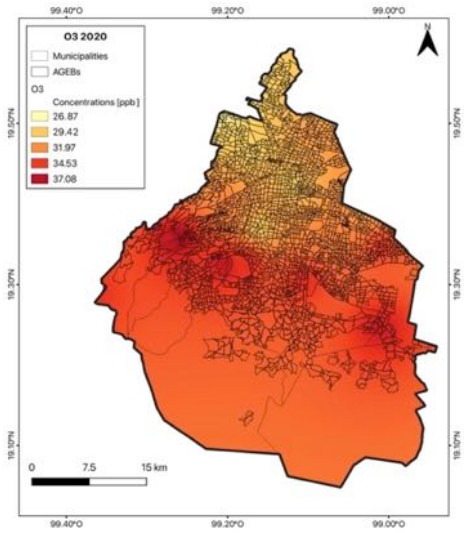

Figure 5.3 Average O_3 concentrations in 2020

5.3.2. Urban Marginalisation

The Urban Marginalisation Degree data suggests that between 2000 and 2020, there has been a decrease in the percentage of AGEBs that fall under the high and very high categories of urban marginalisation. At the same time, there has been an increase in the percentage of AGEBs that fall under the very low and low categories and a decrease in the percentage of AGEBs that fall under the medium category. To summarise, there has been an overall shift towards lower levels of urban marginalisation in the areas represented by the AGEBs in Mexico City. See Figure 5.4.

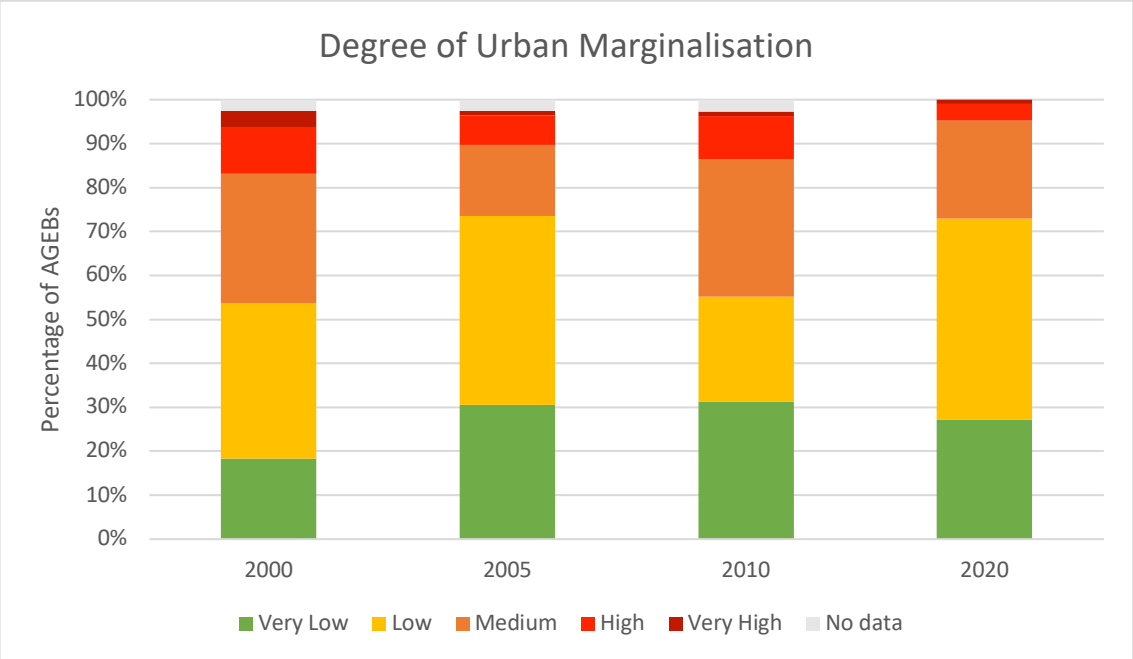

Figure 5.4 Degree of Urban Marginalisation in Mexico City over time

In terms of the spatial distribution, the data indicates a consistent pattern of higher marginalisation levels in the north, east, and south areas of the city. While disparities have been reducing over time, the aforementioned regions still have higher marginalisation levels compared to the centre

and the western areas of the city. As of 2020, the northernmost, easternmost, and southernmost areas of the city are predominantly categorised as medium, with some high spots and very high spots, while the centre and east areas remain mostly very low to low in degree of marginalisation.

See Figure 5.5 and Figure 5.6 for the overall evolution of the Urban Marginalisation Index and Annex II. Urban Marginalisation Index, for full-size maps of the UMI across the studied years.

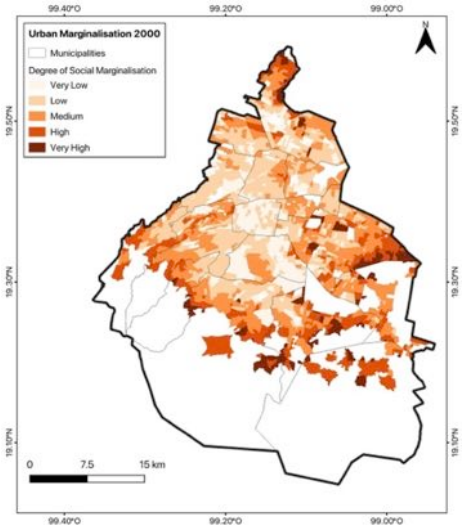

Figure 5.5 Urban Marginalisation Index in 2000

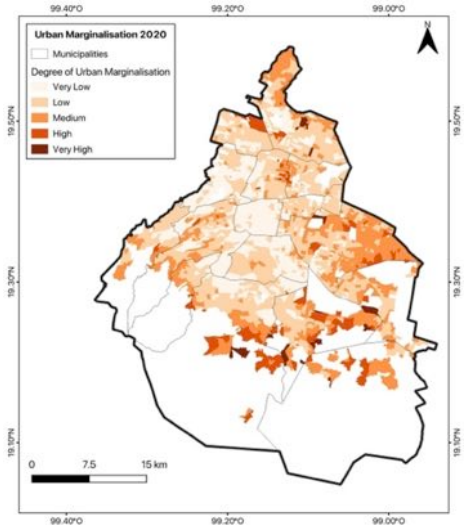

Figure 5.6 Urban Marginalisation Index in 2020

The obtained weighted Cohen's Kappa values for each pair of years are as follows:

- Year 2000 to 2005: Weighted Kappa = 0.182 (Slight agreement)
- Year 2005 to 2010: Weighted Kappa = 0.4228 (Moderate agreement)
- Year 2010 to 2020: Weighted Kappa = 0.3418 (Fair agreement)

The obtained weighted Cohen's Kappa values provide insights into the consistency of the Urban Marginalisation Index (UMI) categorisations over time. The Kappa values reveal varying levels of agreement over time. While the Kappa values do not directly capture the magnitude of change in the UMI values or indicate the direction of change, they provide an assessment of the agreement between the UMI categorisations. In other words, they reveal the extent to which the UMI categorisations remain stable or consistent across consecutive years, despite the evolving socioeconomic conditions.

It is important to note that the interpretation of these Kappa values should be considered alongside the overall trend towards lower levels of urban marginalisation indicated by the UMI data. The observed agreement, although varying in strength, suggests that there is some stability or consistency in the categorisations of marginality captured by the Urban Marginalisation Index.

5.3.3. Poverty Percentages

The poverty rates in Mexico City have been reported differently for 2015 and 2020. While EVALUA (2022) reported a decrease from 60.9% in 2015 to 57.4% in 2020 in their “Poverty Measurement in Mexico City Municipalities, 2015 and 2020” report, a self-made calculation using the Social Development Index database from EVALUA (2020) resulted in a poverty rate of 67.68% for 2020.

It should be noted that the 2015 poverty rates used for this analysis were only available in ranges per AGEB, and not as a continuous variable, which limits the accuracy of any comparison with 2020 data. Additionally, the poverty rates for 2015 were retrieved from CONEVAL (2018) and those for 2020 were self-calculated based on information from EVALUA (2020). Although both institutions retrieved their data from the National Institute of Statistics and Geography (INEGI), there may be differences in the way they calculate poverty. Therefore, any comparison between poverty rates for these two years using this information should be interpreted with caution.

See Figure 5.7 and Figure 5.8 for the evolution of poverty rates from 2015 to 2020 and Annex III. Poverty Percentages for full-size maps.

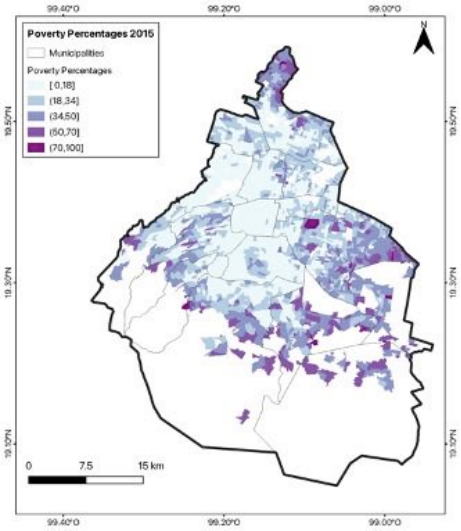

Figure 5.7 Poverty Percentages in 2015

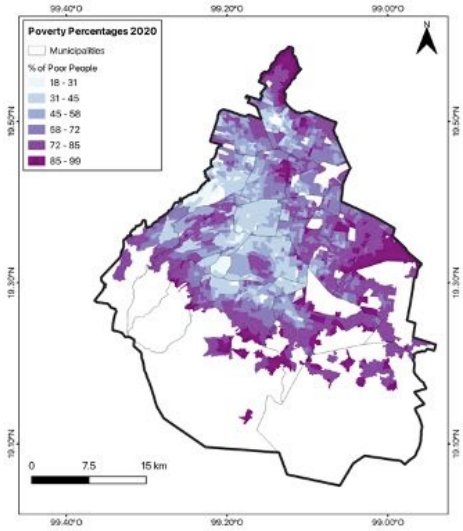

Figure 5.8 Poverty Percentages in 2020

5.4. Spatial Lag Model – Maximum Likelihood Estimation

For these regression analyses, the dependent variables were the Urban Marginalisation Index and the Poverty Percentages, and the independent variables were the air pollutants (SO_2, CO, NO_x, O_3, PM_{10}, and $PM_{2.5}$). A summary of the coefficients of the regressions is shown in Table 5.3, and the complete reports for each regressions are presented in Annex VI. Spatial Lag Model – Maximum Likelihood Estimation.

Table 5.3 Summary of Spatial Lag Model Coefficients – Maximum Likelihood Estimation

Year	O_3	CO	NOx	SO_2	PM_{10}	$PM_{2.5}$	Rho	R-squared
2000 UMI	**0.036*** **	**0.334*** **	-0.003	0.005	**0.037*** **	ND	0.824	0.700
2005 UMI	**0.019*** **	-0.131	0.002	**-0.016** **	**0.005** **	**0.023*** **	0.811	0.704
2010 UMI	**0.024*** **	**-0.163***	**0.006***	**-0.020** **	0.002	**0.030*** **	0.829	0.749
2020 UMI	0.001	-0.047	0.000	0.000	0.000	**0.002** **	0.736	0.571
2015 P %	**0.124*** **	-0.086	0.022	**-0.155*** **	**0.048*** **	**0.018** **	0.687	0.532
2020 P %	**0.800** **	-34.972	-0.018	1.160	0.166	**1.190** **	0.857	0.770

*Note: The coefficients with *** are statistically significant at $p < 0.001$, with ** at $p < 0.01$ and with * at $p < 0.05$*

Urban Marginalisation Index

The results of the spatial lag models highlight significant associations between the Urban Marginalisation Index (UMI) and air pollutant concentrations in Mexico City over the years. Higher levels of O_3 and $PM_{2.5}$ consistently coincide with higher marginalisation in the area at very strong or strong significance levels.

In the year 2000, UMI shows positive and significant relationships with O_3, CO, and PM_{10}, indicating that areas with higher UMI tend to exhibit higher concentrations of these pollutants. The positive spatial lag coefficient Rho suggests spatial autocorrelation, where neighbouring areas with high UMI also have high pollutant concentrations.

In 2005, a notable change occurs in the UMI-air pollutant relationship. Alongside O_3 and PM_{10}, higher UMI values become positively associated with increased concentrations of $PM_{2.5}$[1]. However, a contrasting pattern emerges with SO_2, where higher UMI values are linked to lower concentrations of this pollutant. This shift suggests a more complex and nuanced relationship between UMI and air pollution during this period.

By 2010, the relationships between UMI and air pollutants continue to evolve. O_3 and $PM_{2.5}$ remain positively associated with UMI, while SO_2 retains its negative association. Notably, NO_x now exhibits a positive association with UMI, and the significance of the PM_{10} relationship diminishes. Additionally, CO shows a negative association with UMI, contrasting with the positive association observed in 2000.

In 2020, the only statistically significant relationship is found with $PM_{2.5}$. This may indicate a change in the dynamics or spatial patterns of UMI and air pollution. The lower spatial lag coefficient suggests weaker spatial autocorrelation, suggesting a more dispersed pattern of UMI and air pollutants this year.

Poverty Percentages

The results of the spatial lag models reveal significant associations between Poverty Percentages (% P) and air pollutant concentrations in Mexico City for the two studied years. Consistently, higher levels of O_3 and $PM_{2.5}$ align with higher poverty rates in the area. Additionally, in the year 2015, a positive and significant relationship is observed between poverty percentages and PM_{10} concentrations.

5.5. Bivariate Local Moran's I Spatial Autocorrelation

The following subsections provide an overview of the results of Bivariate Local Moran's Spatial Autocorrelation for Urban Marginalisation Index and Poverty Percentages. Some relevant Moran Cluster Maps are presented below and the full-size Moran Scatterplots and the Moran Cluster Maps are shown in Annex VI. LISA Cluster Maps.

5.5.1. Urban Marginalisation Index

Table 5.4 presents the Bivariate Local Moran's I Index, showcasing the relationship between each air pollutant and the Urban Marginalisation Index (UMI) over the years in Mexico City. This table provides insights into how the association between these variables has evolved. Notably, consistent positive spatial autocorrelations were observed for O_3, PM_{10}, and $PM_{2.5}$, indicating

[1] It is important to note that $PM_{2.5}$ were not being monitored in Mexico City in the year 2000, indicating that this relationship represents the introduction of a new variable rather than a change in an existing one.

clustering patterns of high or low values in nearby locations. Conversely, negative spatial autocorrelations were found for NO_x and SO_2.

Of particular interest, O_3 and $PM_{2.5}$ consistently exhibited higher Moran's Index values. However, it is essential to recognise that the strength and direction of these relationships may vary across different regions within Mexico City. In other words, specific neighbourhoods may demonstrate a more pronounced positive spatial autocorrelation between a particular pollutant and urban marginalisation, while other areas may exhibit a weaker or even negative association. This highlights the spatial heterogeneity in the relationship between air pollutants and urban marginalisation within the city.

Table 5.4 Bivariate Local Moran's I Index Summary for Urban Marginalisation Index

Year	O_3	CO	NOx	SO_2	PM_{10}	$PM_{2.5}$
2000	**0.168**	0.069	-0.106	-0.097	0.249	NA
2005	**0.237**	-0.174	-0.95	-0.291	0.048	**0.345**
2010	**0.280**	-0.074	-0.054	-0.313	0.015	**0.373**
2020	**0.151**	0.115	-0.144	-0.201	0.182	**0.263**

Table 5.5 provides an overview of the percentages of AGEB (local administrative units) categorized as High-High and High-Low for the LISA Cluster Maps between the Urban Marginalisation Index and each air pollutant over the studied years.

Notably, O_3, PM_{10}, and $PM_{2.5}$ consistently exhibit higher percentages of High-High associations, indicating the presence of spatial clusters where areas with higher urban marginalization and higher concentrations of these pollutants are spatially concentrated. This suggests a spatial relationship between urban marginalization and the levels of O_3, PM_{10}, and $PM_{2.5}$, where neighbouring AGEBs with higher UMI tend to have higher concentrations of these pollutants.

Table 5.5 Percentage of AGEBs that fall within High-High and High-Low categories for air pollutants and Urban Marginalisation Index

Pollutant / Year	High-High (% of AGEBs)				High-Low (% of AGEBs)			
	2000	2005	2010	2020	2000	2005	2010	2020
O_3	8.2	10.83	10.87	10.84	14.50	15.14	15.74	12.73
CO	9.33	2.26	6.01	9.20	14.02	10.28	10.91	13.78
NOx	8.24	2.60	3.81	3.66	13.18	12.71	11.21	11.51
SO_2	6.25	2.09	2.71	2.86	12.33	11.26	8.80	10.39
PM_{10}	10.85	8.06	4.70	10.38	17.14	16.59	17.47	18.40
$PM_{2.5}$	ND	10.79	11.04	10.76	ND	18.29	18.65	18.70

Ozone (O_3)

The Bivariate Local Moran's Index analysis indicates a consistent positive spatial autocorrelation between O_3 concentrations and the Urban Marginalization Index in Mexico City over the studied years. Even though the index has had an overall decrease, the concentration of high-high pairs, representing areas of both high O_3 and high marginalisation, has been on the rise with a slightly higher number of clusters seen in recent years. The percentages of AGEBs falling into each category indicate that around one-quarter of AGEBs in Mexico City have been exposed to higher O_3 levels, regardless of their marginalisation status. However, the percentage of AGEBs falling into the High O_3 - High Marginalisation category has increased from 8.2% to 10.84% over time, indicating a growing clustering of O_3 pollution in high marginalisation areas primarily located in

the south and east of the city. Figure 5.9 and Figure 5.10 show the overall evolution of Bivariate Moran's cluster map for O_3.

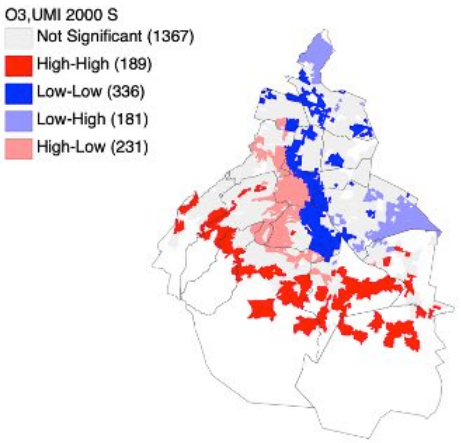

Figure 5.9 LISA Cluster Map for O3 and Urban Marginalisation Index in 2000

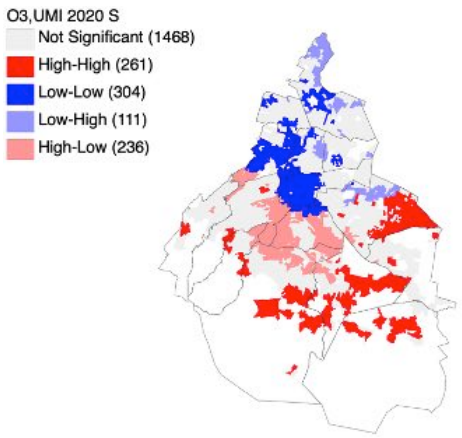

Figure 5.10 LISA Cluster Map for O_3 and Urban Marginalisation Index in 2020

Carbon Monoxide (CO)

The Bivariate Local Moran's Index analysis indicates that there is not a consistent pattern of correlation between the CO concentrations and the Urban Marginalization Index in Mexico City over the studied years, with the relationship between the two variables fluctuating over time. The percentages of AGEBs falling into each category indicate that a proportion, ranging from 12% to 23%, of AGEBs in Mexico City have been exposed to higher levels of CO pollution, irrespective of their marginalization status. The location of High CO - High Marginalization clusters category has been inconsistent over time, with the clusters moving between the south and the east of the city.

Nitrogen Oxides (NOx)

The Bivariate Local Moran's Index analysis indicates a consistent negative spatial autocorrelation between NOx concentrations and the Urban Marginalization Index in Mexico City over the studied years, suggesting that high levels of NOx pollution are not clustered in specific areas of the city. The percentages of AGEBs falling into each category show that a proportion, ranging from 15% to 21%, of AGEBs in Mexico City have been exposed to the higher levels of NOx pollution. Moreover, the percentage of AGEBs falling into the High-High category has had an overall decrease over time, while the percentage of AGEBs falling into the High-Low category has remained consistently significantly higher, indicating that, in general, NOx pollution is not disproportionately affecting marginalized areas of the city, but rather is distributed more evenly. However, since 2005, there is a small cluster of High -High values in the north of the city.

Sulphur Dioxide (SO_2)

The Bivariate Local Moran's Index analysis indicates a consistent negative spatial autocorrelation between SO_2 concentrations and the Urban Marginalization Index in Mexico City over the studied years, suggesting that, in general, high levels of SO_2 pollution are not clustered in specific areas of the city. The percentages of AGEBs falling into each category show that a proportion ranging

from 11% to 19%, of AGEBs in Mexico City, have been exposed to higher levels of SO_2 pollution. Moreover, the percentage of AGEBs falling into the High-High category has had an overall decrease time, while the percentage of AGEBs falling into the High-Low category has remained consistently significantly higher, indicating that SO_2 pollution is not disproportionately affecting marginalized areas of the city. However, there is a small but consistent cluster of High-High values located in the north of the city that has persisted throughout all years.

Particulate Matter (PM_{10})

The Bivariate Local Moran's Index analysis indicates a consistent positive spatial autocorrelation between PM_{10} concentrations and the Urban Marginalization Index in Mexico City over the studied years, suggesting that high levels of PM_{10} pollution are clustered in specific areas of the city. The percentages of AGEBs falling into each category show that at least one-quarter of AGEBs in Mexico City have been exposed to higher levels of PM_{10} concentrations, regardless of their socioeconomic status. Moreover, the percentage of AGEBs falling into the High-High category has fluctuated over time. The High-High clusters have remained consistently in the east and the north of the city.

In 2010, a significant concentration of PM_{10} pollutants was observed in the northeast of the city. This localized hotspot of high concentration had a profound impact on the overall Moran's Index calculation. As a result, the Moran's Index appeared lower because the high concentrations in other areas were overshadowed and masked by this extreme value in the northeast. This localized hotspot acted as an outlier, distorting the spatial pattern analysis and making it less sensitive to the presence of high concentrations in other areas of the city. Thus, it is important to recognize that although other areas also had higher pollutant concentrations, their significance and contribution were diminished in the Moran's Index due to the dominance of the extreme concentration in the northeast.

Particulate Matter ($PM_{2.5}$)

The Bivariate Local Moran's Index analysis indicates a consistent positive spatial autocorrelation between $PM_{2.5}$ concentrations and the Urban Marginalisation Index in Mexico City over the studied years, suggesting that high levels of $PM_{2.5}$ pollution are clustered in specific areas of the city. The percentages of AGEBs falling into each category show that a proportion of around 29%, of AGEBs in Mexico City have been exposed to higher levels of $PM_{2.5}$ concentrations, regardless of their socioeconomic status. Moreover, the percentage of AGEBs falling into the High-High category has remained between 10 and 11% over time. The High-High clusters have remained consistently in the east and the north of the city.

5.5.2. Poverty Percentages

Table 5.6 displays the Bivariate Local Moran's Index between each air pollutant and the poverty rates in Mexico City for the years 2015 and 2020. For 2020, the findings are consistent with those for the Urban Marginalisation Index, revealing positive spatial autocorrelations for CO, O_3, PM_{10}, and $PM_{2.5}$, and a negative one for NO_x and SO_2.

Table 5.6 Bivariate Local Moran's I Index Summary for Poverty Percentages

Year	O_3	CO	NOx	SO_2	PM_{10}	$PM_{2.5}$
2015	0.225	-0.155	-0.232	-0.240	-0.008	-0.107
2020	0.163	0.147	-0.143	-0.209	0.243	0.323

Table 5.7 provides an overview of the percentages of AGEB that fall within the High-High and High-Low categories for the LISA Cluster Maps between Poverty Percentages and each air pollutant over the studied years.

There are significant differences between both years, probably related to the origin of the poverty data, however, the results from 2020 where O_3, PM_{10} and $PM_{2.5}$ have higher percentages are consistent with those for Urban Marginalisation Index.

Table 5.7 Percentage of AGEBs that fall within High-High and High-Low categories for air pollutants and Poverty Percentages

Pollutant / Year	High-High (% of AGEBs)		High-Low (% of AGEBs)	
	2015	2020	2015	2020
O_3	12.61	17.31	15.68	14.83
CO	2.66	13.28	9.36	14.45
NOx	2.74	5.38	6.53	11.72
SO_2	2.45	2.86	7.93	10.38
PM_{10}	10.50	16.68	12.48	19.71
$PM_{2.5}$	2.45	15.97	11.13	20.00

The Bivariate Local Moran's Index analysis indicates that there is a consistent positive spatial autocorrelation between O_3 concentrations and poverty percentages in Mexico City, with High-High clusters located in the south of the city. Moreover, positive spatial autocorrelations were also found for CO, PM_{10} and $PM_{2.5}$ in 2020.

High-High clusters are consistent for CO, NO_x, SO_2, PM_{10} and $PM_{2.5}$, indicating clustering of these pollutants in areas with higher percentages of poverty primarily located in the northernmost part of the city. High-High clusters of PM_{10} and $PM_{2.5}$ are also located in the east of the city. Figure 5.11 and Figure 5.12 show the overall evolution of Bivariate Moran's cluster map for PM_{10}. In 2020 there were more high-poverty areas with high concentrations of PM_{10} compared to low-poverty areas with high PM_{10} concentrations, indicating that a larger proportion of the population living in poverty was exposed to higher levels of PM_{10}.

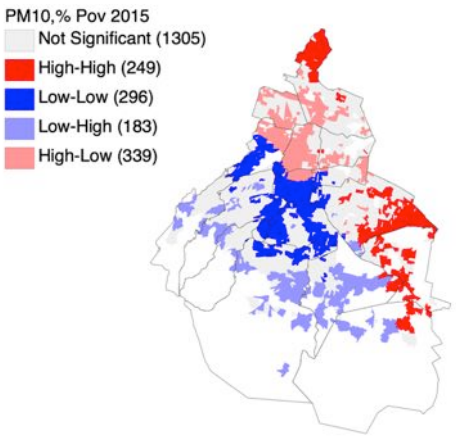

Figure 5.11 LISA Cluster Map for PM2.5 and Poverty in 2015

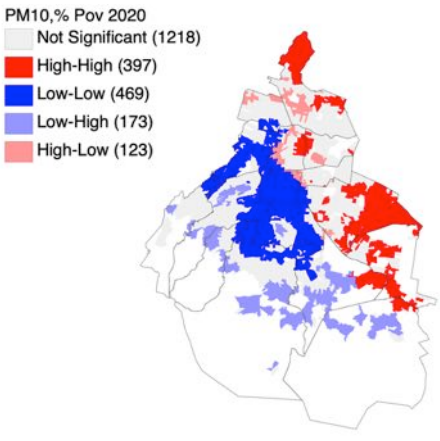

Figure 5.12 LISA Cluster Map for $PM_{2.5}$ and Poverty in 2020

The percentages of AGEBs falling in each category reveal that areas with higher concentrations of pollutants and higher percentages of poverty have increased for all pollutants, while areas with high concentrations of pollutants and lower percentages of poverty have mostly decreased.

In 2020, there was a notable increase in the number of High-High AGEBs for $PM_{2.5}$. This increase can be attributed to the significant concentration of $PM_{2.5}$ observed in the east of the city in 2015. The localized hotspot of elevated pollution in 2015 had a substantial impact on Moran's Index calculations. As a result, the number of High-High areas appeared lower than expected, as the extreme concentrations in the east masked the high concentrations in other areas of the city. Therefore, the increase in High-High areas observed in 2020 can be better understood by considering the influence of the concentrated pollution in the east in 2015, which distorted the spatial pattern of poverty and $PM_{2.5}$ concentrations.

The difference between the 2015 and 2020 results is likely influenced by the fact that the 2015 poverty rates used for this analysis were only available in ranges per AGEB, and not as a continuous variable, which limits the accuracy of any comparison with 2020 data. Nevertheless, the spatial patterns of pollutants and poverty are clear, with some geographically located clusters of pollutants in areas with higher percentages of poverty.

6. Discussion

How has the relationship between socioeconomic factors and air pollution distribution in Mexico City changed over time?

The research on air pollution within the context of environmental inequalities in Latin America is limited, with a low proportion of published papers focusing on this topic (Fernández et al., 2023). Among these studies, a consistent pattern emerges, indicating higher concentrations of air pollutants in socially deprived areas (Gouveia et al., 2022). However, the findings from different studies in Mexico City present contrasting results. For instance, Garcia-Burgos et al. (2022) found socioeconomic disparities specifically in O_3 concentrations, while observing no such disparities in the distribution of PM_{10} and $PM_{2.5}$. Conversely, Lome-Hurtado et al. (2020) identified a positive association between deprived socioeconomic conditions and PM_{10}, but a negative association between lower socioeconomic conditions and O_3.

However, the present study, which covers a longer period, reveals a different perspective. Contrary to the previous studies, this research consistently demonstrates positive associations between urban marginalisation, poverty percentages and the concentrations of O_3, PM_{10}, and $PM_{2.5}$ through both, the Spatial Lag Models and the Bivariate Moran's I Index. Notably, the concentrations of O_3 and Particulate Matter in Mexico City often exceed the maximum permissible limits established by both Mexican regulations and the World Health Organisation (SEDEMA et al., 2022).

Mexico City exhibits a complex socio-spatial structure, with diverse social groups coexisting within delegations and municipalities, although there are exceptions. Notably, a distinct spatial pattern emerges, where the urban elite tends to concentrate in central areas while poorer groups disperse towards the outer periphery. This segregation is driven by real estate dynamics, including processes like gentrification, which displace lower-income groups and attract middle-class populations (Aguilar et al., 2015). Additionally, there is a notable pattern of spatial fragmentation and segregation within the city, where specific points of interest are exclusive to particular income groups (Letouzé et al., 2022).

The city's socio-spatial differentiation is historically marked by two axes: north-south and east-west. The southwestern and western areas are consistently associated with socioeconomic privilege and higher social strata, while the eastern areas tend to have lower strata (Duhau, 2003; Schteingart, 2001; Ziccardi, 2016).

This spatial pattern aligns with the spatial distribution of PM_{10} and $PM_{2.5}$ concentrations, where areas with high vehicular intensity and heavy traffic are the main contributors to the generation and suspension of particles, primarily due to transportation activities on roadways (SEDEMA, Báez, et al., 2021). Moreover, industrial activities also play an important role in the distribution of particulate matter in the city.

Cruz et al., (2014) identified significant industrial activities in both the northern and eastern parts of the city, which contribute to the emissions of pollutants in their respective areas. The industrial zones in the northern region are strategically positioned to cater to domestic markets and facilitate trade with the United States. Similarly, the eastern regions of Iztapalapa and La Paz serve as important industrial hubs primarily oriented towards meeting the demands of the city's domestic markets.

These spatial disparities in socio-economic conditions contribute to the unequal distribution of resources and opportunities across the city. However, these disparities extend beyond the socio-economic realm and encompass environmental burdens such as air pollution. These disparities in exposure to air pollutants further contribute to the environmental inequalities experienced by socially or economically disadvantaged communities (Gouveia et al., 2022).

Air pollution exposure can vary among different socioeconomic groups and have implications for housing choices and job opportunities. Fontenla et al. (2019) uncovered that as PM_{10} air pollution levels increase in Mexico City, the prices of houses tend to decrease. This means that individuals living in areas with higher pollution may pay less for their homes compared to those residing in cleaner areas. Additionally, the study revealed that as pollution levels increase, wages tend to be higher. This suggests that individuals working in areas with higher pollution may earn more money compared to those working in cleaner areas. This creates a cycle where socially or economically disadvantaged communities not only live in areas with higher levels of air pollution but also face challenges in accessing better housing options and may be compelled to work in more polluted environments.

In relation to O_3, the topographical characteristics of the semi-closed basin of Mexico City contribute to the circulation of O_3. In the morning, pollutants emitted in the north and northeast are carried by winds towards the southwestern and southern sectors of the basin. However, the presence of mountain ranges restricts ventilation, causing air masses with high levels of O_3 to accumulate in these areas. (Peralta et al., 2021). Consequently, the southern parts of Mexico City consistently exhibit higher concentrations of O_3, importantly this area also corresponds to regions with higher levels of marginalisation and poverty.

This study reveals that specific areas in Mexico City continue to experience high levels of both air pollution and low socioeconomic conditions, highlighting the persistence of socio-environmental disparities. While the overall spatial association between urban marginalisation, poverty percentages, and air pollutant concentrations may have weakened over time, certain pockets within the city remain disproportionately affected.

It is important to note that individuals from lower socioeconomic backgrounds often reside in conditions that amplify their exposure to these pollutants. Moreover, these populations tend to be more vulnerable and experience a higher prevalence of diseases, which can be further exacerbated by poor air quality (Clougherty et al., 2014; Ortiz-Hernández et al., 2015). This is attributed to various factors such as limited access to healthcare services, education, lifestyle choices, and work and transportation-related factors, all of which are associated with socioeconomic disparities (Bautista-Hernández, 2021; Makri & Stilianakis, 2008).

Conversely, wealthier individuals, despite being exposed to high levels of pollutant concentrations in certain areas, possess greater socioeconomic and political resources. These resources provide them with the means and options to effectively avoid or mitigate many environmental health risks (Romero-Lankao et al., 2013).

To what extent have policy and regulatory interventions aimed at reducing air pollution in Mexico City been effective, and how have they impacted disparities in air pollution distribution over time?

To improve air quality in Mexico City, policy and regulatory interventions have been implemented, with a particular emphasis on addressing emissions from mobile sources, since they are recognised as major contributors to air pollution in the city.

It has been claimed by researchers that mobility policies in Mexico City focus on enhancing long-distance daily journeys by increasing mass transport options and thus reducing air pollution, however, this approach contradicts the goal of reducing air pollution since it fails to promote productive activities and services in southern municipalities, from where people have to travel longer distances (Finck Carrales, 2023). These differences between policy priorities and objectives have implications for the effectiveness of interventions targeting mobile sources, which are considered crucial in reducing air pollution in Mexico City.

According to the evaluation of the ProAire[2] program conducted by the Environmental Commission of the Megalopolis (2021), measures targeting mobile sources, such as the Mandatory Vehicle Emission Testing Program and the "Hoy No Circula" program, which restricts vehicle usage on certain days based on license plate numbers, are considered the most effective in reducing emissions in Mexico City. However, studies have shown that these driving restrictions have had minimal impact on overall vehicle travel and pollution reduction (Davis, 2017; Guerra & Millard-Ball, 2017). Additionally, these policies raise equity concerns as uneven enforcement has led to a concentration of exempt vehicles in the city centre, while higher-polluting vehicles may be pushed towards lower-income peripheral neighbourhoods (Guerra & Reyes, 2022). This gives rise to worries regarding the fairness and effectiveness of a program that grants exemptions to wealthier households. As a result, it disproportionately impacts individuals who rely on a single restricted vehicle, particularly those who commute to areas with stricter enforcement measures in place.

There are concerns regarding the adequacy of meeting the objectives related to preventing and controlling pollutant emissions, monitoring vehicle environmental performance, and controlling emissions from mobile sources (Ontiverios Jiménez, 2019). The effectiveness of the Mandatory Vehicle Emission Testing Program has been brought into question, with researchers raising significant concerns about the prevalence of cheating, which allows non-compliant vehicles to pass emission tests and evade the restrictions imposed by the Hoy No Circula program (Oliva, 2015).

These concerns align with Muñoz-Pizza et al.'s (2022) research, which emphasizes a predominant focus on technological solutions and vehicle fleet modernisation by policy makers, limited consideration of alternative approaches, barriers related to dependence on petroleum-based industries, lack of public awareness about the health risks of air pollution, scepticism towards suggested solutions, and the need for stronger regulatory frameworks to ensure air quality.

Policy and regulatory interventions aimed at reducing air pollution in Mexico City have demonstrated a certain degree of effectiveness in decreasing overall pollutant concentrations. Despite criticisms, the stable trend observed in air pollution levels since 2010 suggests a positive impact of these measures (SEDEMA et al., 2021). However, it is important to acknowledge that certain pollutants, such as PM_{10}, $PM_{2.5}$, and O_3, still often exceed permissible limits, indicating the need for further action.

[2] ProAire programs are management instruments that establish actions to prevent and reverse trends in air quality deterioration.

7. Conclusion

This research underscores the persistent socio-environmental disparities in Mexico City and emphasizes the importance of comprehensive and integrated approaches for the development of air pollution control policies. The study consistently demonstrates positive associations between urban marginalisation, poverty percentages, and the concentrations of O_3, PM_{10}, and $PM_{2.5}$ across the studied years. It reveals that pollution sources in Mexico City, like in other parts of the world, are disproportionately located in low-income neighborhoods, consequently, the concentrations of pollutants tends to be higher in these areas. Moreover, as air pollution increases, housing prices go down, perpetuating the low-income status of these communities.

Scientific studies indicate that current air quality policies have not effectively achieved objectives related to emissions prevention, environmental performance monitoring, and control of mobile source emissions in Mexico City. These findings have raised concerns about equity in air pollution management. Although progress has been made in reducing overall air pollutant concentrations, pollutants such as PM_{10}, $PM_{2.5}$, and O_3 still frequently exceed acceptable limits. Importantly, these concentrations are often higher in areas with lower socioeconomic status, where populations tend to be more vulnerable, highlighting the urgent need for further action.

Mobility policies need to adopt a comprehensive approach that goes beyond relying solely on restrictive measures, which, although useful in some cases, are not sufficient on their own. The focus should steer towards targeting the root causes of the issue, one of which is the large population that commutes daily to the city. It is important to acknowledge that certain policies may currently prioritise addressing the symptoms rather than the underlying core problem.

By tackling the underlying factors of pollution with policies that lead to improvements in regional infrastructure, promote decentralised economic development and enhance public transportation systems, the root causes of pollution can be better addressed, leading to significant and enduring change. For improving the overall well-being of the Mexico City, we must focus on sustainable solutions that take into account the bigger picture and prioritise measures that reduce pollution.

8. Limitations

The use of interpolation techniques, particularly inverse distance weighting (IDW), introduces uncertainty and error into air pollution distribution estimates. Even though IDW is commonly used for air pollutants interpolation, this method assumes that closer monitoring points have a greater influence on estimated values, which oversimplifies the complex dispersion patterns and may yield less accurate results, especially in areas with spatial variations. Furthermore, IDW does not consider the underlying physical processes governing pollutant dispersion.

Additionally, calculating yearly averages of pollutants within the AGEBs has its limitations. It assumes uniform pollution levels within a given area, potentially neglecting spatial variability and leading to a less accurate representation of distribution patterns. Moreover, the use of yearly averages fails to account for temporal variations in pollution levels, such as diurnal, seasonal, and annual fluctuations. Moreover, relying on data from a limited number of monitoring stations may result in incomplete spatial coverage, thereby limiting the representation of air pollution levels across the study area.

Lastly, the utilisation of poverty rates from different sources and their varying presentation introduces potential inconsistencies and bias in the analysis. Despite these limitations, this study

provides a valuable temporal overview of the evolving relationship between air pollutants and socioeconomic conditions.

9. References

Aguilar, A. G., Romero, P., & Hernández, J. (2015). Segregación socio-residencial en la Ciudad de México. Dinámica del patrón territorial a nivel local, 2000-2010. In *Segregación Urbana y Espacios de Exclusión. Ejemplos de México y América Latina*.

Agyeman, J., & Evans, B. (2004). 'Just Sustainability': The Emerging Discourse of Environmental Justice in Britain? *The Geographical Journal*, *170*(2), 155–164.

Ahrens, D. (2009). *Meteorology Today* (9th ed.). Brooks/Cole CENGAGE Learning.

Alfaro-Moreno, E., Martínez, L., García-Cuellar, C., Bonner, J. C., Murray, J. C., Rosas, I., Rosales, S. P. de L., & Osornio-Vargas, A. R. (2002). Biologic effects induced in vitro by PM10 from three different zones of Mexico City. *Environmental Health Perspectives*, *110*(7), 715–720. https://doi.org/10.1289/ehp.02110715

Alves, B. (2023). *Most polluted cities in Latin America 2021*. Statista. https://www.statista.com/statistics/1029132/latin-america-air-pollution-city/

Anselin, L. (1988). Lagrange Multiplier Test Diagnostics for Spatial Dependence and Spatial Heterogeneity. *Geographical Analysis*, *20*(1), 1–17. https://doi.org/10.1111/j.1538-4632.1988.tb00159.x

Anselin, L. (1999). *Bruton Center School of Social Sciences University of Texas at Dallas Richardson, TX 75083-0688*.

Anselin, L. (2005). *Exploring Spatial Data with GeoDa: A Workbook*. https://www.geos.ed.ac.uk/~gisteac/fspat/geodaworkbook.pdf

Anselin, L. (2017). *Spatial Regression 10. Specification Tests (2)*. https://spatial.uchicago.edu/sites/spatial.uchicago.edu/files/10_specification_tests_2_slides.pdf

Anselin, L., Bera, A. K., Florax, R., & Yoon, M. J. (1996). Simple diagnostic tests for spatial dependence. *Regional Science and Urban Economics*, *26*(1), 77–104. https://doi.org/10.1016/0166-0462(95)02111-6

Bautista-Hernández, D. A. (2021). Mode choice in commuting and the built environment in México City. Is there a chance for non-motorized travel? *Journal of Transport Geography*, *92*, 103024. https://doi.org/10.1016/j.jtrangeo.2021.103024

Borja-Aburto, V. H., Loomis, D. P., Bangdiwala, S. I., Shy, C. M., & Rascon-Pacheco, R. A. (1997). Ozone, Suspended Particulates, and Daily Mortality in Mexico City. *American Journal of Epidemiology*, *145*(3), 258–268. https://doi.org/10.1093/oxfordjournals.aje.a009099

Branis, M., & Linhartova, M. (2012). Association between unemployment, income, education level, population size and air pollution in Czech cities: Evidence for environmental inequality? A pilot national scale analysis. *Health & Place*, *18*(5), 1110–1114. https://doi.org/10.1016/j.healthplace.2012.04.011

Bravo, A. H., Sosa, E. R., Sánchez, A. P., Jaimes, P. M., & Saavedra, R. M. I. (2002). Impact of wildfires on the air quality of Mexico City, 1992–1999. *Environmental Pollution*, *117*(2), 243–253. https://doi.org/10.1016/S0269-7491(01)00277-9

Brulle, R. J., & Pellow, D. N. (2006). ENVIRONMENTAL JUSTICE: Human Health and Environmental Inequalities. *Annual Review of Public Health*, *27*(1), 103–124. https://doi.org/10.1146/annurev.publhealth.27.021405.102124

Bullard, R. D. (2000). *Dumping in Dixie: Race, Class and Environmental Quality* (3rd ed). Westview Press.

Carbajal-Arroyo, L., Miranda-Soberanis, V., Medina-Ramón, M., Rojas-Bracho, L., Tzintzun, G., Solís-Gutiérrez, P., Méndez-Ramírez, I., Hurtado-Díaz, M., Schwartz, J., & Romieu, I. (2011). Effect of PM10 and O3 on infant mortality among residents in the Mexico City Metropolitan Area: A case-crossover analysis, 1997–2005. *Journal of Epidemiology & Community Health*, *65*(8), 715–721. https://doi.org/10.1136/jech.2009.101212

Carvalho, C., Del Campo, A. G., & de Carvalho Cabral, D. (2022). Scales of inequality: The role of spatial extent in environmental justice analysis. *Landscape and Urban Planning*, *221*, 104369. https://doi.org/10.1016/j.landurbplan.2022.104369

Chatziioannou, I., Alvarez-Icaza, L., & Bakogiannis, E. (2020). A structural analysis method for the promotion of Mexico City´s integral plan of mobility. *Cogent Engineering*, *7*(1). Scopus. https://doi.org/10.1080/23311916.2020.1759395

Chi, G., & Zhu, J. (2019). Models dealing with spatial dependence. In *Spatial Regression Models for the Social Sciences* (Vol. 14, p. 272). SAGE Publications, Inc.

Clark, L. P., Millet, D. B., & Marshall, J. D. (2014). National Patterns in Environmental Injustice and Inequality: Outdoor NO2 Air Pollution in the United States. *PLOS ONE*, *9*(4), e94431. https://doi.org/10.1371/journal.pone.0094431

Clougherty, J. E., Shmool, J. L. C., & Kubzansky, L. D. (2014). The Role of Non-Chemical Stressors in Mediating Socioeconomic Susceptibility to Environmental Chemicals. *Current Environmental Health Reports*, *1*(4), 302–313. https://doi.org/10.1007/s40572-014-0031-y

Cohen, A. J., Brauer, M., Burnett, R., Anderson, H. R., Frostad, J., Estep, K., Balakrishnan, K., Brunekreef, B., Dandona, L., Dandona, R., Feigin, V., Freedman, G., Hubbell, B., Jobling, A., Kan, H., Knibbs, L., Liu, Y., Martin, R., Morawska, L., … Forouzanfar, M. H. (2017). Estimates and 25-year trends of the global burden of disease attributable to ambient air pollution: An analysis of data from the Global Burden of Diseases Study 2015. *Lancet (London, England)*, *389*(10082), 1907–1918. https://doi.org/10.1016/S0140-6736(17)30505-6

CONAFOR. (2023). Estadísticas de Incendios. *Sistema Nacional de Información Forestal*. https://snif.cnf.gob.mx/estadisticas-de-incendios/

CONAPO. (2021a). *Índice de Marginación Urbana 2020: Nota técnico-metodológica*. https://www.gob.mx/cms/uploads/attachment/file/685307/Nota_t_cnica_IMU_2020.pdf

CONAPO. (2021b). *Índices de marginación 2020*. gob.mx. http://www.gob.mx/conapo/documentos/indices-de-marginacion-2020-284372

CONAPO. (2023). *Índice de marginación (carencias poblacionales) por localidad, municipio y entidad—Índice de marginación urbana por AGEB, 2000-2010—Datos.gob.mx/busca*. Datos Abiertos. https://datos.gob.mx/busca/dataset/indice-de-marginacion-carencias-poblacionales-por-localidad-municipio-y-entidad/resource/082aadb4-8d92-4f09-9ed4-e9439b35ff16

CONEVAL. (2018). *Índice de pobreza urbana por AGEB*. Portal de Datos Abiertos de la Ciudad de México. https://datos.cdmx.gob.mx/dataset/indice-de-pobreza-urbana-por-ageb

Cruz, F., Garza, G., Cruz, F., & Garza, G. (2014). Configuración microespacial de la industria en la Ciudad de México a inicios del siglo XXI. *Estudios demográficos y urbanos*, *29*(1), 9–52.

Damián, A. (2020). *Un diagnóstico de la desigualdad socio territorial* (p. 440) [Diagnóstico]. Consejo de Evaluación del Desarrollo Social de la Ciudad de México. https://www.evalua.cdmx.gob.mx/storage/app/media/DIES20/ciudad-de-mexico-2020-un-diagnostico-de-la-desigualdad-socio-territorial.pdf

Data México. (2020). *Ciudad de México: Economía, empleo, equidad, calidad de vida, educación, salud y seguridad pública*. Data México. https://datamexico.org/es/profile/geo/ciudad-de-mexico-cx

Davis, L. W. (2017). Saturday Driving Restrictions Fail to Improve Air Quality in Mexico City. *Scientific Reports*, *7*(1), 41652. https://doi.org/10.1038/srep41652

de Foy, B., Krotkov, N. A., Bei, N., Herndon, S. C., Huey, L. G., Zavala, M., & Molina, L. T. (2009). Hit from both sides: Tracking industrial and volcanic plumes in Mexico City with surface measurements and OMI SO2 retrievals during the MILAGRO field campaign. *Atmos. Chem. Phys.*

De Matteis, S., Forastiere, F., Baldacci, S., Maio, S., Tagliaferro, S., Fasola, S., Cilluffo, G., La Grutta, S., & Viegi, G. (2022). Issue 1 - “Update on adverse respiratory effects of outdoor

air pollution". Part 1): Outdoor air pollution and respiratory diseases: A general update and an Italian perspective. *Pulmonology*, *28*(4), 284–296. https://doi.org/10.1016/j.pulmoe.2021.12.008

Deligiorgi, D., & Philippopoulos, K. (2011). Spatial Interpolation Methodologies in Urban Air Pollution Modeling: Application for the Greater Area of Metropolitan Athens, Greece. In *Advanced Air Pollution*. IntechOpen. https://www.intechopen.com/chapters/17390

Díaz-Esteban, Y., Barrett, B. S., & Raga, G. B. (2022). Circulation patterns influencing the concentration of pollutants in central Mexico. *Atmospheric Environment*, *274*, 118976. https://doi.org/10.1016/j.atmosenv.2022.118976

Duhau, E. (2003). División social del espacio metropolitano y movilidad residencial. *Papeles de Población*, *36*.

EVALUA. (2022). *Medición de la pobreza en las Alcaldías de la Ciudad de México, 2015 y 2020*. EVALUA. https://www.evalua.cdmx.gob.mx/storage/app/media/2022/diresta/NBI_2015-2020.pdf

EVALUA. (2020). *Medición del Índice de Desarrollo Social, 2020*. Consejo de Evaluación del Desarrollo Social de la Ciudad de México. https://www.evalua.cdmx.gob.mx/principales-atribuciones/medicion-del-indice-de-desarrollo-social-de-las-unidades-territoriales/medicion-del-indice-de-desarrollo-social-de-las-unidades-territoriales

Ezcurra, E. (1991, April). Las inversiones térmicas. *Revista Ciencias*, *22*. https://www.revistacienciasunam.com/en/170-revistas/revista-ciencias-22/1538-las-inversiones-t%C3%A9rmicas.html

Fairburn, J., Walker, G., & Smith, G. (2005). *Investigating environmental justice in Scotland: Links between measures of environmental quality and social deprivation* (Project UE4(03)01). Institute for Environment and Sustainability Research, Staffordshire University. https://eprints.staffs.ac.uk/1828/1/1828.pdf

Fecht, D., Fischer, P., Fortunato, L., Hoek, G., de Hoogh, K., Marra, M., Kruize, H., Vienneau, D., Beelen, R., & Hansell, A. (2015). Associations between air pollution and socioeconomic characteristics, ethnicity and age profile of neighbourhoods in England and the Netherlands. *Environmental Pollution*, *198*, 201–210. https://doi.org/10.1016/j.envpol.2014.12.014

Fernández, I. C., Koplow-Villavicencio, T., & Montoya-Tangarife, C. (2023). Urban environmental inequalities in Latin America: A scoping review. *World Development Sustainability*, *2*, 100055. https://doi.org/10.1016/j.wds.2023.100055

Finck Carrales, J. C. (2023). Mobility regulations and urban projects in Mexico City: An accessibility focus on territorial inequalities. *Case Studies on Transport Policy*, *11*, 100939. https://doi.org/10.1016/j.cstp.2022.100939

Fontenla, M., Ben Goodwin, M., & Gonzalez, F. (2019). Pollution and the choice of where to work and live within Mexico City. *Latin American Economic Review*, *28*(1), 11. https://doi.org/10.1186/s40503-019-0072-6

García-Burgos, J., Miquelajauregui, Y., Vega, E., Namdeo, A., Ruíz-Olivares, A., Mejía-Arangure, J. M., Resendiz-Martinez, C. G., Hayes, L., Bramwell, L., Jaimes-Palomera, M., Entwistle, J., Núñez-Enríquez, J. C., Portas, A., & McNally, R. (2022). Exploring the Spatial Distribution of Air Pollution and Its Association with Socioeconomic Status Indicators in Mexico City. *Sustainability*, *14*(22), Article 22. https://doi.org/10.3390/su142215320

Garza, G. (1996). Uncontrolled air pollution in Mexico City. *Cities*, *13*(5), 315–328. https://doi.org/10.1016/0264-2751(96)00019-4

Gobierno de la Ciudad de México. (2020). *Inicia Gobierno capitalino renovación de Metrobús*. Gobierno de La Ciudad de México: Jefatura de Gobierno. https://jefaturadegobierno.cdmx.gob.mx/comunicacion/nota/inicia-gobierno-capitalino-renovacion-de-metrobus

Gobierno de la Ciudad de México. (2022). Renovación de autobuses RTP. *Gobierno CDMX*. https://gobierno.cdmx.gob.mx/noticias/renovacion-de-autobuses-rtp/

Goutham Priya, M., & Jayalakshmi, S. (2018). Evaluation of Interpolation Techniques for Air Quality Monitoring using Statistical Error Metrics â˜' A Review. *International Journal of Engineering Research & Technology*, *6*(7). https://doi.org/10.17577/IJERTCONV6IS07019

Gouveia, N., Slovic, A. D., Kanai, C. M., & Soriano, L. (2022). Air Pollution and Environmental Justice in Latin America: Where Are We and How Can We Move Forward? *Current Environmental Health Reports*, *9*(2), 152–164. https://doi.org/10.1007/s40572-022-00341-z

Guerra, E., & Millard-Ball, A. (2017). Getting around a license-plate ban: Behavioral responses to Mexico City's driving restriction. *Transportation Research Part D: Transport and Environment*, *55*, 113–126. https://doi.org/10.1016/j.trd.2017.06.027

Guerra, E., & Reyes, A. (2022). Examining behavioral responses to Mexico City's driving restriction: A mixed methods approach. *Transportation Research Part D: Transport and Environment*, *104*, 103191. https://doi.org/10.1016/j.trd.2022.103191

Hajat, A., Hsia, C., & O'Neill, M. S. (2015). Socioeconomic Disparities and Air Pollution Exposure: A Global Review. *Current Environmental Health Reports*, *2*(4), 440–450. https://doi.org/10.1007/s40572-015-0069-5

Hartmann, K., Krois, J., & Waske, B. (2018). *E-Learning Project SOGA: Statistics and Geospatial Data Analysis*. Freie Universitaet Berlinn. https://www.geo.fu-berlin.de/en/v/soga/Geodata-analysis/geostatistics/Inverse-Distance-Weighting/index.html

Hodzic, A., Wiedinmyer, C., Salcedo, D., & Jimenez, J. L. (2012). Impact of Trash Burning on Air Quality in Mexico City. *Environmental Science & Technology*, *46*(9), 4950–4957. https://doi.org/10.1021/es203954r

INEGI. (2000). *Marco geoestadístico municipal 2000 (Censo General de Población y Vivienda 2000)*. Mapas. https://www.inegi.org.mx/app/biblioteca/ficha.html?upc=702825292843

INEGI. (2004). *Cartografía Geoestadística Urbana 2004, Distrito Federal*. Mapas. https://www.inegi.org.mx/app/biblioteca/ficha.html?upc=889463083542

INEGI. (2010). *Marco geoestadístico 2010 versión 5.0 (Censo de Población y Vivienda 2010)*. Mapas. https://www.inegi.org.mx/app/biblioteca/ficha.html?upc=702825292812

INEGI. (2020a). *AGEB Rurales (Áreas geoestadísticas básicas rurales)*. Portal de Datos Abiertos de la CDMX. https://datos.cdmx.gob.mx/dataset/ageb-rurales-areas-geoestadisticas-basicas-rurales

INEGI. (2020b). *AGEB Urbanas (Áreas geoestadísticas básicas urbanas)*. Portal de Datos Abiertos de la CDMX. https://datos.cdmx.gob.mx/dataset/ageb-urbanas-areas-geoestadisticas-basicas-urbanas

INEGI. (2020c). *Censo de Población y Vivienda 2020*. Instituto Nacional de Estadística, Geografía e Informática. https://www.inegi.org.mx/programas/ccpv/2020/#Datos_abiertos

Islas-Camargo, A., Bohara, A. K., Department of EconomicsThe New Mexico University, USA1915 Roma Ave. Albuquerque, NM 87131, USA, & Herrera Ramos, J. M. (2022). Economic disparities in pollution-related mortality in three municipalities of the Metropolitan Area of the Valley of Mexico. *Atmósfera*, *35*(4), 755–779. https://doi.org/10.20937/ATM.52962

Jazcilevich, A. D., García, A. R., & Caetano, E. (2005). Locally induced surface air confluence by complex terrain and its effects on air pollution in the valley of Mexico. *Atmospheric Environment*, *39*(30), 5481–5489. https://doi.org/10.1016/j.atmosenv.2005.05.046

Jerrett, M., Burnett, R. T., Ma, R., Pope, C. A. I., Krewski, D., Newbold, K. B., Thurston, G., Shi, Y., Finkelstein, N., Calle, E. E., & Thun, M. J. (2005). Spatial Analysis of Air Pollution and Mortality in Los Angeles. *Epidemiology*, *16*(6), 727. https://doi.org/10.1097/01.ede.0000181630.15826.7d

Kamboj, K., Sisodiya, S., Mathur, A. K., Zare, A., & Verma, P. (2022). Assessment and Spatial Distribution Mapping of Criteria Pollutants. *Water, Air, & Soil Pollution*, *233*(3), 82. https://doi.org/10.1007/s11270-022-05522-y

Knibbs, L. D., & Barnett, A. G. (2015). Assessing environmental inequalities in ambient air pollution across urban Australia. *Spatial and Spatio-Temporal Epidemiology*, *13*, 1–6. https://doi.org/10.1016/j.sste.2015.03.001

Kopas, J., York, E., Jin, X., Harish, S. P., Kennedy, R., Shen, S. V., & Urpelainen, J. (2020). Environmental Justice in India: Incidence of Air Pollution from Coal-Fired Power Plants. *Ecological Economics*, *176*, 106711. https://doi.org/10.1016/j.ecolecon.2020.106711

Landis, J. R., & Koch, G. G. (1977). The Measurement of Observer Agreement for Categorical Data. *Biometrics*, *33*(1), 159–174. https://doi.org/10.2307/2529310

Legorreta, J. (1991, April). La grave contaminación atmosférica de la Ciudad de México—Revista Ciencias. *Revista Ciencias*, *22*. https://www.revistacienciasunam.com/pt/170-revistas/revista-ciencias-22/1539-la-grave-contaminaci%C3%B3n-atmosf%C3%A9rica-de-la-ciudad-de-m%C3%A9xico.html

Leo, A., Morillón, D., & Silva, R. (2017). Review and analysis of urban mobility strategies in Mexico. *Case Studies on Transport Policy*, *5*(2), 299–305. https://doi.org/10.1016/j.cstp.2016.11.008

Letouzé, E., Nieto, B. F., Romero, G., Ricard, J., Vazquez, D., & Maya, L. A. C. (2022). *Parallel Worlds: Revealing the Inequity of Access to Urban Spaces in Mexico City Through Mobility Data*.

Link, B. G., & Phelan, J. (1995). Social Conditions As Fundamental Causes of Disease. *Journal of Health and Social Behavior*, *35*, 80. https://doi.org/10.2307/2626958

Lome-Hurtado, A., Touza-Montero, J., & White, P. C. L. (2020). Environmental Injustice in Mexico City: A Spatial Quantile Approach. *Exposure and Health*, *12*(2), 265–279. https://doi.org/10.1007/s12403-019-00310-2

Lynch, J., & Kaplan, G. (2000). Socioeconomic Position. In *Social Epidemiology* (pp. 13–35). Oxford University Press. http://hdl.handle.net/2027.42/51520

Makri, A., & Stilianakis, N. I. (2008). Vulnerability to air pollution health effects. *International Journal of Hygiene and Environmental Health*, *211*(3–4), 326–336. https://doi.org/10.1016/j.ijheh.2007.06.005

Manisalidis, I., Stavropoulou, E., Stavropoulos, A., & Bezirtzoglou, E. (2020). Environmental and Health Impacts of Air Pollution: A Review. *Frontiers in Public Health*, *8*, 14. https://doi.org/10.3389/fpubh.2020.00014

McLeod, H., Langford, I. H., Jones, A. P., Stedman, J. R., Day, R. J., Lorenzoni, I., & Bateman, I. J. (2000). The relationship between socio-economic indicators and air pollution in England and Wales: Implications for environmental justice. *Regional Environmental Change*, *1*(2), 78–85. https://doi.org/10.1007/PL00011536

Molina, L. T., & Molina, M. J. (2004). Improving Air Quality in Megacities: Mexico City Case Study. *Annals of the New York Academy of Sciences*, *1023*(1), 142–158. https://doi.org/10.1196/annals.1319.006

Moreno-Jiménez, A., Cañada-Torrecilla, R., Vidal-Domínguez, M. J., Palacios-García, A., & Martínez-Suárez, P. (2016). Assessing environmental justice through potential exposure to air pollution: A socio-spatial analysis in Madrid and Barcelona, Spain. *Geoforum*, *69*, 117–131. https://doi.org/10.1016/j.geoforum.2015.12.008

Muñoz-Pizza, D. M., Villada-Canela, M., Rivera-Castañeda, P., Osornio-Vargas, Á., Martínez-Cruz, A. L., & Texcalac-Sangrador, J. L. (2022). Barriers and opportunities to incorporate scientific evidence into air quality management in Mexico: A stakeholders' perspective. *Environmental Science & Policy*, *129*, 87–95. https://doi.org/10.1016/j.envsci.2021.12.022

Niedzwiecki, M. M., Rosa, M. J., Solano-González, M., Kloog, I., Just, A. C., Martínez-Medina, S., Schnaas, L., Tamayo-Ortiz, M., Wright, R. O., Téllez-Rojo, M. M., & Wright, R. J. (2020). Particulate air pollution exposure during pregnancy and postpartum depression symptoms in women in Mexico City. *Environment International*, *134*, 105325. https://doi.org/10.1016/j.envint.2019.105325

Olguín Lacunza, M. (2022, February 17). En invierno, mala calidad del aire. *Gaceta UNAM*. https://www.gaceta.unam.mx/en-invierno-mala-calidad-del-aire/

Oliva, P. (2015). Environmental Regulations and Corruption: Automobile Emissions in Mexico City. *Journal of Political Economy*, *123*(3), 686–724. https://doi.org/10.1086/680936

O'Neill, M. S., Bell, M. L., Ranjit, N., Cifuentes, L. A., Loomis, D., Gouveia, N., & Borja-Aburto, V. H. (2008). Air Pollution and Mortality in Latin America: The Role of Education. *Epidemiology*, *19*(6), 810. https://doi.org/10.1097/EDE.0b013e3181816528

Ontiverios Jiménez, M. (2019). Análisis de la eficacia, eficiencia y equidad de los programas para reducir las emisiones de ozono troposférico en la Ciudad de México. *Journal of Economic Literature*, *16*(48). https://www.scielo.org.mx/pdf/eunam/v16n48/1665-952X-eunam-16-48-239.pdf

Ortiz-Hernández, L., Pérez-Salgado, D., & Tamez-González, S. (2015). Desigualdad socioeconómica y salud en México. *Rev Med Inst Mex Seguro Soc.*, *53*(3), 336–347.

Pastor, M., Sadd, J., & Hipp, J. (2001). Which Came First? Toxic Facilities, Minority Move-In, and Environmental Justice. *Journal of Urban Affairs*, *23*(1), 1–21. https://doi.org/10.1111/0735-2166.00072

Pearce, J., & Kingham, S. (2008). Environmental inequalities in New Zealand: A national study of air pollution and environmental justice. *Geoforum*, *39*(2), 980–993. https://doi.org/10.1016/j.geoforum.2007.10.007

Peralta, O., Ortínez-Alvarez, A., Torres-Jardón, R., Suárez-Lastra, M., Castro, T., & Ruíz-Suárez, L. G. (2021). Ozone over Mexico City during the COVID-19 pandemic. *The Science of the Total Environment*, *761*, 143183. https://doi.org/10.1016/j.scitotenv.2020.143183

Pyle, D. M., & Mather, T. A. (2005). The regional influence of volcanic emissions from Popocatéptl, Mexico: Discussion of "Measurement of aerosol particles, gases and flux radiation in the Pico de Orizaba Nacional Park, and its relationship to air pollution transport", Márquez et al., 2005, Atmospheric Environment, 39, 3877–3890. *Atmospheric Environment*, *39*(34), 6475–6478. https://doi.org/10.1016/j.atmosenv.2005.07.022

Raga, G. B., Kok, G. L., Baumgardner, D., Báez, A., & Rosas, I. (1999). Evidence for volcanic influence on Mexico City aerosols. *Geophysical Research Letters*, *26*(8), 1149–1152. https://doi.org/10.1029/1999GL900154

Rawls, J. (1999). *A theory of justice* (Rev. ed). Belknap Press of Harvard University Press.

Rentschler, J., & Leonova, N. (2022, May 18). *Air pollution kills – Evidence from a global analysis of exposure and poverty*. https://blogs.worldbank.org/developmenttalk/air-pollution-kills-evidence-global-analysis-exposure-and-poverty

Rojas-Martinez, R., Perez-Padilla, R., Olaiz-Fernandez, G., Mendoza-Alvarado, L., Moreno-Macias, H., Fortoul, T., McDonnell, W., Loomis, D., & Romieu, I. (2007). Lung Function Growth in Children with Long-Term Exposure to Air Pollutants in Mexico City. *American Journal of Respiratory and Critical Care Medicine*, *176*(4), 377–384. https://doi.org/10.1164/rccm.200510-1678OC

Romero-Lankao, P., Qin, H., & Borbor-Cordova, M. (2013). Exploration of health risks related to air pollution and temperature in three Latin American cities. *Social Science & Medicine*, *83*, 110–118. https://doi.org/10.1016/j.socscimed.2013.01.009

Romieu, I., Gouveia, N., & Cifuentes, L. A. (2012). *Multicity Study of Air Pollution and Mortality in Latin America (The ESCALA Study)* (Research Report No. 171). https://www.healtheffects.org/publication/multicity-study-air-pollution-and-mortality-latin-america-escala-study

Samoli, E., Stergiopoulou, A., Santana, P., Rodopoulou, S., Mitsakou, C., Dimitroulopoulou, C., Bauwelinck, M., de Hoogh, K., Costa, C., Marí-Dell'Olmo, M., Corman, D., Vardoulakis, S., & Katsouyanni, K. (2019). Spatial variability in air pollution exposure in relation to socioeconomic indicators in nine European metropolitan areas: A study on environmental inequality. *Environmental Pollution*, *249*, 345–353. https://doi.org/10.1016/j.envpol.2019.03.050

Schlosberg, D. (2007). *Defining environmental justice: Theories, movements, and nature*. Oxford University Press.

Schteingart, M. (2001). La división social del espacio en las ciudades. *PERFILES LATINOAMERICANOS*, |*9*.

SEDEMA. (n.d.). *El monitoreo de la calidad del aire*. Dirección de Monitoreo Atmosférico. Retrieved 19 March 2023, from http://www.aire.cdmx.gob.mx/default.php?opc=%27ZaBhnmI=%27

SEDEMA. (2023). *Datos derivados del Monitoreo Atmosférico—Contaminante*. Dirección de Monitoreo Atmosférico. http://www.aire.cdmx.gob.mx/default.php?opc=%27aKBhnmI=%27&opcion=Zg==

SEDEMA, Báez, A. A. A., Hernández, A. M., Rivera, C. C., Molina, G. G., Rosas, L. E. C., Mendoza, L. I. L., Trujillo, M. S. O., Ramírez, O. S., Morales, O. L., Hernández Gordillo Lavana, O. U., Camacho Rodríguez, P., Paz Ramírez, P., Mendoza Pelcastre, S., Siles Tapia, S. P., Diego Santos, V., & Reyes Aguilar, Y. (2021). *Inventario de Emisiones de la Zona Metropolitana del Valle de México 2018* (Inventario de emisiones, p. 86). Secretaría del Medio Ambiente de la Ciudad de México, SEDEMA.

SEDEMA, Jaimes Palomera, M., Reséndiz Martínez, C. G., & Rivera Hernández, O. (2022). *Calidad del aire en la Ciudad de México, Informe 2019* (Informe 2019; Calidad del aire en la Ciudad de México). Secretaría del Medio Ambiente de la Ciudad de México, SEDEMA.

SEDEMA, SMAGEM, SEMARNATH, & SEMARNAT. (2021). *Programa de gestión para mejorar la calidad del aire en la Zona Metropolitana del Valle de México. ProAire 2021-2030*.

Shukla, K., Kumar, P., Mann, G. S., & Khare, M. (2020). Mapping spatial distribution of particulate matter using Kriging and Inverse Distance Weighting at supersites of megacity Delhi. *Sustainable Cities and Society*, *54*, 101997. https://doi.org/10.1016/j.scs.2019.101997

Steurer, N., & Bonilla, D. (2016). Building sustainable transport futures for the Mexico City Metropolitan Area. *Transport Policy*, *52*, 121–133. https://doi.org/10.1016/j.tranpol.2016.06.002

Stevens, G. A., Dias, R. H., & Ezzati, M. (2008). The effects of 3 environmental risks on mortality disparities across Mexican communities. *Proceedings of the National Academy of Sciences*, *105*(44), 16860–16865. https://doi.org/10.1073/pnas.0808927105

Ugalde-Resano, R., Riojas-Rodríguez, H., Texcalac-Sangrador, J. L., Cruz, J. C., & Hurtado-Díaz, M. (2022). Short term exposure to ambient air pollutants and cardiovascular emergency department visits in Mexico city. *Environmental Research*, *207*, 112600. https://doi.org/10.1016/j.envres.2021.112600

United Church of Christ. (1987). *Toxic Wastes and Race In the United States: A National Report on the Racial and Socio-Economic Characteristics of Communities with Hazardous Waste Sites.* (Exhibit 13). United Church of Christ. https://www.nrc.gov/docs/ML1310/ML13109A339.pdf

US EPA, O. (2021, September 15). *EPA Research: Environmental Justice and Air Pollution* [Overviews and Factsheets]. https://www.epa.gov/ej-research/epa-research-environmental-justice-and-air-pollution

US EPA, O. (2022, September 6). *Learn About Environmental Justice* [Overviews and Factsheets]. https://www.epa.gov/environmentaljustice/learn-about-environmental-justice

Venter, Z. S., Figari, H., Krange, O., & Gundersen, V. (2023). Environmental justice in a very green city: Spatial inequality in exposure to urban nature, air pollution and heat in Oslo, Norway. *Science of The Total Environment*, *858*, 160193. https://doi.org/10.1016/j.scitotenv.2022.160193

WHO. (2022). *Ambient (outdoor) air pollution*. World Health Organization. https://www.who.int/news-room/fact-sheets/detail/ambient-(outdoor)-air-quality-and-health

Ziccardi, A. (2016). Poverty and urban inequality: The case of Mexico City metropolitan region *: Poverty and urban inequality. *International Social Science Journal*, *65*(217–218), 205–219. https://doi.org/10.1111/issj.12070

Annex I. Air Quality Monitoring Stations

Table 9.1 Air quality monitoring stations

Code	Name	Municipality	State
ACO	Acolman	Acolman	State of Mexico
AJU	Ajusco	Tlalpan	Mexico City
AJM	Ajusco Medio	Tlalpan	Mexico City
ATI	Atizapán	Atizapán de Zaragoza	State of Mexico
BJU	Benito Juarez	Benito Juárez	Mexico City
CAM	Camarones	Azcapotzalco	Mexico City
CCA	Centro de Ciencias de la Atmósfera	Coyoacán	Mexico City
TEC	Cerro del Tepeyac	Gustavo A. Madero	Mexico City
CHO	Chalco	Chalco	State of Mexico
COR	CORENA	Xochimilco	Mexico City
CUA	Cuajimalpa	Cuajimalpa de Morelos	Mexico City
CUT	Cuautitlán	Cuautitlán Izcalli	State of Mexico
DIC	Diconsa	Tlalpan	Mexico City
EAJ	Ecoguardas Ajusco	Tlalpan	Mexico City
EDL	Ex Convento Desierto de los Leones	Cuajimalpa de Morelos	Mexico City
FAC	FES Acatlán	Naucalpan de Juárez	State of Mexico
FAR	FES Aragón	Nezahualcóyotl	State of Mexico
GAM	Gustavo A. Madero	Gustavo A. Madero	Mexico City
HGM	Hospital General de México	Cuauhtémoc	Mexico City
INN	Investigaciones Nucleares	Ocoyoacac	State of Mexico
IZT	Iztacalco	Iztacalco	Mexico City
LPR	La Presa	Tlalnepantla de Baz	State of Mexico
LAA	Laboratorio de Análisis Ambiental	Gustavo A. Madero	Mexico City
IBM	Legaria	Miguel Hidalgo	Mexico City
LOM	Lomas	Miguel Hidalgo	Mexico City
LLA	Los Laureles	Ecatepec de Morelos	State of Mexico
MER	Merced	Venustiano Carranza	Mexico City
MGH	Miguel Hidalgo	Miguel Hidalgo	Mexico City
MPA	Milpa Alta	Milpa Alta	Mexico City
MON	Montecillo	Texcoco	State of Mexico
MCM	Museo de la Ciudad de México	Cuauhtémoc	Mexico City
NEZ	Nezahualcóyotl	Nezahualcóyotl	State of Mexico
PED	Pedregal	Álvaro Obregón	Mexico City
SAG	San Agustín	Ecatepec de Morelos	State of Mexico
SNT	San Nicolás Totolapan	La Magdalena Contreras	Mexico City
SFE	Santa Fe	Cuajimalpa de Morelos	Mexico City
SAC	Santiago Acahualtepec	Iztapalapa	Mexico City
TAH	Tláhuac	Xochimilco	Mexico City
TLA	Tlalnepantla	Tlalnepantla de Baz	State of Mexico
TLI	Tultitlán	Tultitlán	State of Mexico
UIZ	UAM Iztapalapa	Iztapalapa	Mexico City
UAX	UAM Xochimilco	Coyoacán	Mexico City
VIF	Villa de las Flores	Coacalco de Berriozábal	State of Mexico
XAL	Xalostoc	Ecatepec de Morelos	State of Mexico

Source: (SEDEMA, n.d.)

Annex II. Urban Marginalisation Index

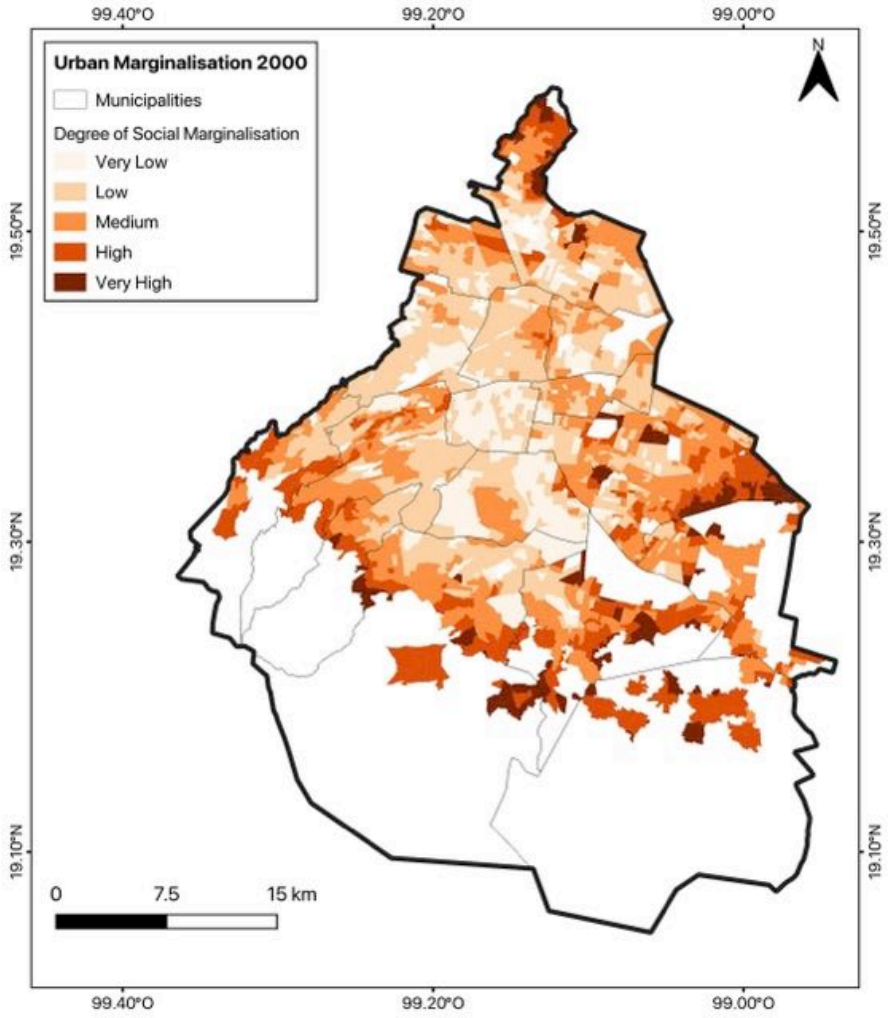

Figure 9.1 Urban Marginalisation Index in 2000

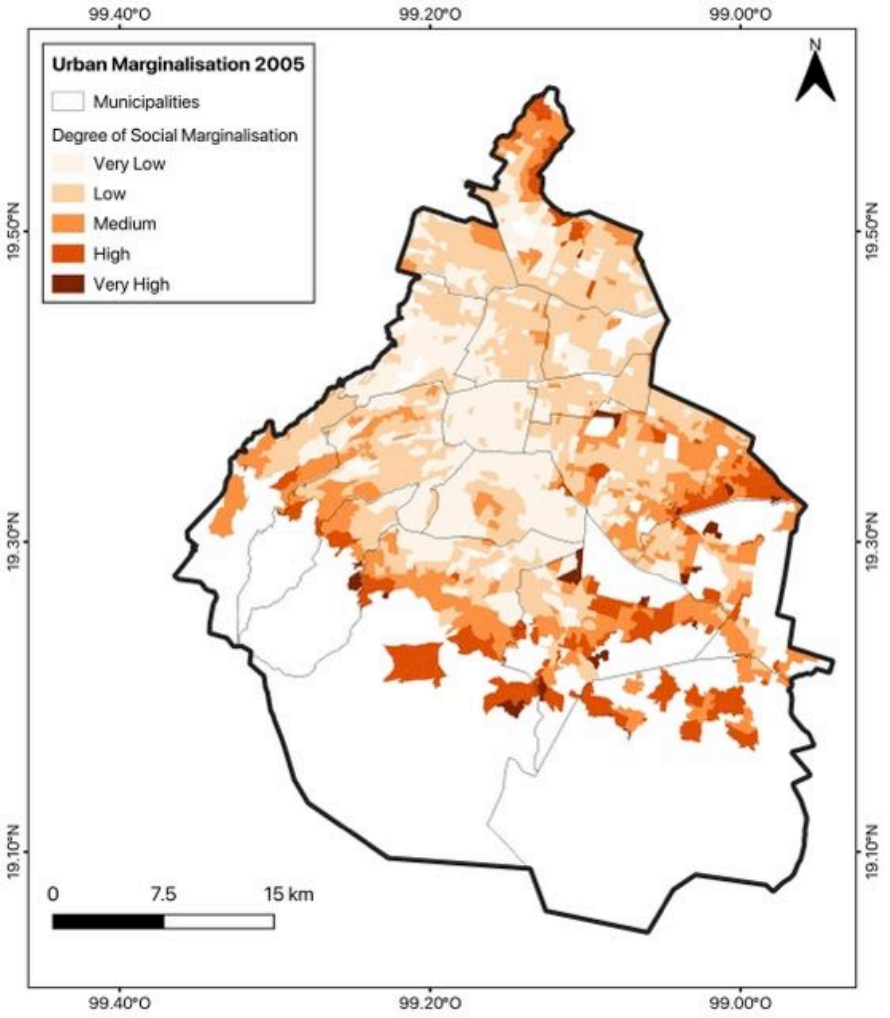

Figure 9.2 Urban Marginalisation Index in 2005

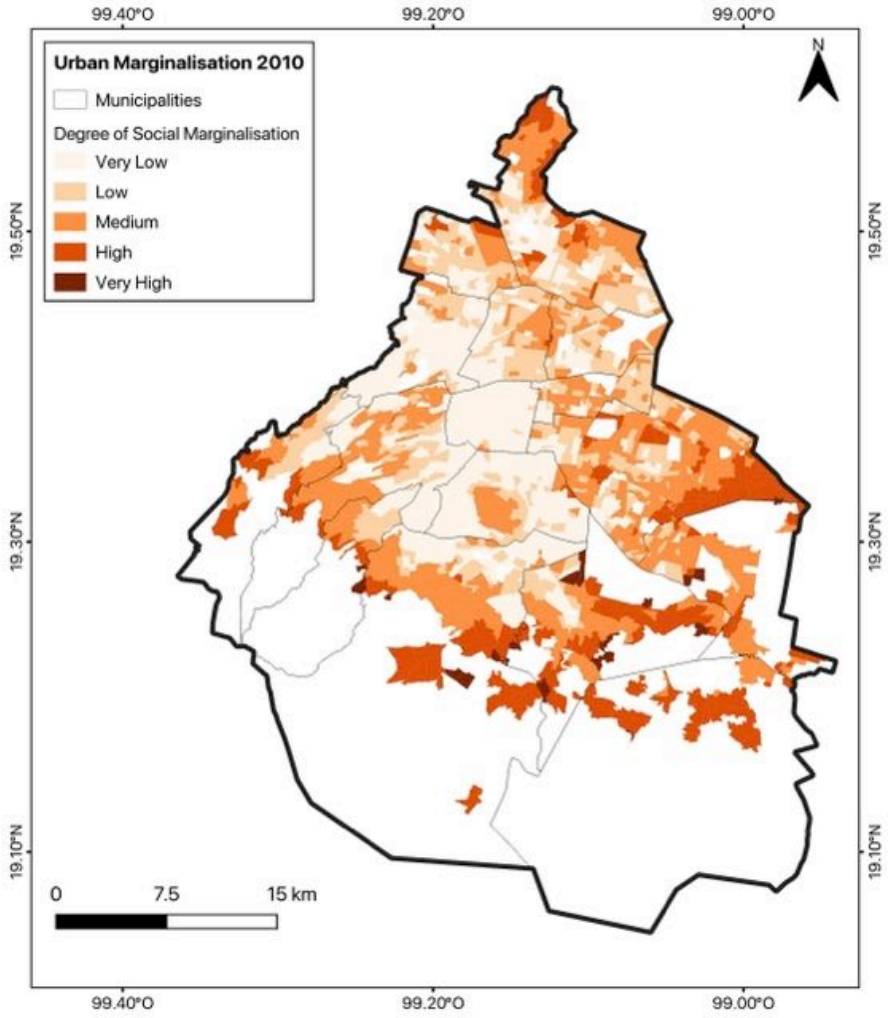

Figure 9.3 Urban Marginalisation Index in 2010

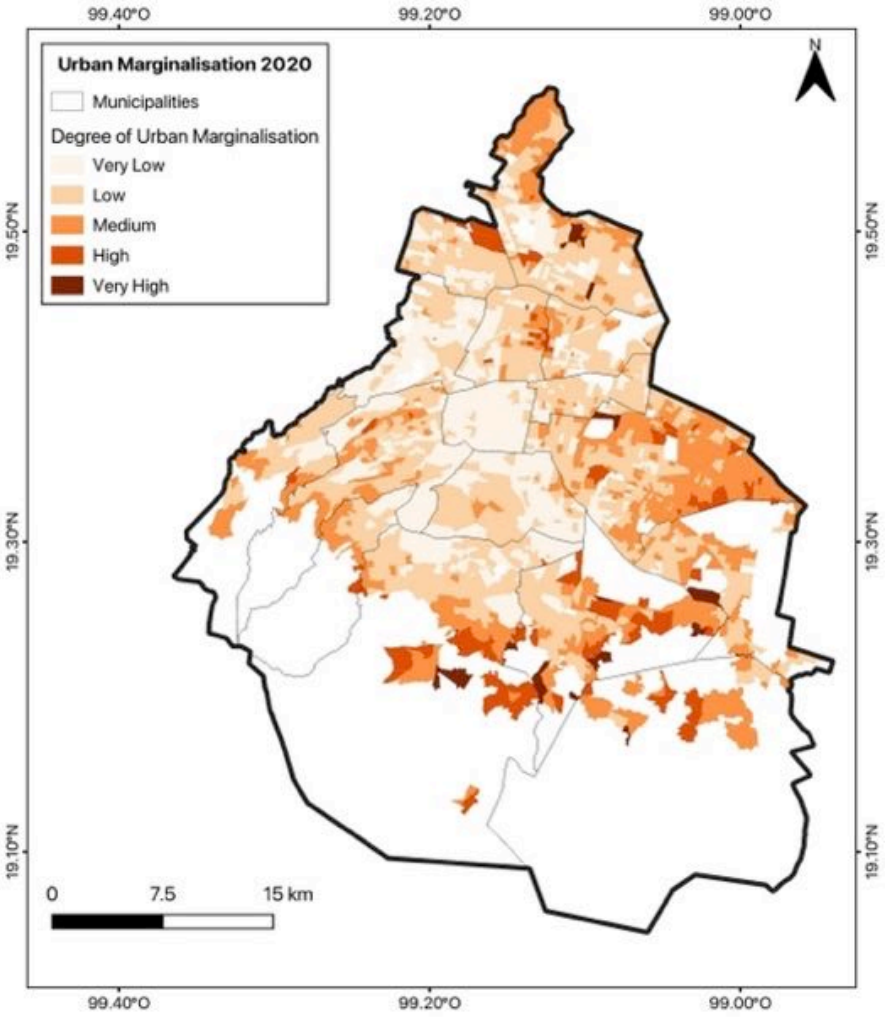

Figure 9.4 Urban Marginalisation Index in 2020

Source: The 2000, 2005 and 2010 layers were self-made with data from CONAPO (2023) and INEGI (2000, 2004, 2010), the layer from 2020 was retrieved from CONAPO (2021b)

Annex III. Poverty Percentages

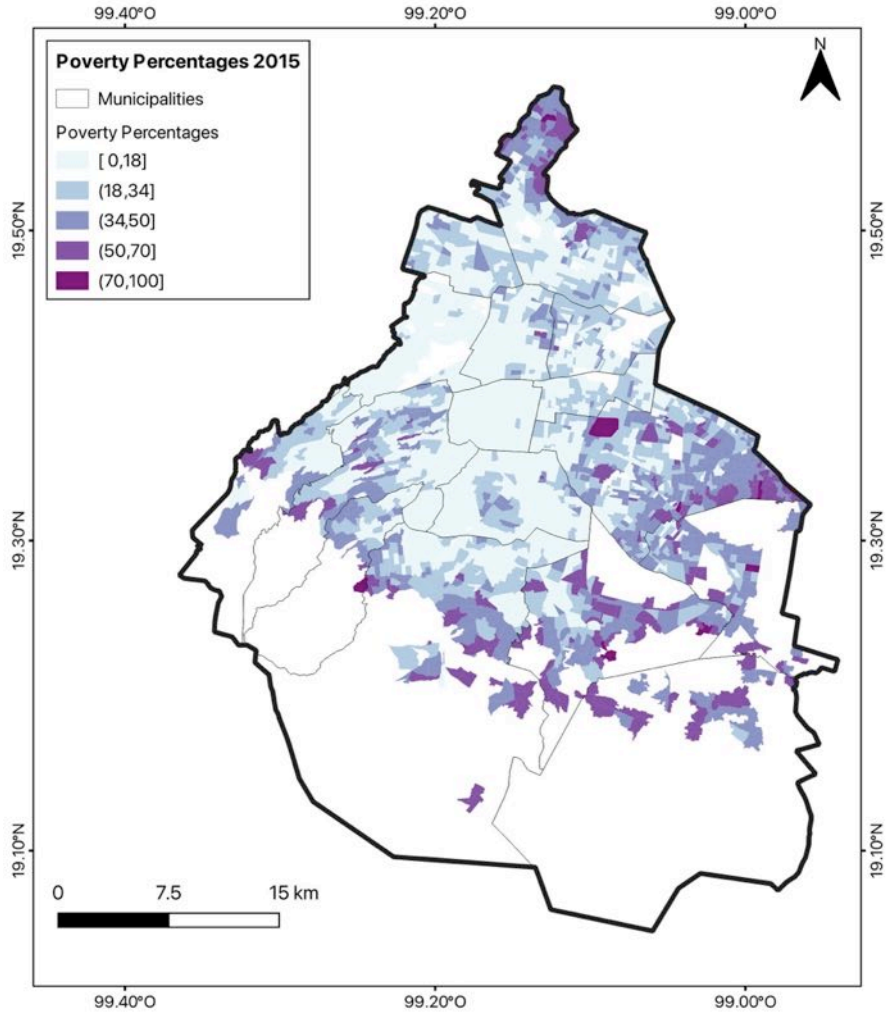

Figure 9.5 Poverty percentages in Mexico City in 2015

Source: Self-made with data from CONEVAL (2018)

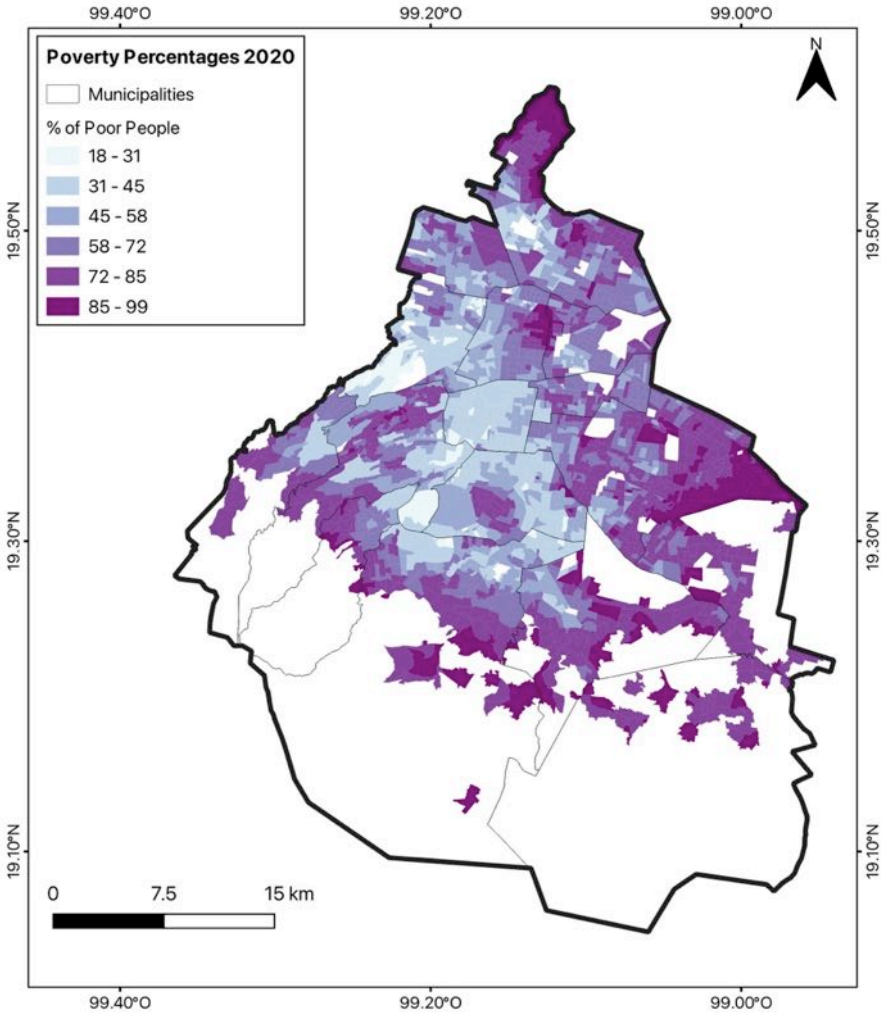

Figure 9.6 Poverty percentages in Mexico City in 2020

Source: Self-made with data from EVALUA (2020)

Annex IV. Air Quality Stations Used for the Interpolations

Table 9.2 Air quality stations used for the interpolations

Pollutant	Year	Stations	
		#	Stations Key
O_3	2000	19	AZC, BJU, CES, CUA, FAC, HAN, LAG, MER, MON, PED, PLA, SAG, TAC, TAH, TAX, TLA, TPN, UIZ, XAL
	2005	18	AZC, CES, CUA, FAC, HAN, LAG, MER, MON, PED, PLA, SAG, SUR, TAC, TAH, TAX, TLA, UIZ, XAL
	2010	22	ACO, AZC, CES, CHO, COY, CUA, FAC, IZT, LAG, MER, MON, PED, PLA, SAG, SUR, TAC, TAH, TAX, TLA, TPN, UIZ, XAL
	2015	25	AJM, AJU, BJU, CAM, CCA, CHO, COY, CUA, CUT, FAC, GAM, HGM, INN, IZT, LLA, MER, MGH, NEZ, PED, SAG, TLA, TPN, UAX, UIZ, XAL
	2020	22	ATI, BJU, CAM, CCA, CUT, FAC, FAR, GAM, INN, MER, MGH, MON, NEZ, PED, SAC, SAG, SFE, TAH, TLA, UAX, UIZ, VIF
CO	2000	21	ARA, ATI, AZC, BJU, CES, FAC, HAN, IMP, LAG, MER, NET, PED, PLA, SAG, TAC, TAX, TLA, TLI, UIZ, VAL, VIF, XAL
	2005	22	ARA, ATI, AZC, CES, FAC, HAN, IMP, LAG, MER, MIN, PED, PLA, SAG, SUR TAC, TAX, TLA, TLI, UIZ, VAL, VIF, XAL
	2010	15	CHO, FAC, IMP, IZT, LAG, MER, PED, SAG, SUR, TAC, TAX, TLA, TLI, UIZ, XAL
	2015	19	AJM, BJU, CAM, CCA, CHO, CUA, FAC, HGM, INN, IZT, MER, MGN, NEZ, PED, SAG, TLA, UAX, UIZ, XAL
	2020	18	ATI, BJU, CAM, FAC, FAR, INN, MER, MGH, NEZ, PED, SAC, SAG, SFE, TAH, TLA, UAX, UIZ, VIF
NOx	2000	16	ATI, AZC, BHU, CES, FAC, HAN, LAG, MER , PED, PLA, SAG, TAC, TAX, TLI, UIZ, VIF
	2005	18	ATI, AZC, CES, FAC, HAN, LAG, MER, PED, PLA, SAG, SUR, TAC, TAX, TLA, TLI, UIZ, VIF, XAL
	2010	16	ATI, AZC, CES, FAC, IZT, LAG, MER, PED, SAG, SUR, TAC, TAX, TLA, TLI, UIZ, XAL
	2015	18	AJM, CAM, CCA, CUA, CUT, FAC, HGM, IZT, MER, MGH, MON, NEZ, PED, SAG, TLA, UAX, UIZ, XAL
	2020	18	ATI, CAM ,CCA, CUT, FAC, MER, MGH, MON, NEZ, PED, SAC, SAG, SFE, TAH, TLA, UAX, UIZ, VIF
SO_2	2000	25	ARA, ATI, AZC, BJU, CES, FAC, HAN, LAG, LPR, LVI, MER, NET PED, PLA, SAG, SUR, TAC, TAH, TAX, TLA, TLI, UIZ, VAL VIF, XAL
	2005	23	ARA, ATI, AZC, BJU, CES, HAN, LAG, LPR, LVI, MER, PED, PLA, SAG, SUR, TAC, TAH, TAX TLA, TLI, UIZ, VAL, VIF, XAL
	2010	21	ACO, ATI, AZC, CES, CHO, FAC, IZT, LAG, LVI, MER, PED, PLA, SAG, SUR, TAC, TAH, TAX, TLA, TLI, UIZ, XAL
	2015	18	AJM, CAM, CCA, CHO, CUT, FAC, HGM, IZT, LLA, MER, MGH, NEZ, PED, SAG, TLA, UAX, UIZ, XAL
	2020	19	ATI, BJU, CAM, CCA, CUT, FAC, FAR, INN, MER, MGH, MON, NEZ, PED, SFE, TAH, TLA, UAX, UIZ, VIF
PM_{10}	2000	10	CES, LVI, MER, NET, PED, TAH, TLA, TLI, VIF, XAL
	2005	13	CES, FAC, HAN, LVI, MER, PED, PLA, SAG, SUR, TAX, TLA, VIF, XAL
	2010	13	CES, FAC, IZT, LVI, MER , PED, SAG, SUR, TAH, TAX, TLA, TLI, XAL
	2015	16	AJM, BJU, CAM, CHO, CUA, CUT, FAC, HGM, IZT, MER, MGH, PED, SAG, SUR, TLA, UIZ
	2020	13	ATI, BJU, CAM, CUT, FAC, INN, MER, PED, SAG, SFE, TLA, UIZ, VIF
$PM_{2.5}$	2005	8	CAM, COY, MER, PER, SAG, SJA, TLA, UIZ

Pollutant	Year	Stations	
		#	Stations Key
	2010	8	ACO, CAM, COY, PER, SAG, SJA, TLA, UIZ
	2015	14	BJU, CAM, CCA, FAR, INN, MER, NEZ, PED, SAC, SAG, SFE, TLA, UAX, UIZ
	2020	14	BJU, CAM, CCA, FAR, INN, MER, NEZ, PED, SAC, SAG, SFE, TLA, UAX, UIZ

Annex V. Air Pollutant Interpolations

Ozone (O_3)

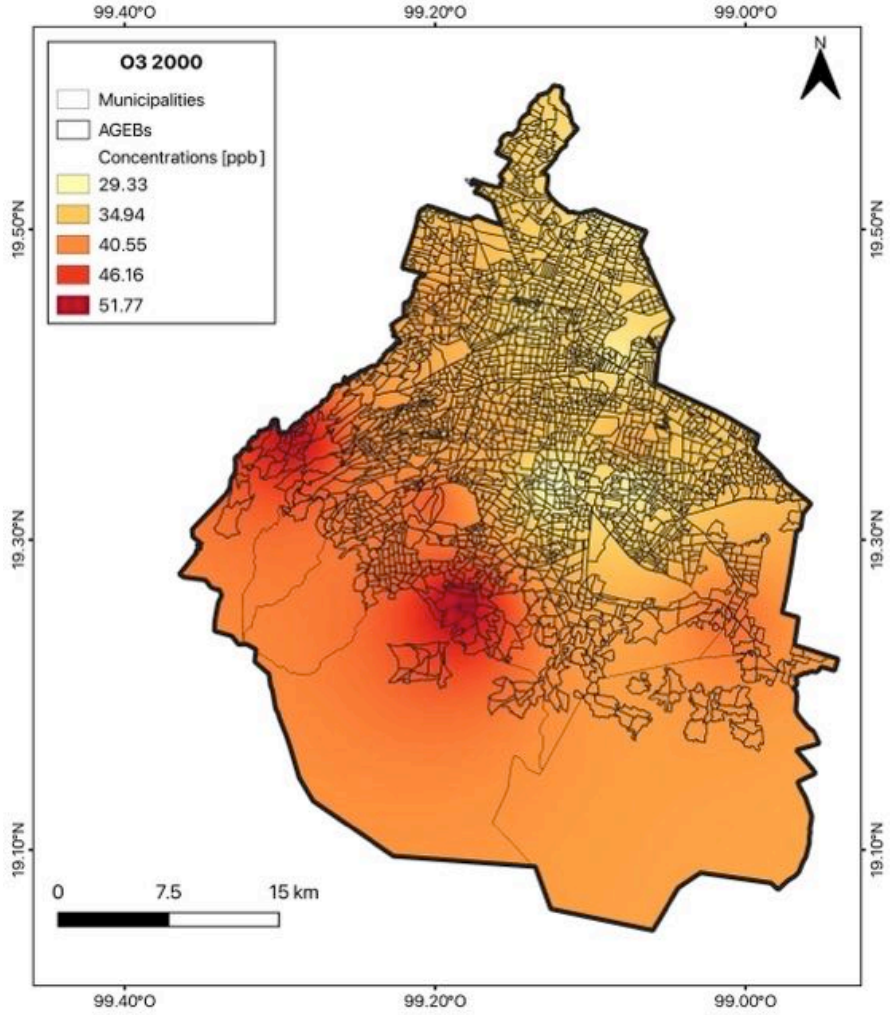

Figure 9.7 Average O_3 concentrations in 2000

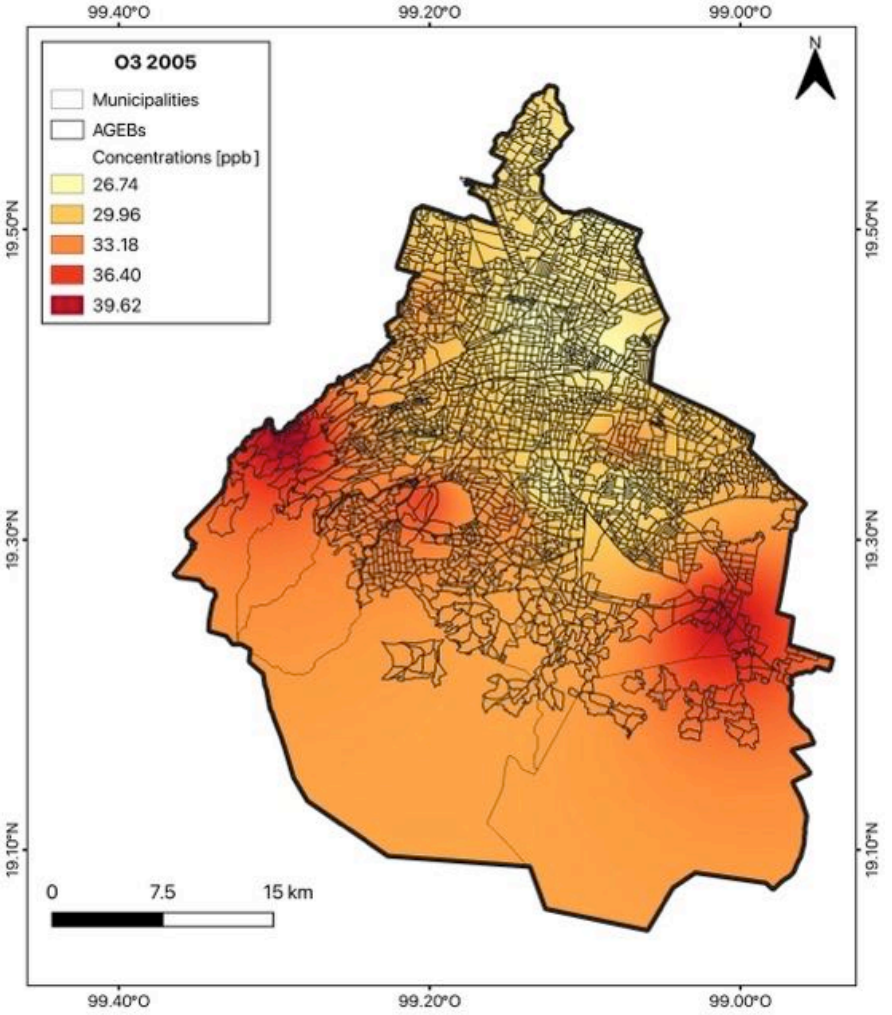

Figure 9.8 Average O_3 concentrations in 2005

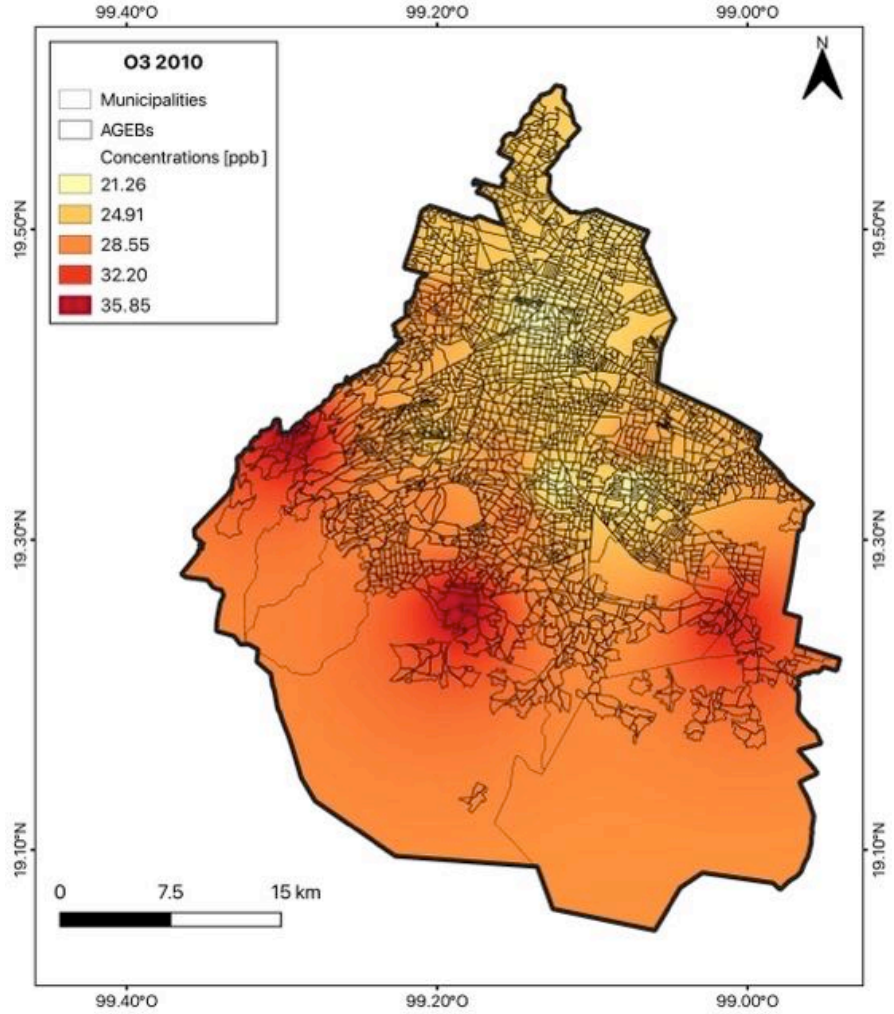

Figure 9.9 Average O3 concentrations in 2010

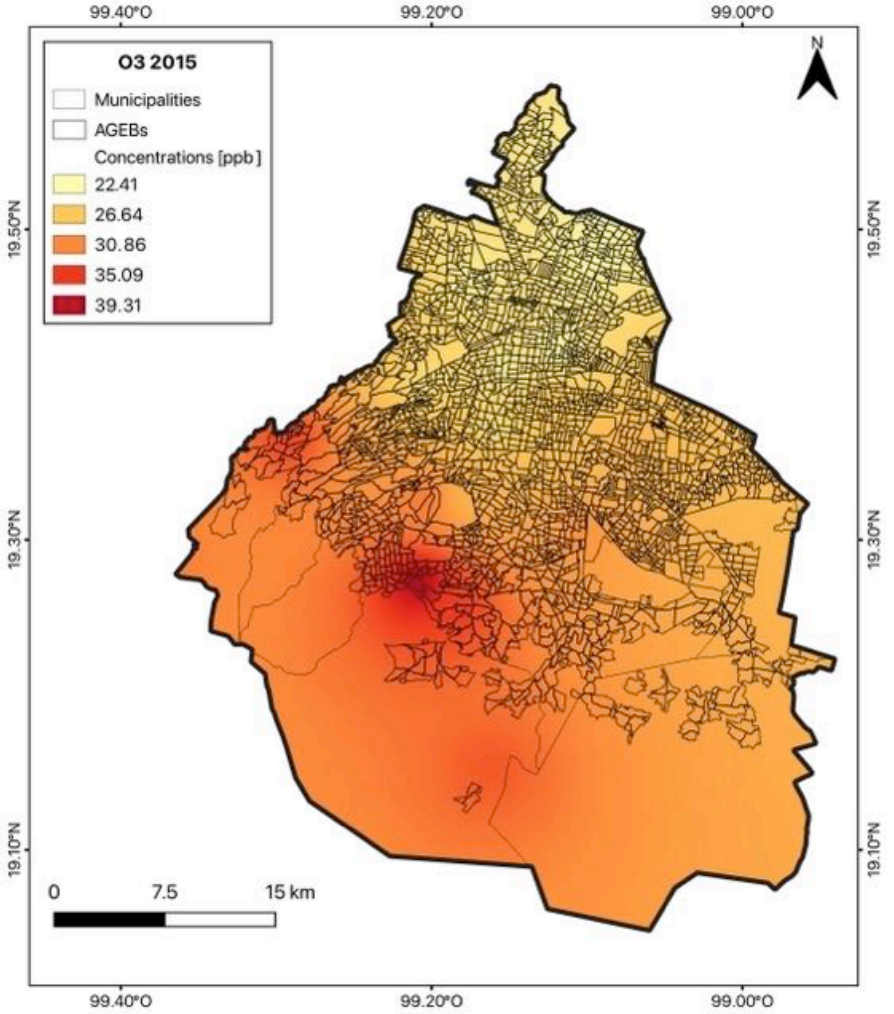

Figure 9.10 Average O_3 concentrations in 2015

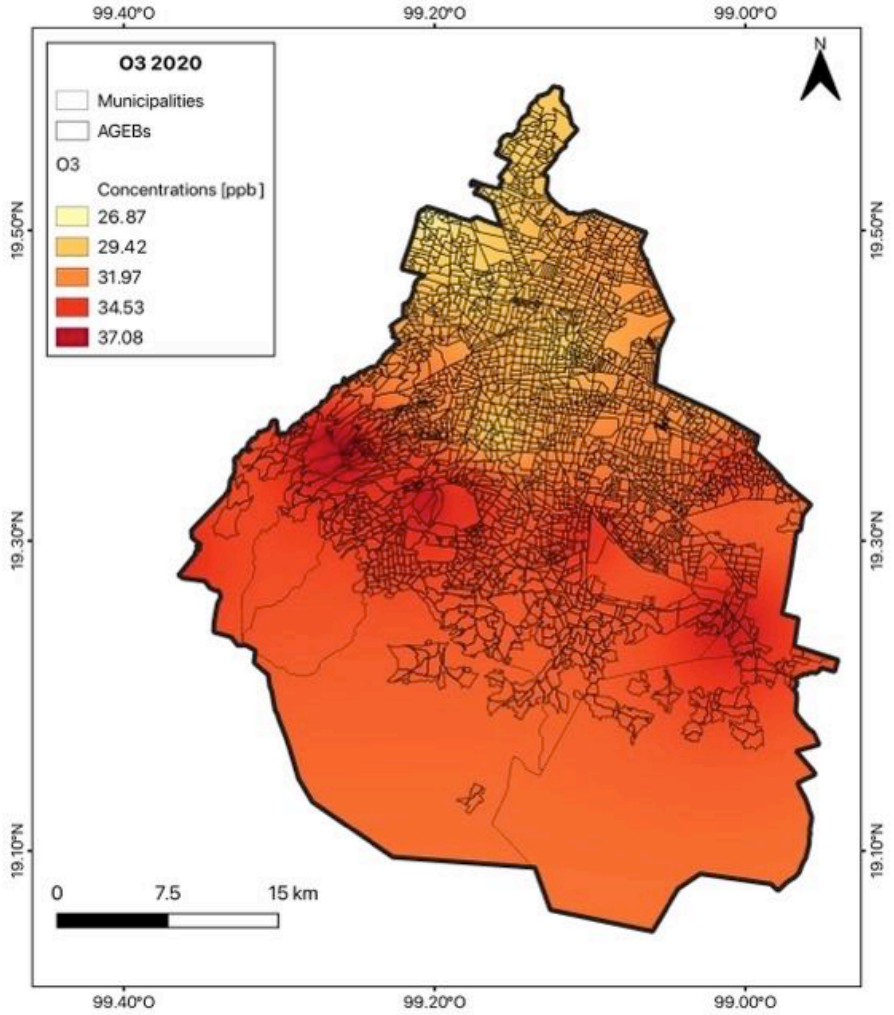

Figure 9.11 Average O3 concentrations in 2020

Carbon Monoxide (CO)

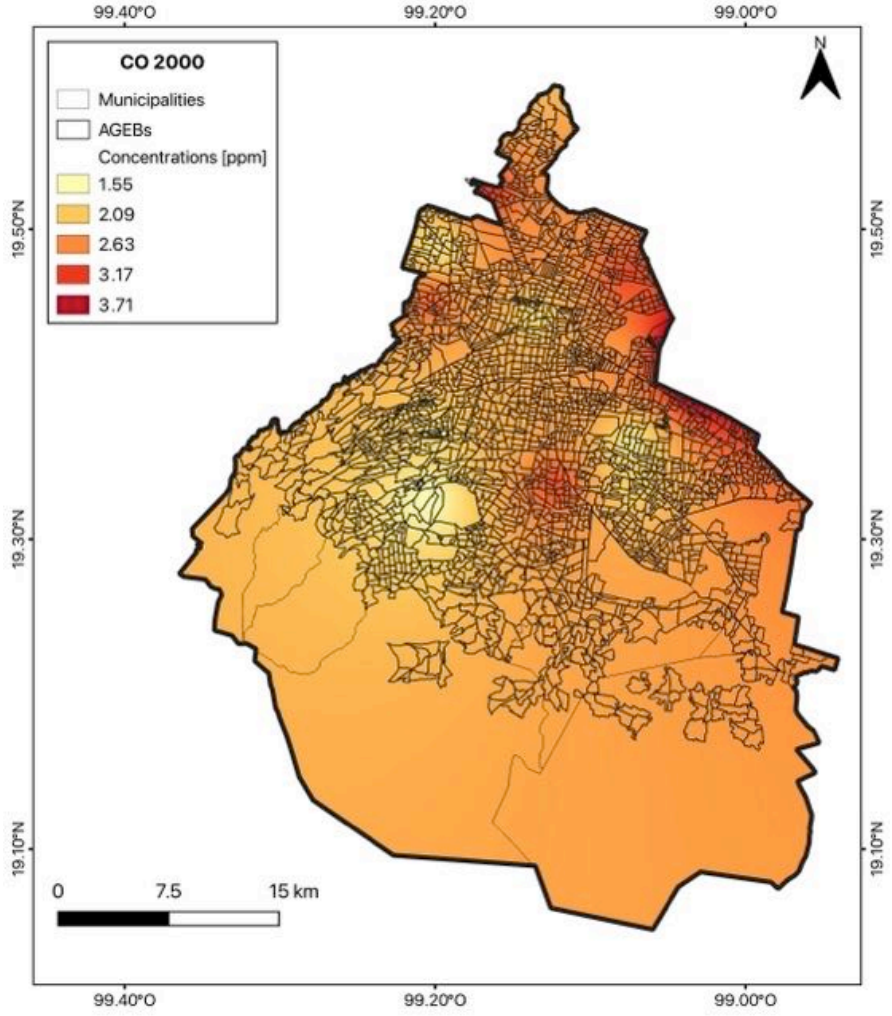

Figure 9.12 Average CO concentrations in 2000

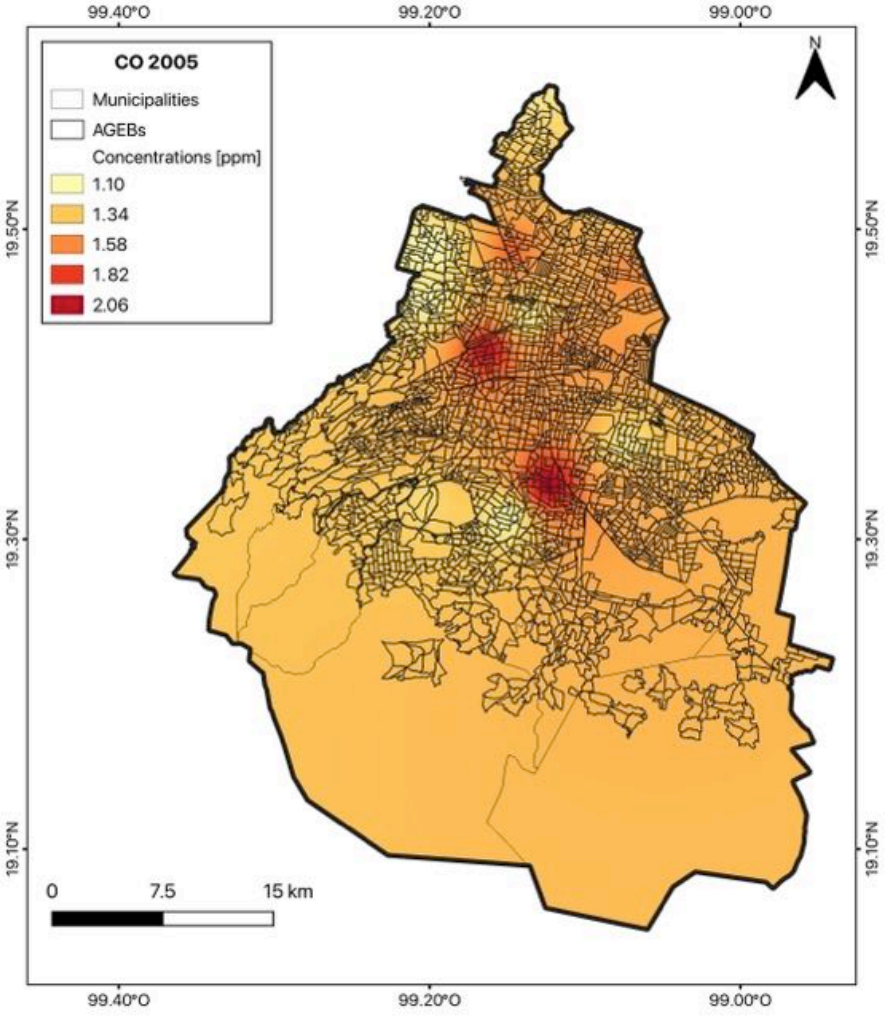

Figure 9.13 Average CO concentrations in 2005

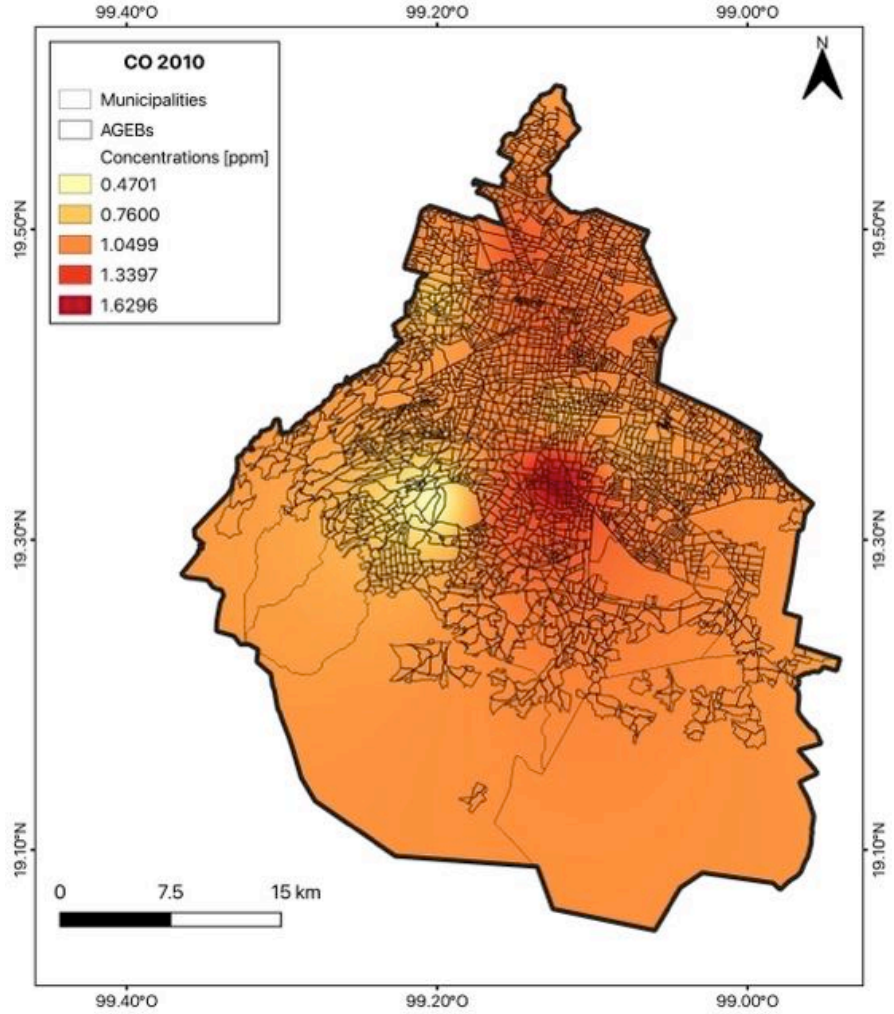

Figure 9.14 Average CO concentrations in 2010

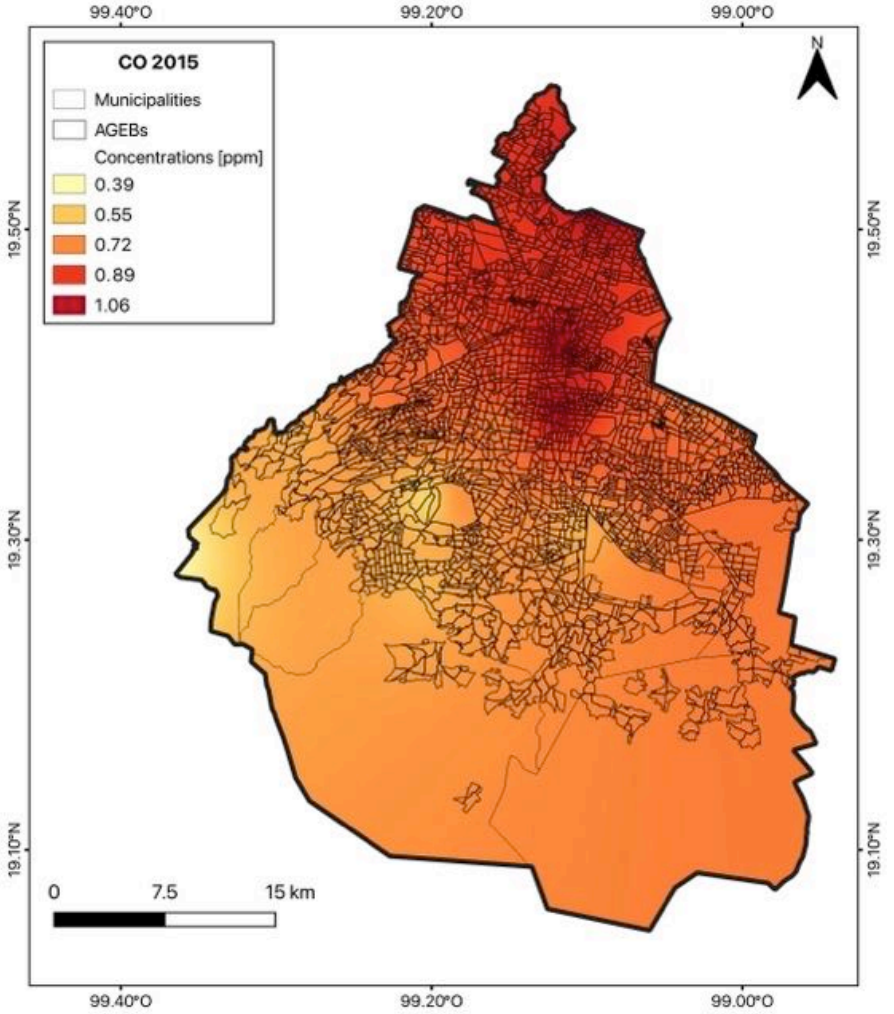

Figure 9.15 Average CO concentrations in 2015

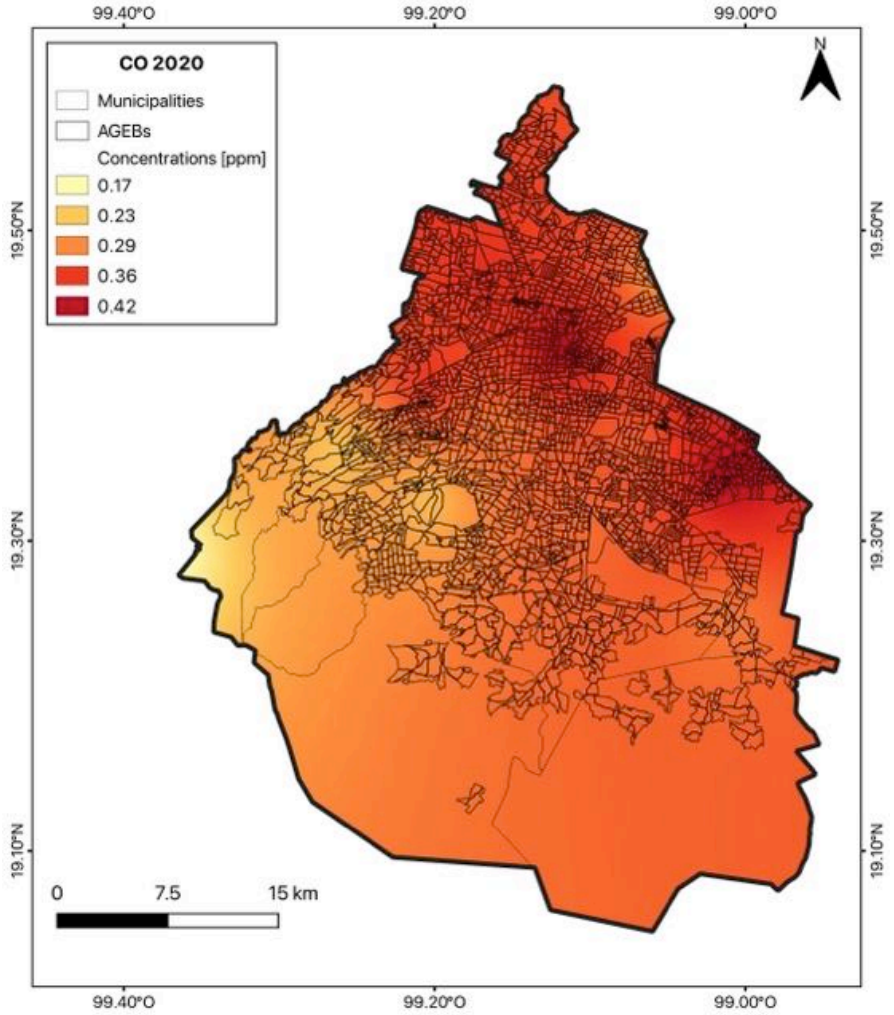

Figure 9.16 Average CO concentrations in 2020

Nitrogen Oxides (NOx)

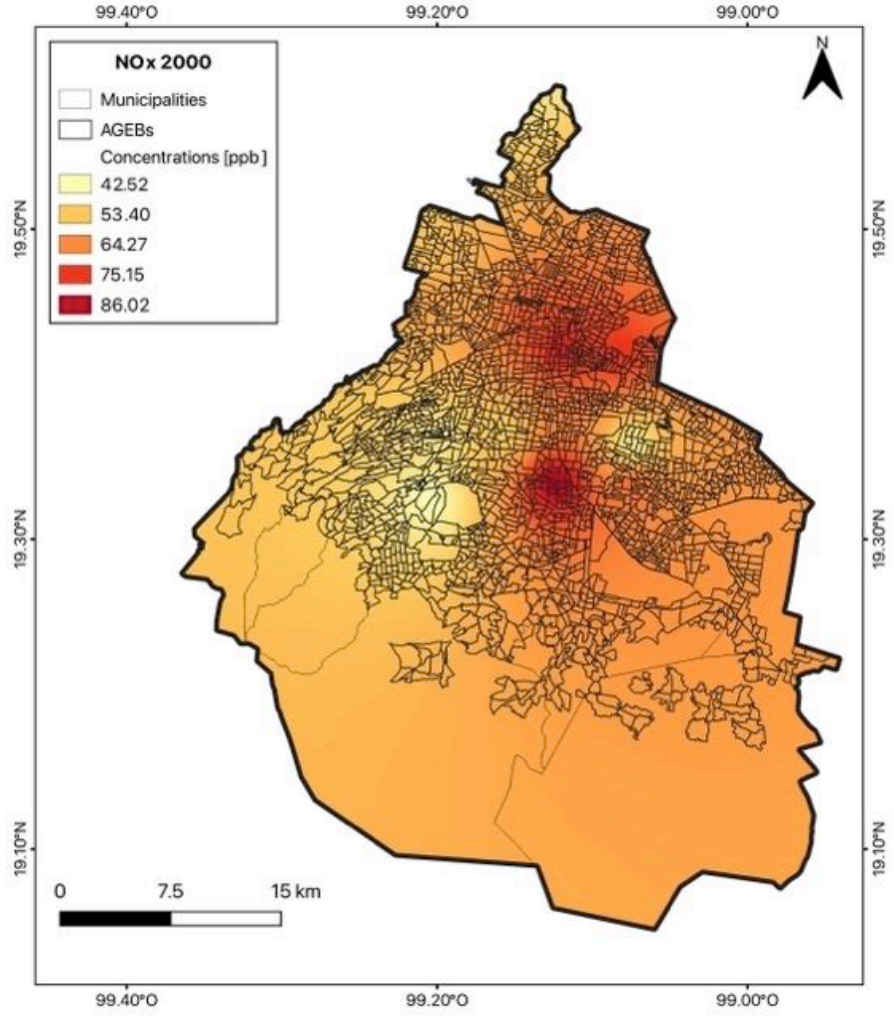

Figure 9.17 Average NOx concentrations in 2000

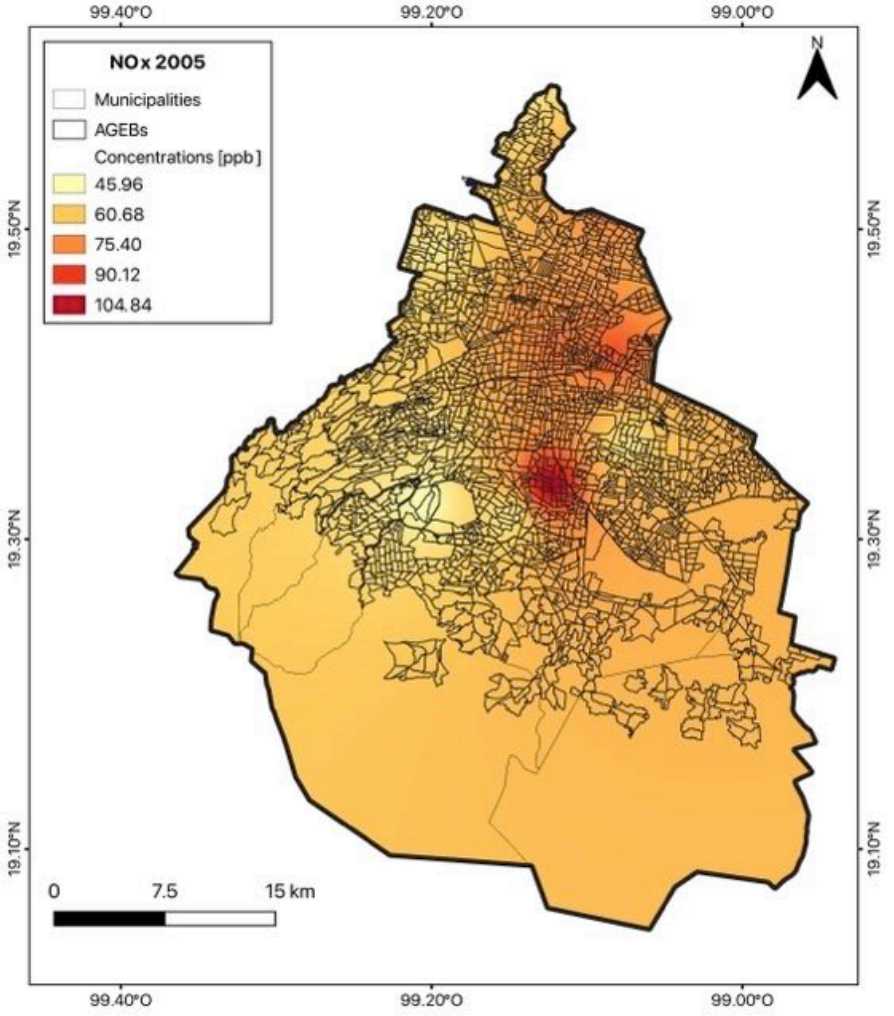

Figure 9.18 Average NOx concentrations in 2005

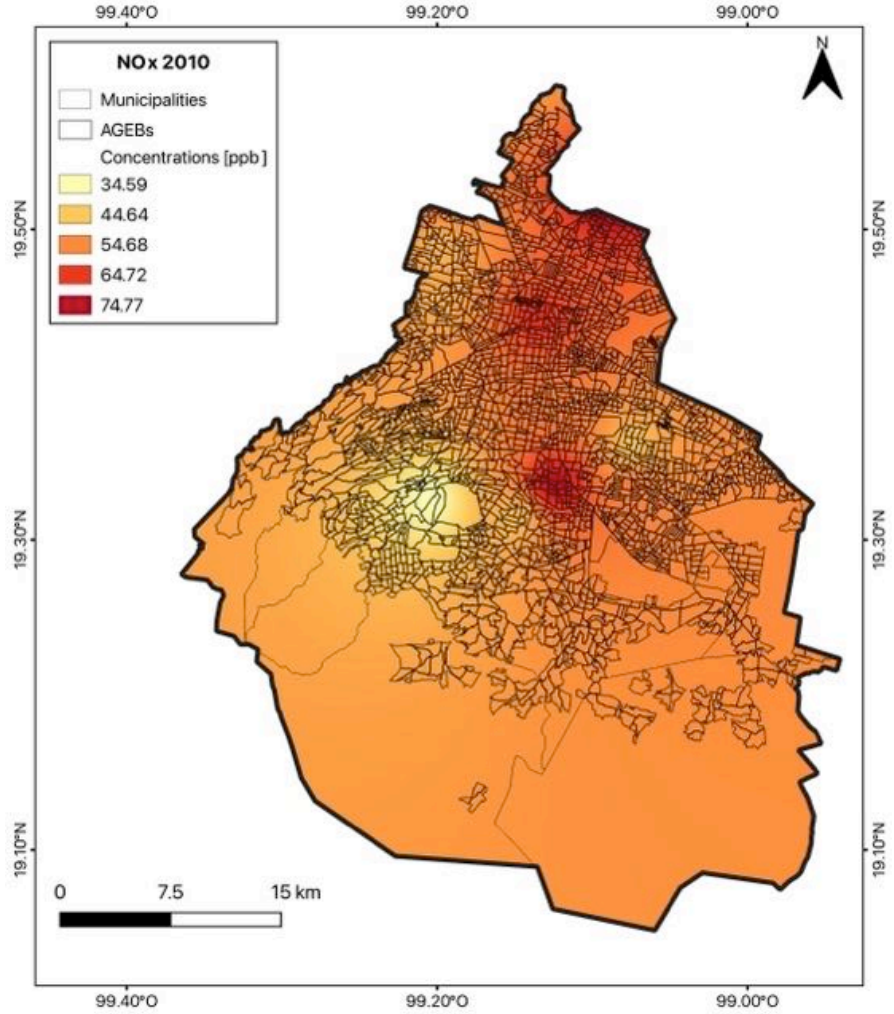

Figure 9.19 Average NOx concentrations in 2010

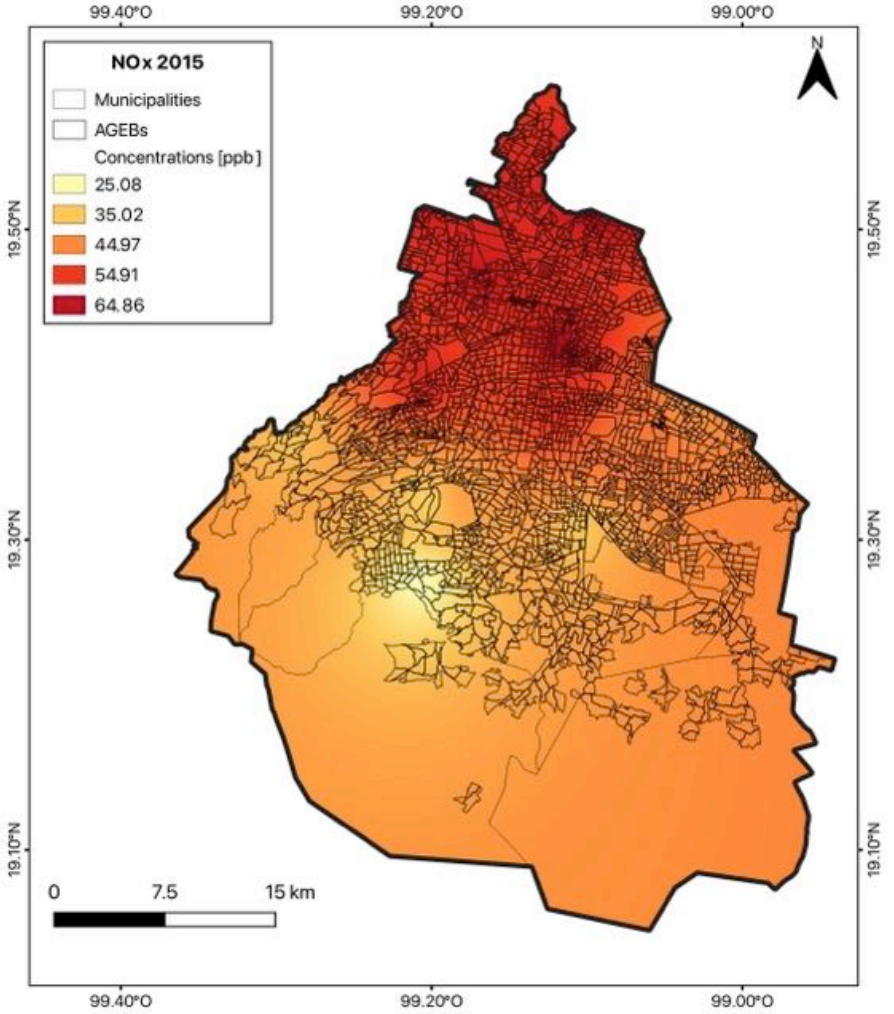

Figure 9.20 Average NOx concentrations in 2015

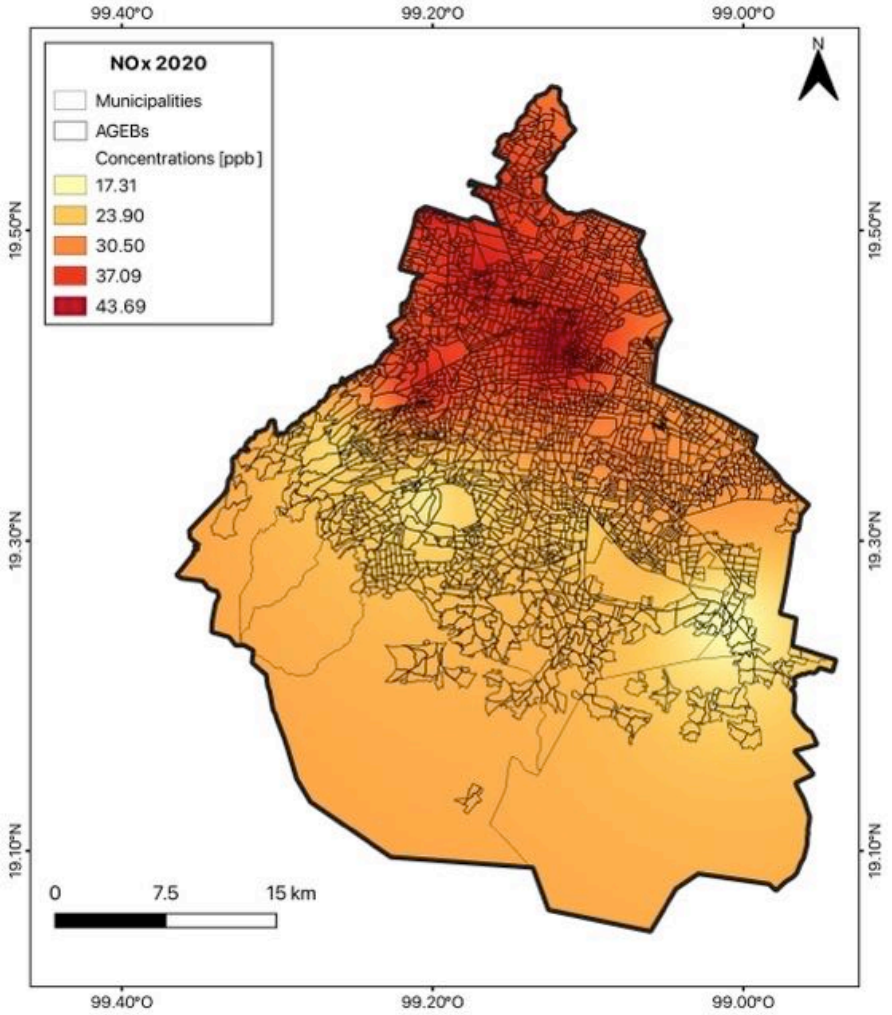

Figure 9.21 Average NOx concentrations in 2020

Sulphur Dioxide (SO_2)

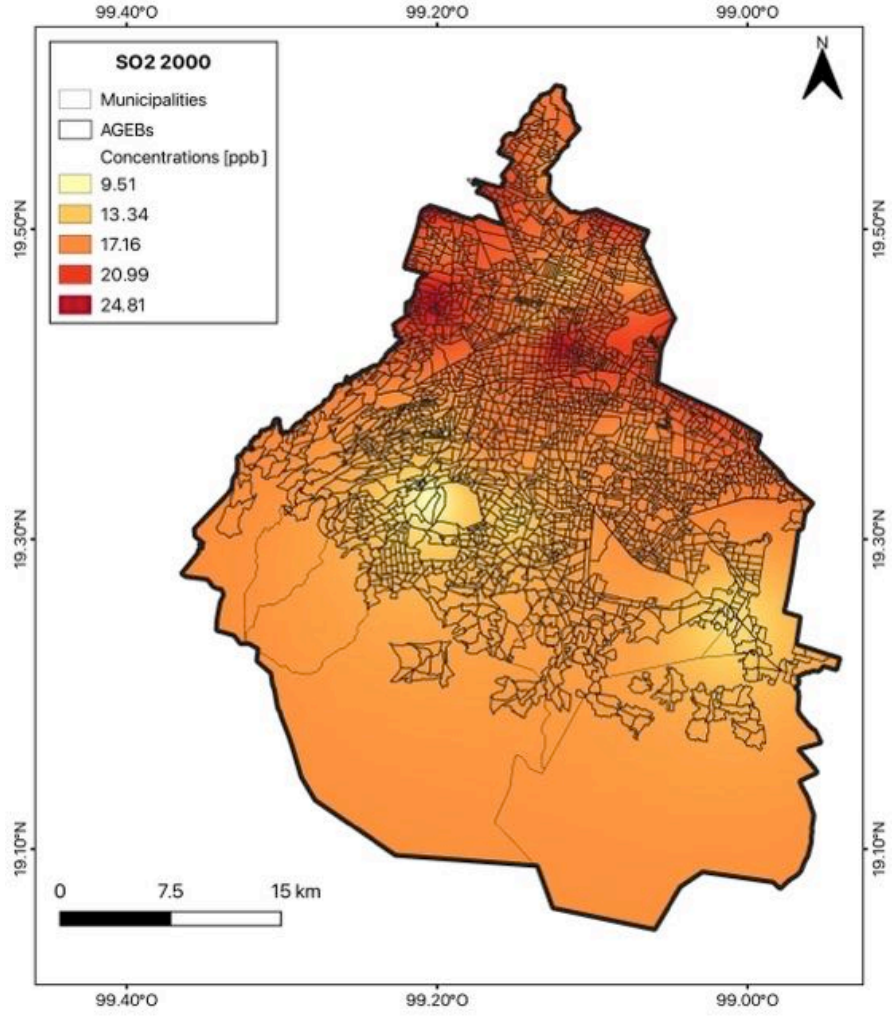

Figure 9.22 Average SO_2 concentrations in 2000

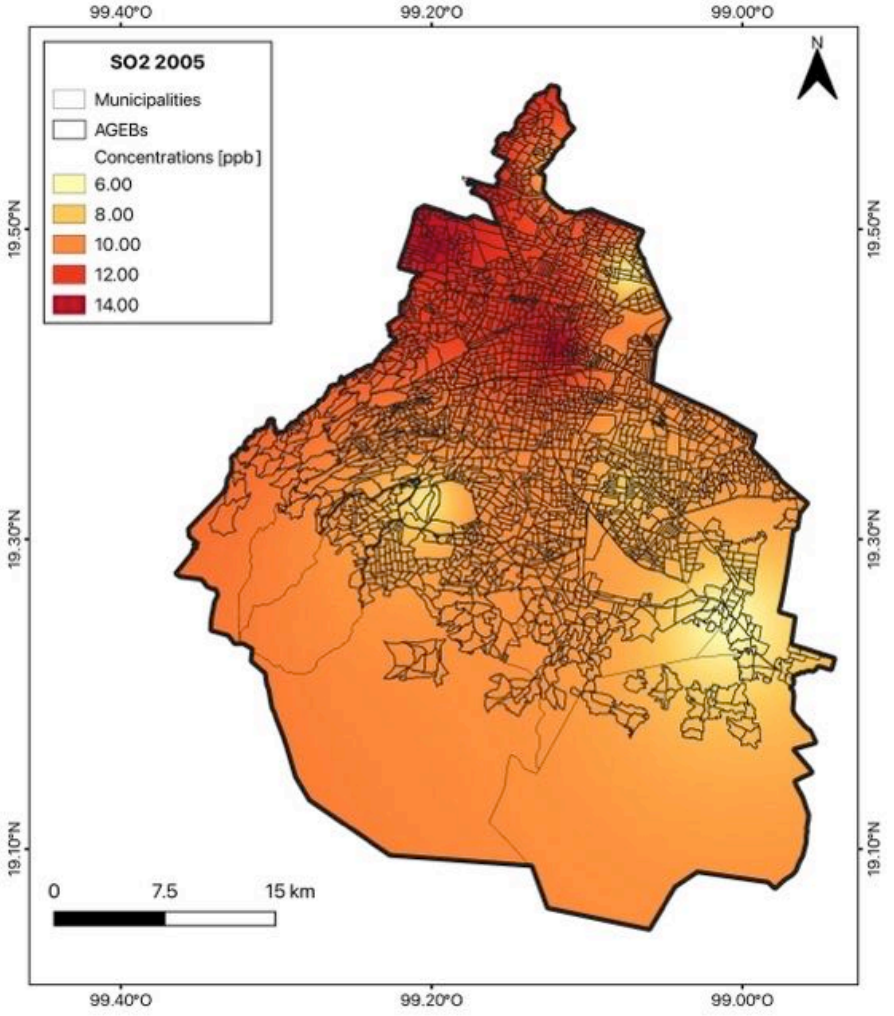

Figure 9.23 Average SO_2 concentrations in 2005

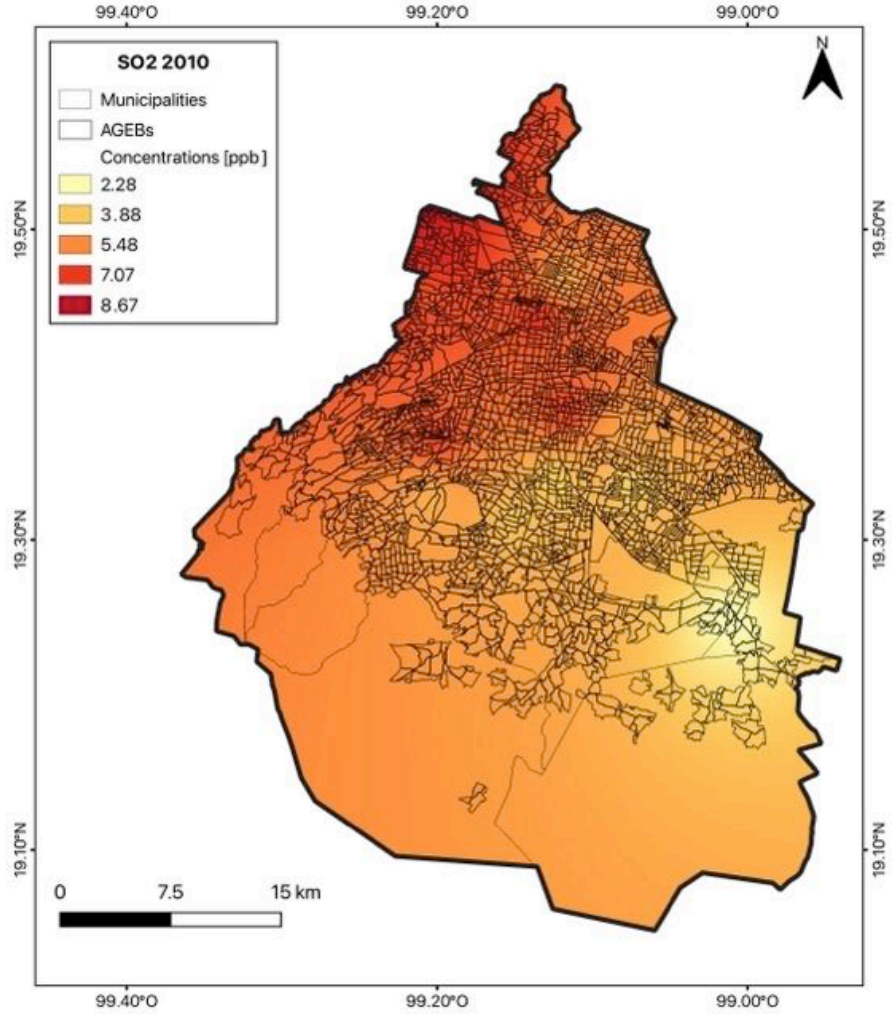

Figure 9.24 Average SO_2 concentrations in 2010

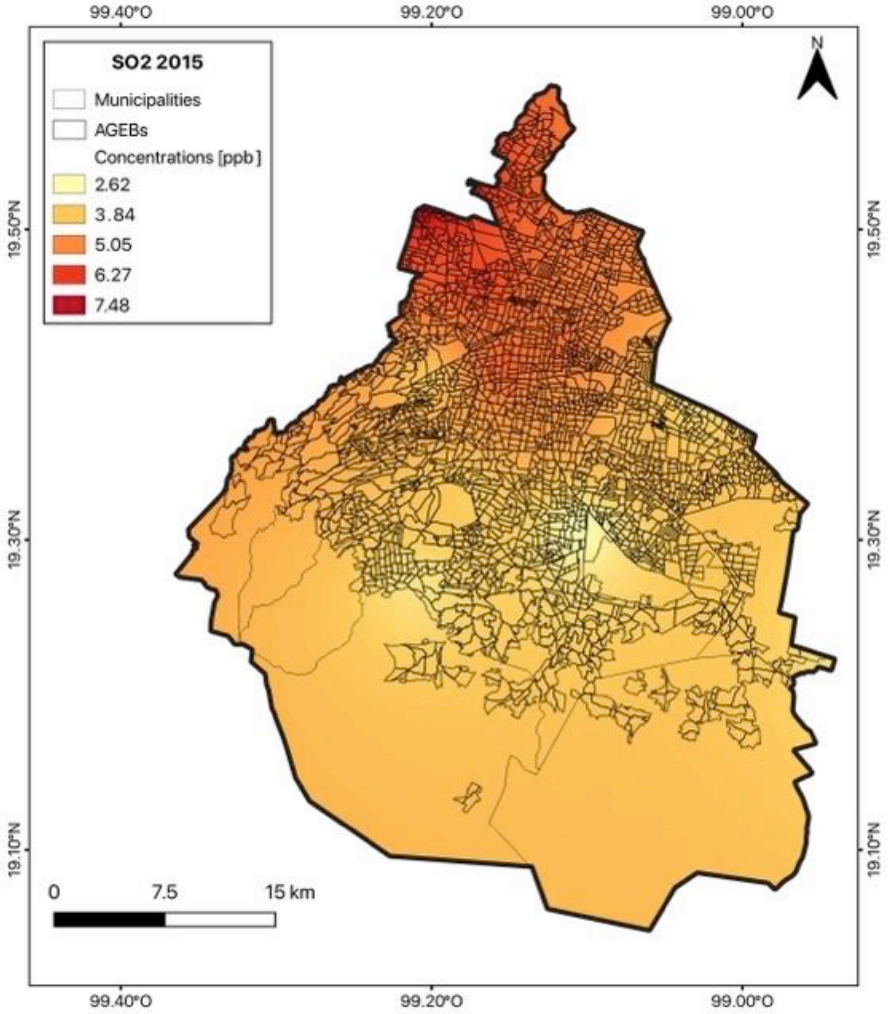

Figure 9.25 Average SO_2 concentrations in 2015

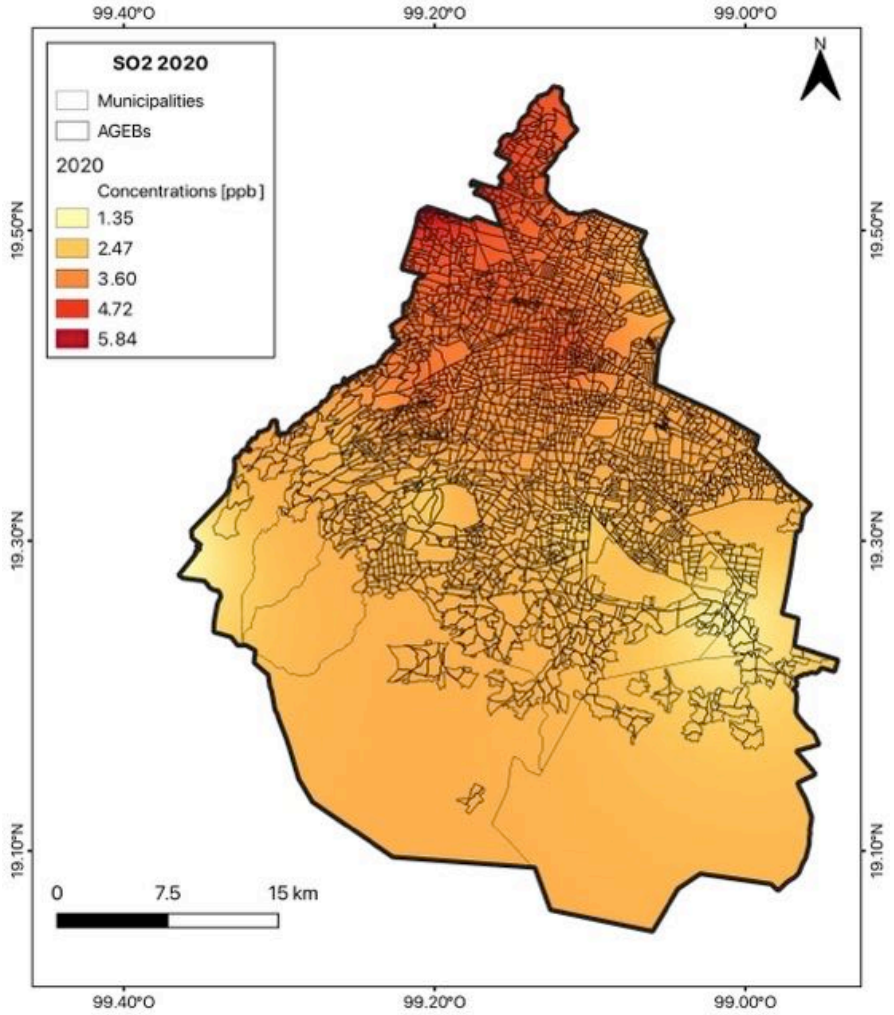

Figure 9.26 Average SO_2 concentrations in 2020

Particulate Matter (PM_{10})

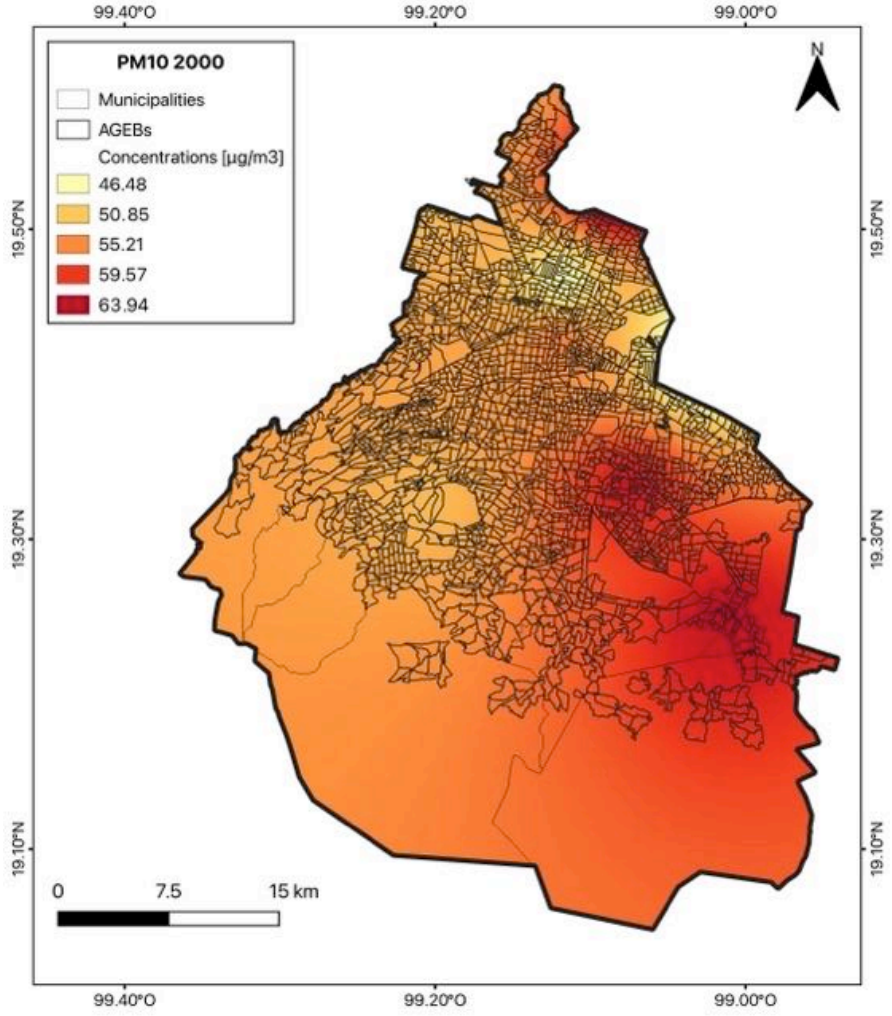

Figure 9.27 Average PM_{10} concentrations in 2000

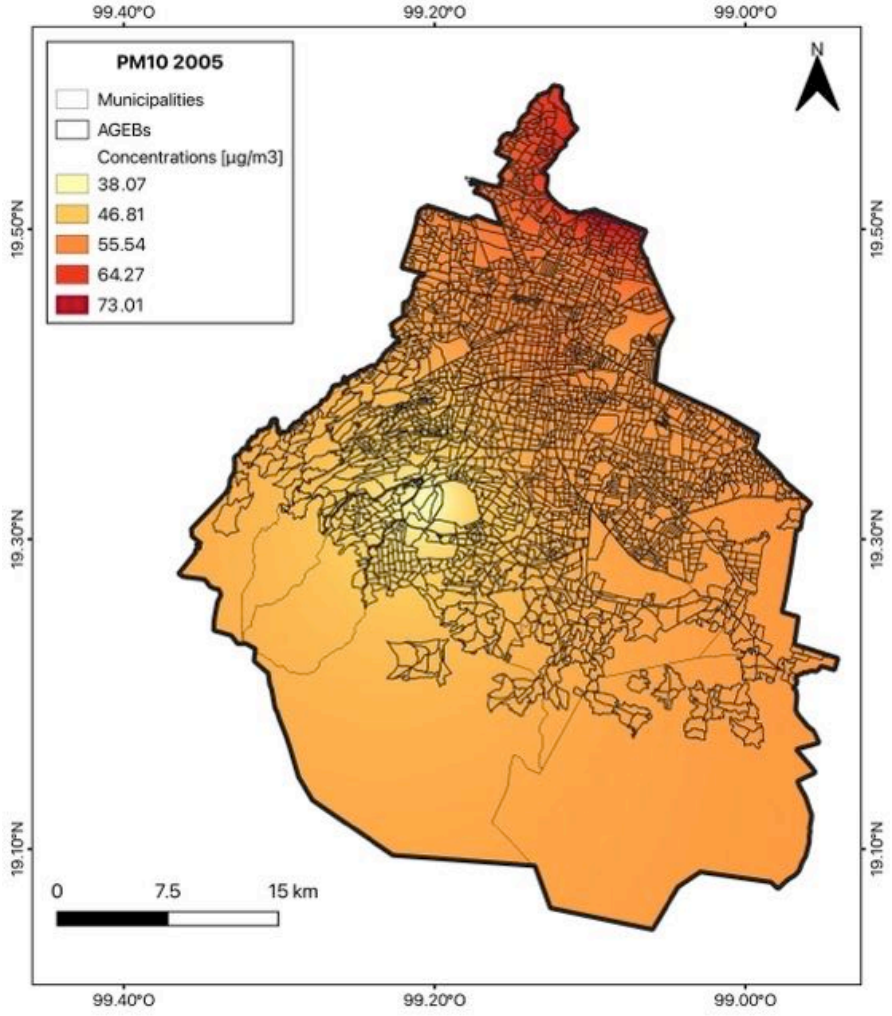

Figure 9.28 Average PM_{10} concentrations in 2005

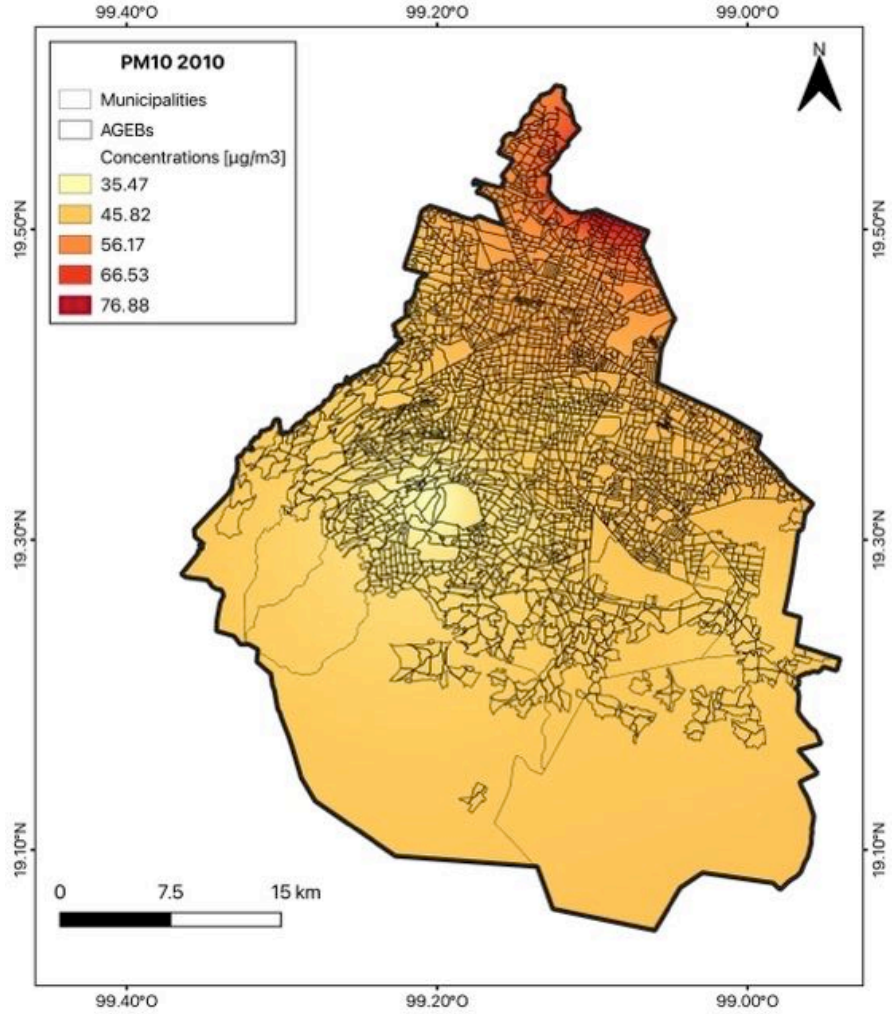

Figure 9.29 Average PM_{10} concentrations in 2010

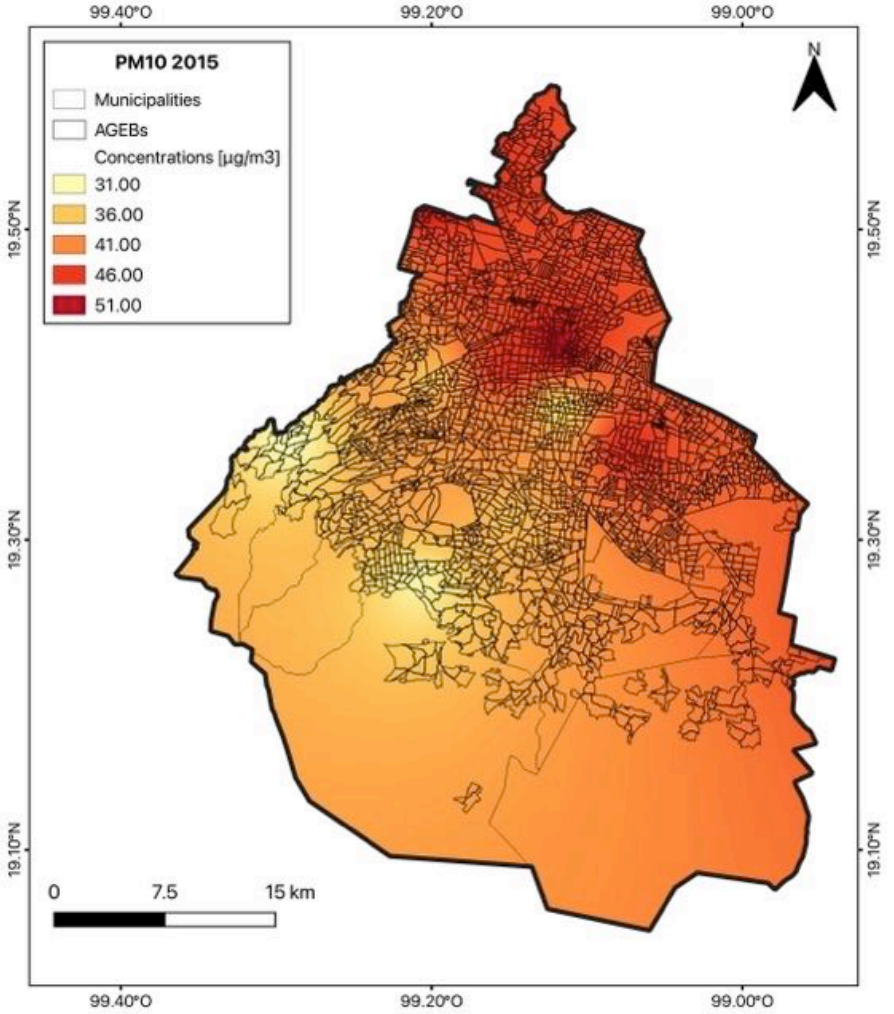

Figure 9.30 Average PM_{10} concentrations in 2015

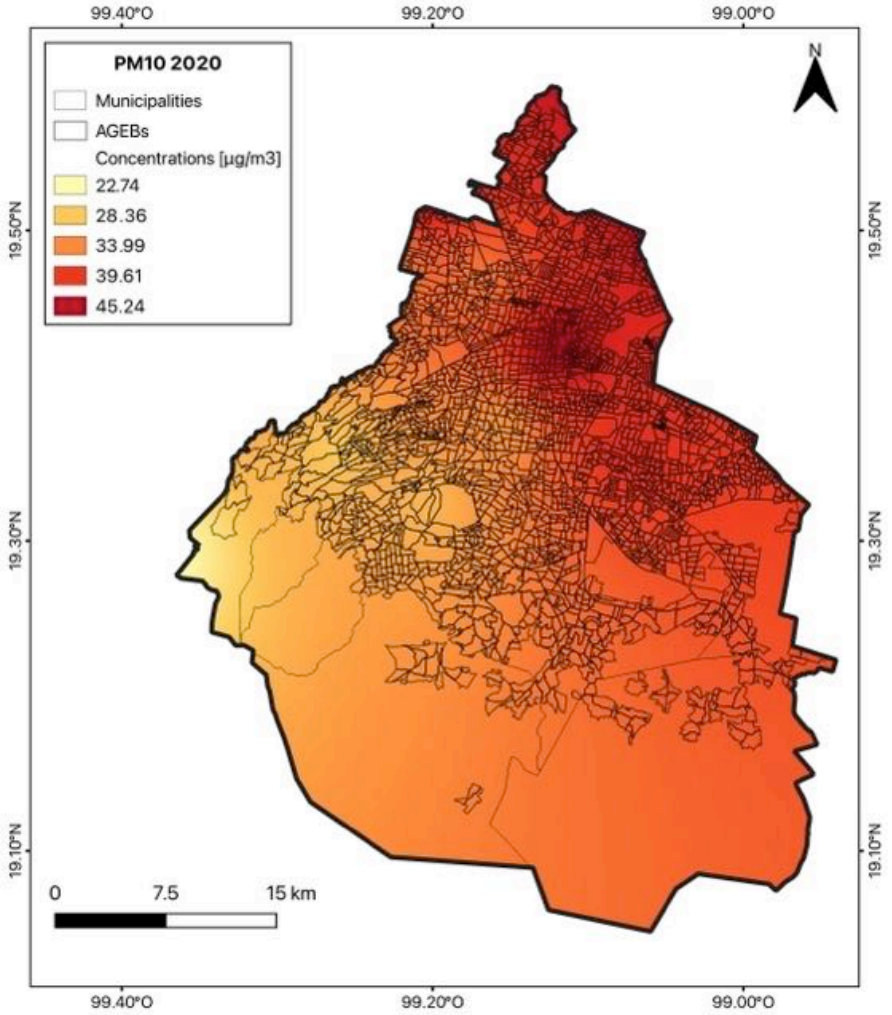

Figure 9.31 Average PM_{10} concentrations in 2020

Particulate Matter ($PM_{2.5}$)

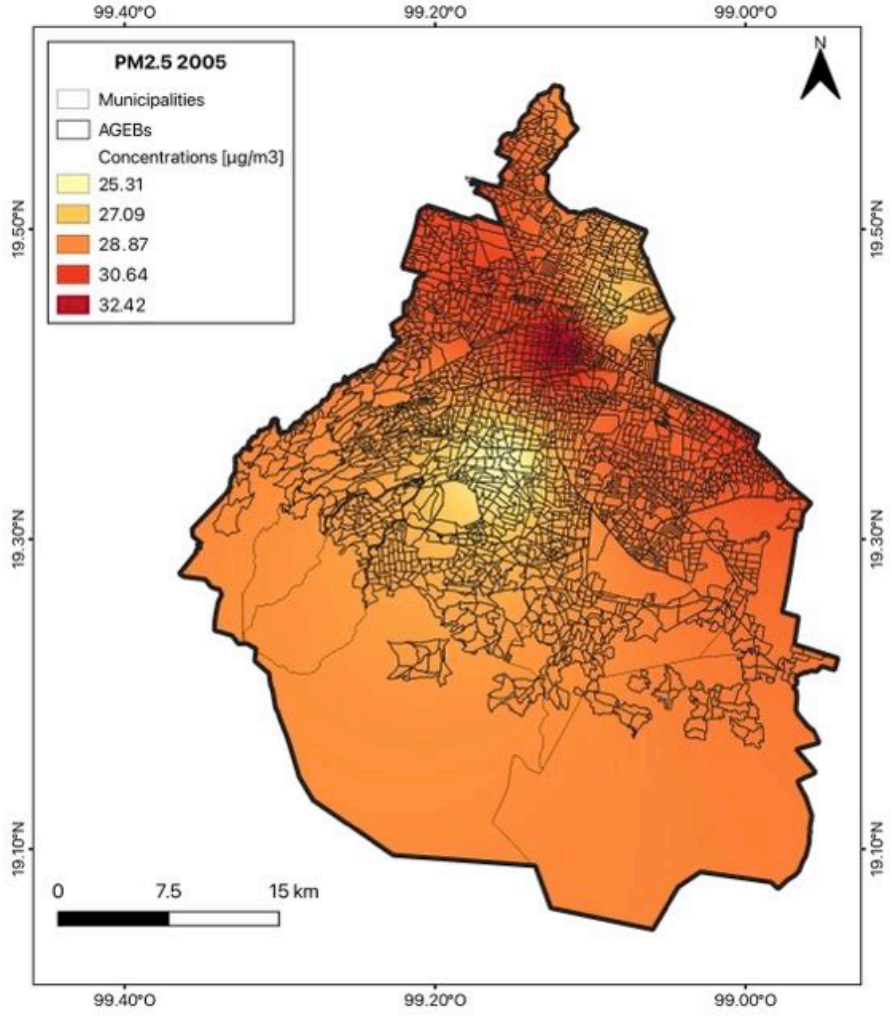

Figure 9.32 Average $PM_{2.5}$ concentrations in 2005

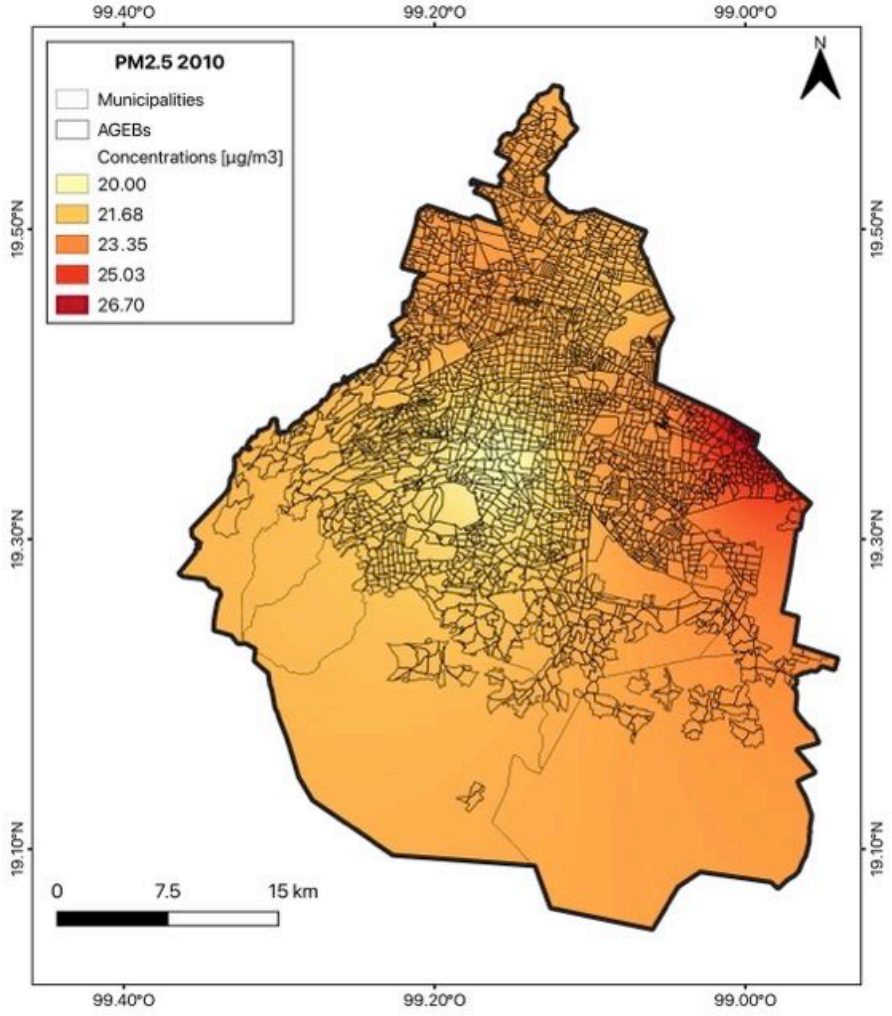

Figure 9.33 Average $PM_{2.5}$ concentrations in 2010

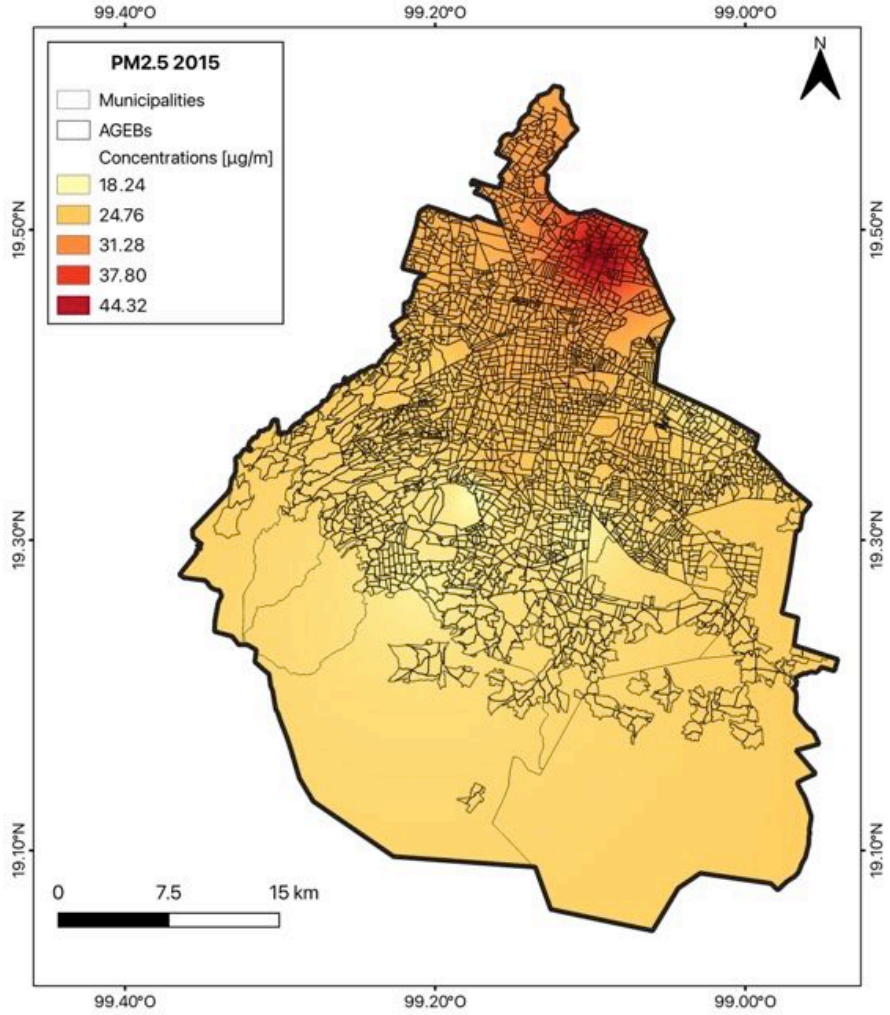

Figure 9.34 Average $PM_{2.5}$ concentrations in 2015

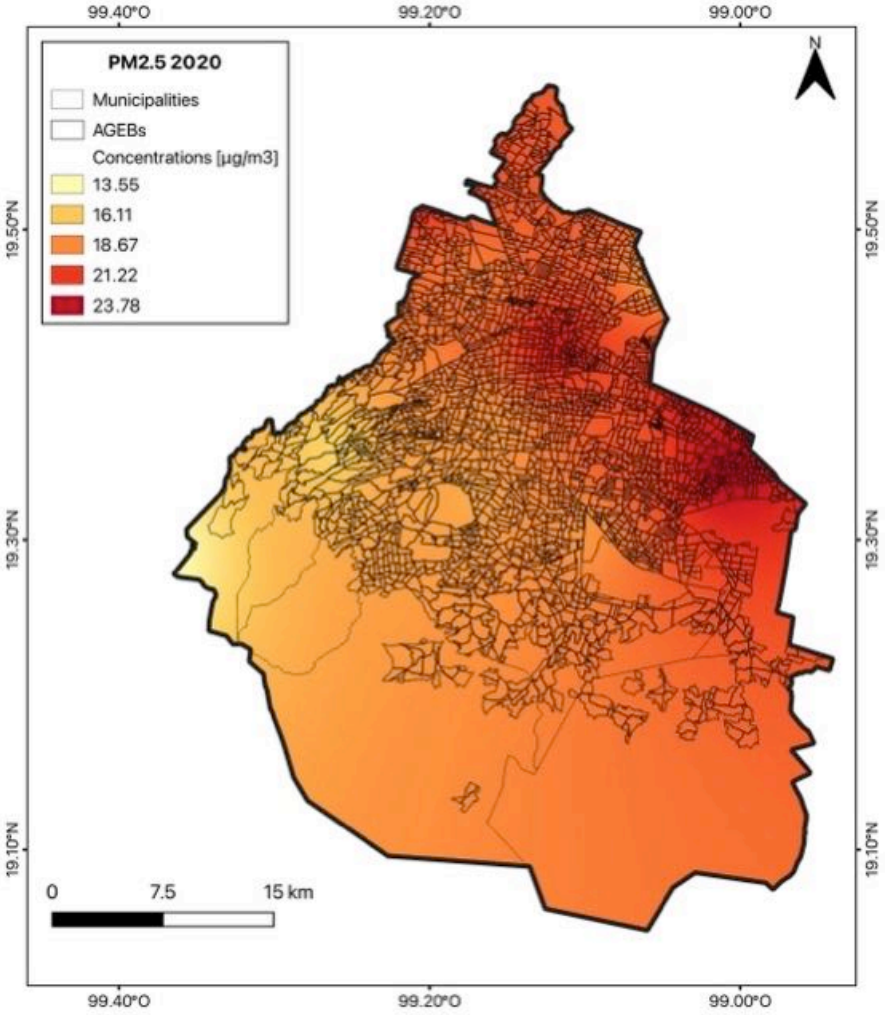

Figure 9.35 Average $PM_{2.5}$ concentrations in 2020

Annex VI. Spatial Lag Model – Maximum Likelihood Estimation

Ordinary Least Squares Estimation (Urban Marginalisation Index 2000)

```
REGRESSION
----------
SUMMARY OF OUTPUT: ORDINARY LEAST SQUARES ESTIMATION
Data set            :  Zonal 2000
Dependent Variable  :    UMI 2000  Number of Observations: 2304
Mean dependent var  :    -1.93832  Number of Variables   :    6
S.D. dependent var  :      1.4783  Degrees of Freedom    : 2298

R-squared           :    0.178938  F-statistic           :     100.163
Adjusted R-squared  :    0.177151  Prob(F-statistic)     :           0
Sum squared residual:     4134.11  Log likelihood        :    -3942.72
Sigma-square        :       1.799  Akaike info criterion :     7897.45
S.E. of regression  :     1.34127  Schwarz criterion     :      7931.9
Sigma-square ML     :     1.79432
S.E of regression ML:     1.33952

------------------------------------------------------------------------------
       Variable      Coefficient      Std.Error    t-Statistic   Probability
------------------------------------------------------------------------------
          CONSTANT      -17.3984       0.993124      -17.5188      0.00000
                O3      0.119379      0.0114709       10.4071      0.00000
                CO       1.50091       0.124518       12.0537      0.00000
               NOX    -0.0268308     0.00536848      -4.99784      0.00000
               SO2      0.016056      0.0163963      0.979246      0.32756
              PM10       0.16076     0.00960104         16.744      0.00000
------------------------------------------------------------------------------

REGRESSION DIAGNOSTICS
MULTICOLLINEARITY CONDITION NUMBER   97.807038
TEST ON NORMALITY OF ERRORS
TEST                   DF           VALUE             PROB
Jarque-Bera             2           162.7725          0.00000

DIAGNOSTICS FOR HETEROSKEDASTICITY
RANDOM COEFFICIENTS
TEST                   DF           VALUE             PROB
Breusch-Pagan test      5            83.7601          0.00000
Koenker-Bassett test    5            65.8838          0.00000

DIAGNOSTICS FOR SPATIAL DEPENDENCE
FOR WEIGHT MATRIX : Zonal2000
   (row-standardized weights)
TEST                            MI/DF        VALUE          PROB
Moran's I (error)              0.6487       51.1332        0.00000
Lagrange Multiplier (lag)           1      2573.3229        0.00000
Robust LM (lag)                     1         5.7484        0.01650
Lagrange Multiplier (error)         1      2567.5842        0.00000
Robust LM (error)                   1         0.0097        0.92156
Lagrange Multiplier (SARMA)         2      2573.3326        0.00000
============================== END OF REPORT ==============================
```

Urban Marginalisation Index

2000

```
REGRESSION
----------
SUMMARY OF OUTPUT: SPATIAL LAG MODEL - MAXIMUM LIKELIHOOD ESTIMATION
Data set            : Zonal 2000
Spatial Weight      : Zonal2000
Dependent Variable  :    UMI 2000  Number of Observations: 2304
Mean dependent var  :    -1.93832  Number of Variables   :    7
S.D. dependent var  :      1.4783  Degrees of Freedom    : 2297
Lag coeff.   (Rho)  :    0.824102

R-squared           :    0.700353  Log likelihood        :    -2992.56
Sq. Correlation     : -            Akaike info criterion :     5999.12
Sigma-square        :    0.654838  Schwarz criterion     :     6039.32
S.E of regression   :     0.80922

------------------------------------------------------------------------------
       Variable       Coefficient     Std.Error       z-value    Probability
------------------------------------------------------------------------------
        W_UMI 2000      0.824102      0.0129254        63.7582     0.00000
          CONSTANT      -4.41291       0.668713       -6.59911     0.00000
               SO2    0.00508281     0.00989253       0.513803     0.60739
                CO      0.333932      0.0785543        4.25096     0.00002
               NOX   -0.00321434     0.00324666      -0.990044     0.32215
                O3     0.0359411      0.0073223        4.90844     0.00000
              PM10     0.0372934     0.00633312        5.88864     0.00000
------------------------------------------------------------------------------

REGRESSION DIAGNOSTICS
DIAGNOSTICS FOR HETEROSKEDASTICITY
RANDOM COEFFICIENTS
TEST                                    DF      VALUE        PROB
Breusch-Pagan test                      5        93.4431     0.00000

DIAGNOSTICS FOR SPATIAL DEPENDENCE
SPATIAL LAG DEPENDENCE FOR WEIGHT MATRIX : Zonal2000
TEST                                    DF      VALUE        PROB
Likelihood Ratio Test                   1     1900.3235     0.00000
============================ END OF REPORT ==============================
```

2005

```
REGRESSION
----------
SUMMARY OF OUTPUT: SPATIAL LAG MODEL - MAXIMUM LIKELIHOOD ESTIMATION
Data set            : Zonal 2005
Spatial Weight      : Zonal2005
Dependent Variable  :    UMI 2005  Number of Observations: 2345
Mean dependent var  :   -0.695497  Number of Variables   :    8
S.D. dependent var  :    0.487758  Degrees of Freedom    : 2337
Lag coeff.   (Rho)  :    0.811388

R-squared           :    0.704083  Log likelihood        :    -425.661
Sq. Correlation     : -            Akaike info criterion :     867.322
Sigma-square        :   0.0704009  Schwarz criterion     :     913.402
S.E of regression   :    0.265332

------------------------------------------------------------------------------
       Variable       Coefficient     Std.Error       z-value    Probability
------------------------------------------------------------------------------
        W_UMI 2005      0.811388      0.0132374        61.2953     0.00000
          CONSTANT      -1.28173       0.279221       -4.59038     0.00000
               NOx    0.00214131     0.00122713        1.74498     0.08099
                CO     -0.131015      0.0713563       -1.83606     0.06635
                O3     0.0189068     0.00425629        4.44208     0.00001
              PM10    0.00497331     0.00194059        2.56278     0.01038
             PM2.5     0.0234408     0.00676377        3.46565     0.00053
               SO2    -0.0162392      0.0051443       -3.15674     0.00160
------------------------------------------------------------------------------

REGRESSION DIAGNOSTICS
DIAGNOSTICS FOR HETEROSKEDASTICITY
RANDOM COEFFICIENTS
TEST                                    DF      VALUE        PROB
Breusch-Pagan test                      6       181.2136     0.00000

DIAGNOSTICS FOR SPATIAL DEPENDENCE
SPATIAL LAG DEPENDENCE FOR WEIGHT MATRIX : Zonal2005
TEST                                    DF      VALUE        PROB
Likelihood Ratio Test                   1     1738.3471     0.00000
============================ END OF REPORT ==============================
```

2010

```
REGRESSION
----------
SUMMARY OF OUTPUT: SPATIAL LAG MODEL - MAXIMUM LIKELIHOOD ESTIMATION
Data set            : Zonal 2010
Spatial Weight      : Zonal2010
Dependent Variable  :    UMI 2010  Number of Observations: 2364
Mean dependent var  :   -0.630613  Number of Variables   :    8
S.D. dependent var  :    0.547308  Degrees of Freedom    : 2356
Lag coeff.   (Rho)  :    0.829215

R-squared           :    0.748770  Log likelihood        :    -523.06
Sq. Correlation     : -            Akaike info criterion :    1062.12
Sigma-square        :    0.075255  Schwarz criterion     :    1108.27
S.E of regression   :    0.274326

------------------------------------------------------------------------------
       Variable       Coefficient     Std.Error       z-value    Probability
------------------------------------------------------------------------------
        W_UMI 2010      0.829215      0.0122951        67.4425     0.00000
          CONSTANT       -1.5698       0.259786       -6.04268     0.00000
                CO     -0.162955       0.082585       -1.97318     0.04848
               NOX    0.00637156     0.00289462        2.20117     0.02772
                O3     0.0240158     0.00385447        6.23064     0.00000
              PM10    0.00191311     0.00210647       0.908207     0.36377
             PM2.5     0.0298667     0.00691673        4.31804     0.00002
               SO2    -0.0201613     0.00768116       -2.62478     0.00867
------------------------------------------------------------------------------

REGRESSION DIAGNOSTICS
DIAGNOSTICS FOR HETEROSKEDASTICITY
RANDOM COEFFICIENTS
TEST                                DF      VALUE         PROB
Breusch-Pagan test                  6       145.3843      0.00000

DIAGNOSTICS FOR SPATIAL DEPENDENCE
SPATIAL LAG DEPENDENCE FOR WEIGHT MATRIX : Zonal2010
TEST                                DF      VALUE         PROB
Likelihood Ratio Test               1      1934.0079      0.00000
============================ END OF REPORT ==============================
```

2020

```
REGRESSION
----------
SUMMARY OF OUTPUT: SPATIAL LAG MODEL - MAXIMUM LIKELIHOOD ESTIMATION
Data set            : Zonal 2020
Spatial Weight      : Zonal2020
Dependent Variable  :    UMI 2020  Number of Observations: 2380
Mean dependent var  :   0.0452134  Number of Variables   :    8
S.D. dependent var  :   0.0167764  Degrees of Freedom    : 2372
Lag coeff.   (Rho)  :    0.736223

R-squared           :    0.571093  Log likelihood        :    7201.01
Sq. Correlation     : -            Akaike info criterion :     -14386
Sigma-square        : 0.000120714  Schwarz criterion     :    -14339.8
S.E of regression   :    0.010987

------------------------------------------------------------------------------
       Variable       Coefficient     Std.Error       z-value    Probability
------------------------------------------------------------------------------
        W_UMI 2020      0.736223      0.0165653        44.4437     0.00000
          CONSTANT    -0.0305117      0.0181707       -1.67917     0.09312
               SO2   0.000136118     0.00124272        0.109532     0.91278
                CO    -0.0468691      0.0270373       -1.73349     0.08301
               NOx  -3.19444e-05    0.000152346       -0.209683     0.83392
                O3   0.000629771    0.000398485         1.58041     0.11401
              PM10   5.95153e-05     0.00015953        0.373066     0.70910
             PM2.5    0.00184311    0.000601504         3.06416     0.00218
------------------------------------------------------------------------------

REGRESSION DIAGNOSTICS
DIAGNOSTICS FOR HETEROSKEDASTICITY
RANDOM COEFFICIENTS
TEST                                DF      VALUE         PROB
Breusch-Pagan test                  6        41.8685      0.00000

DIAGNOSTICS FOR SPATIAL DEPENDENCE
SPATIAL LAG DEPENDENCE FOR WEIGHT MATRIX : Zonal2020
TEST                                DF      VALUE         PROB
Likelihood Ratio Test               1      1253.8374      0.00000
============================ END OF REPORT ==============================
```

Poverty Percentages

2015

```
REGRESSION
----------
SUMMARY OF OUTPUT: SPATIAL LAG MODEL - MAXIMUM LIKELIHOOD ESTIMATION
Data set            : Zonal 2015
Spatial Weight      : Zonal2015
Dependent Variable  :         POB  Number of Observations: 2372
Mean dependent var  :     1.90556  Number of Variables   :    8
S.D. dependent var  :    0.990011  Degrees of Freedom    : 2364
Lag coeff.   (Rho)  :    0.687245

R-squared           :    0.531611  Log likelihood        :   -2579.77
Sq. Correlation     : -           Akaike info criterion :    5175.54
Sigma-square        :    0.459078  Schwarz criterion     :    5221.71
S.E of regression   :    0.677553

------------------------------------------------------------------------------
       Variable       Coefficient     Std.Error       z-value    Probability
------------------------------------------------------------------------------
          W_POB      0.687245      0.0179492        38.2883     0.00000
       CONSTANT      -5.59711        1.15374       -4.85126     0.00000
             O3      0.123641      0.0239852        5.15488     0.00000
             CO    -0.0861484       0.436082      -0.197551     0.84340
            NOx     0.0221812       0.011344        1.95533     0.05054
           PM10     0.0479641     0.00793405        6.04535     0.00000
          PM2.5     0.0179767     0.00591817        3.03755     0.00239
            SO2     -0.154942      0.0431428       -3.59138     0.00033
------------------------------------------------------------------------------

REGRESSION DIAGNOSTICS
DIAGNOSTICS FOR HETEROSKEDASTICITY
RANDOM COEFFICIENTS
TEST                                    DF      VALUE        PROB
Breusch-Pagan test                      6       130.8938     0.00000

DIAGNOSTICS FOR SPATIAL DEPENDENCE
SPATIAL LAG DEPENDENCE FOR WEIGHT MATRIX : Zonal2015
TEST                                    DF      VALUE        PROB
Likelihood Ratio Test                   1      1068.2439     0.00000
============================== END OF REPORT ==============================
```

2020

```
REGRESSION
----------
SUMMARY OF OUTPUT: SPATIAL LAG MODEL - MAXIMUM LIKELIHOOD ESTIMATION
Data set            : Zonal 2020
Spatial Weight      : Zonal2020
Dependent Variable  :      % Poor  Number of Observations: 2380
Mean dependent var  :      64.278  Number of Variables   :    8
S.D. dependent var  :     17.3318  Degrees of Freedom    : 2372
Lag coeff.   (Rho)  :    0.857036

R-squared           :    0.770180  Log likelihood        :   -8660.37
Sq. Correlation     : -           Akaike info criterion :     17336.7
Sigma-square        :     69.0361  Schwarz criterion     :     17382.9
S.E of regression   :      8.3088

------------------------------------------------------------------------------
       Variable       Coefficient     Std.Error       z-value    Probability
------------------------------------------------------------------------------
         W_% Poor      0.857036       0.011205        76.4872     0.00000
         CONSTANT      -37.8029        13.8884       -2.72191     0.00649
              SO2        1.1597       0.941668        1.23154     0.21812
               CO      -34.9723        20.4815       -1.7075      0.08773
              NOx    -0.0175127        0.11521      -0.152007     0.87918
               O3      0.799517       0.304475        2.62589     0.00864
             PM10      0.166194       0.121105        1.37231     0.16997
            PM2.5        1.1904       0.455434        2.61377     0.00896
------------------------------------------------------------------------------

REGRESSION DIAGNOSTICS
DIAGNOSTICS FOR HETEROSKEDASTICITY
RANDOM COEFFICIENTS
TEST                                    DF      VALUE        PROB
Breusch-Pagan test                      6       143.5219     0.00000

DIAGNOSTICS FOR SPATIAL DEPENDENCE
SPATIAL LAG DEPENDENCE FOR WEIGHT MATRIX : Zonal2020
TEST                                    DF      VALUE        PROB
Likelihood Ratio Test                   1      2321.2587     0.00000
============================== END OF REPORT ==============================
```

Annex VII. LISA Cluster Maps

Urban Marginalisation Index

Ozone (O_3)

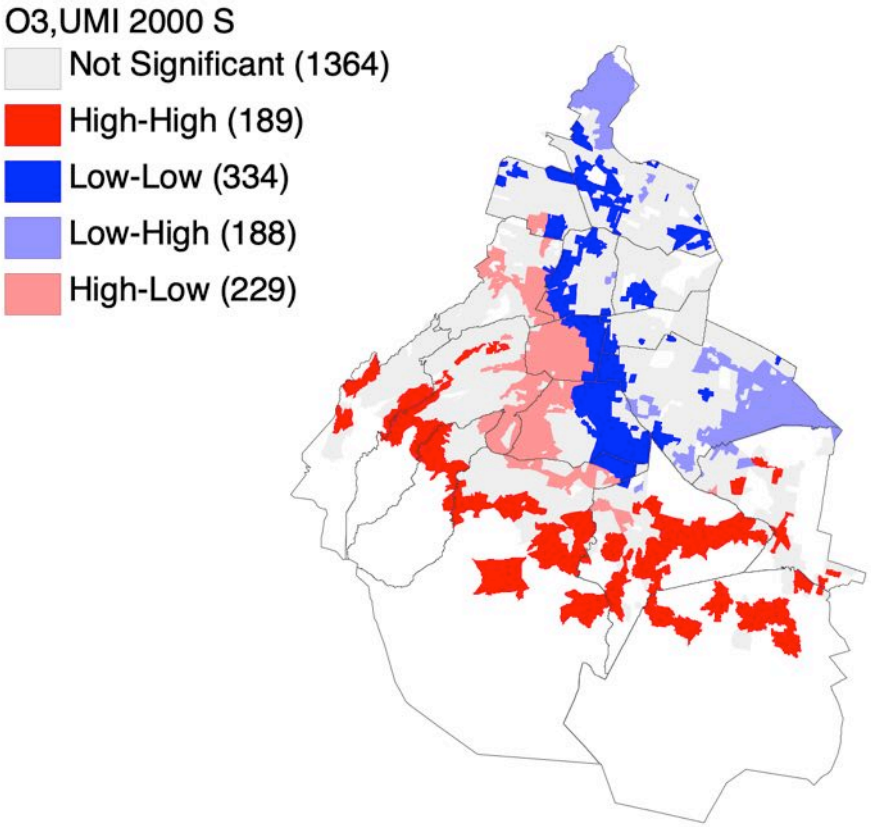

Figure 9.36 LISA Cluster Map for O_3 and Urban Marginalisation Index in 2000

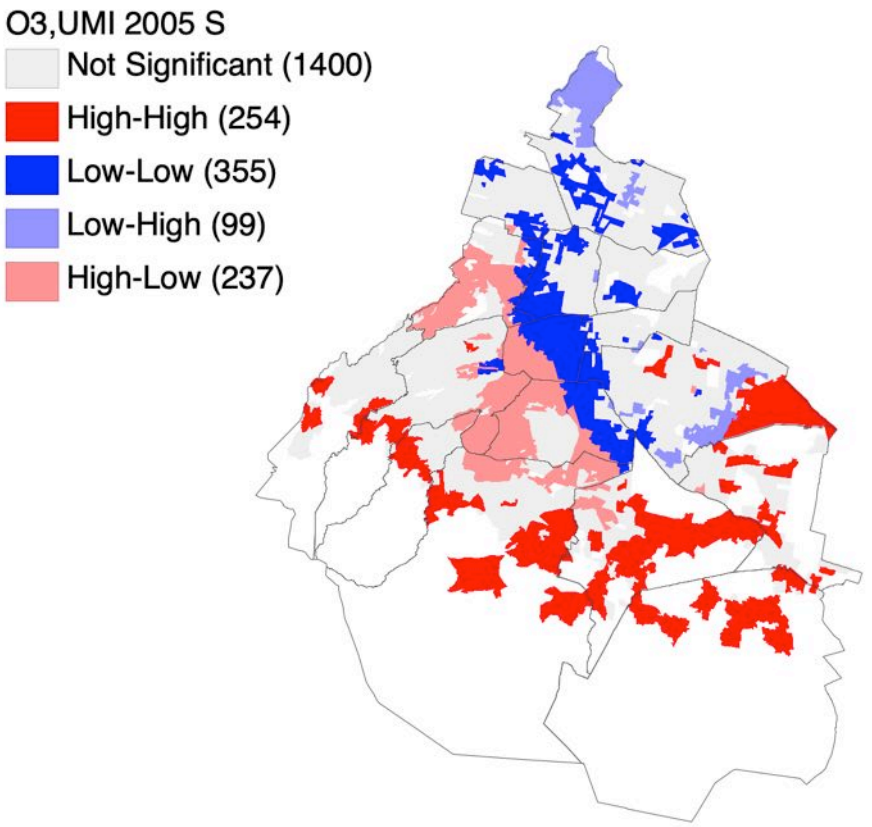

Figure 9.37 LISA Cluster Map for O_3 and Urban Marginalisation Index in 2005

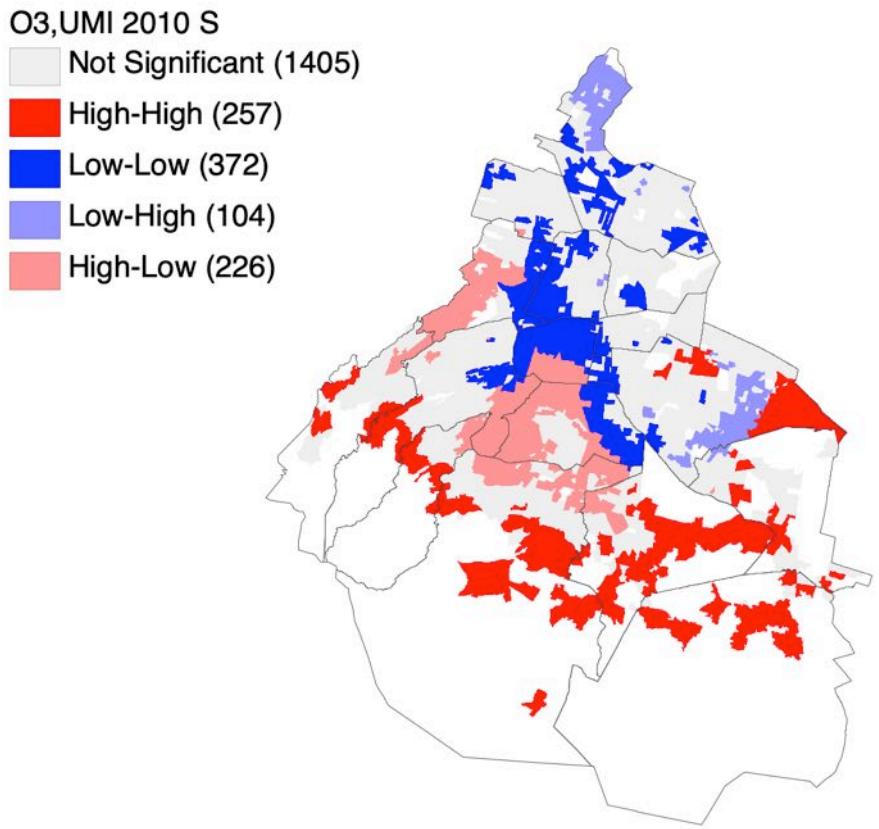

Figure 9.38 LISA Cluster Map for O_3 and Urban Marginalisation Index in 2010

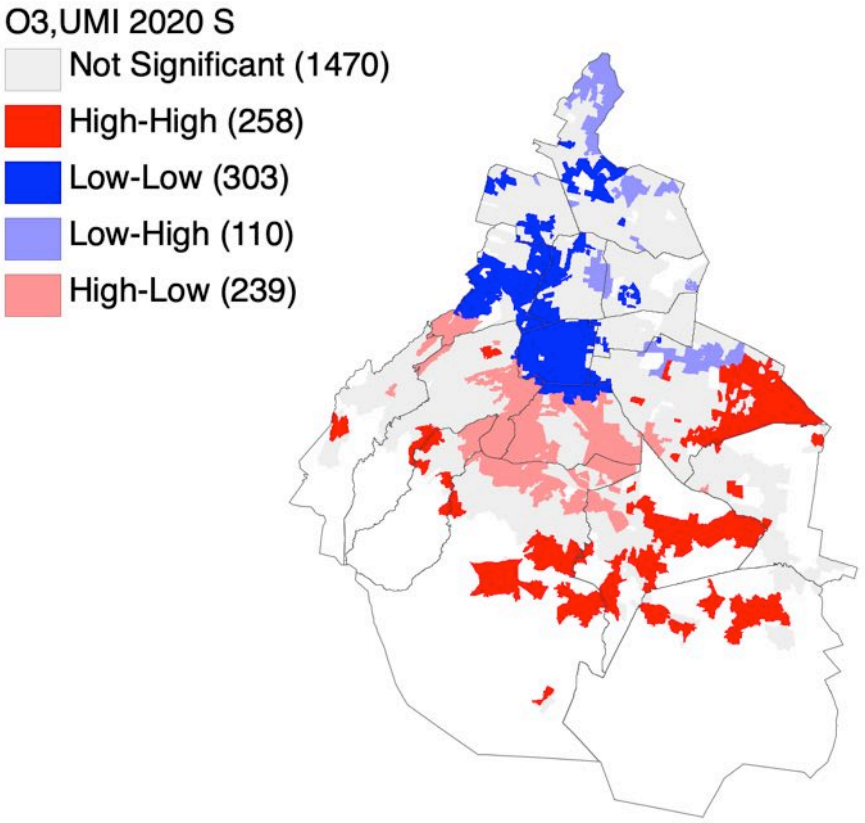

Figure 9.39 LISA Cluster Map for O_3 and Urban Marginalisation Index in 2020

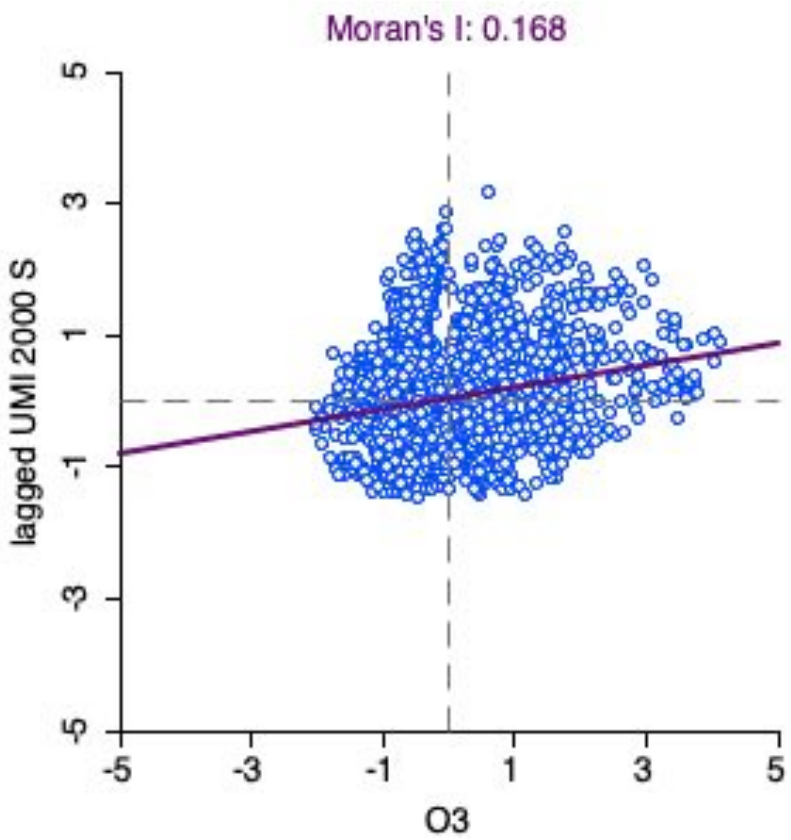

Figure 9.40 Bivariate Moran's I Scatter Plot for O_3 and Urban Marginalisation Index in 2000

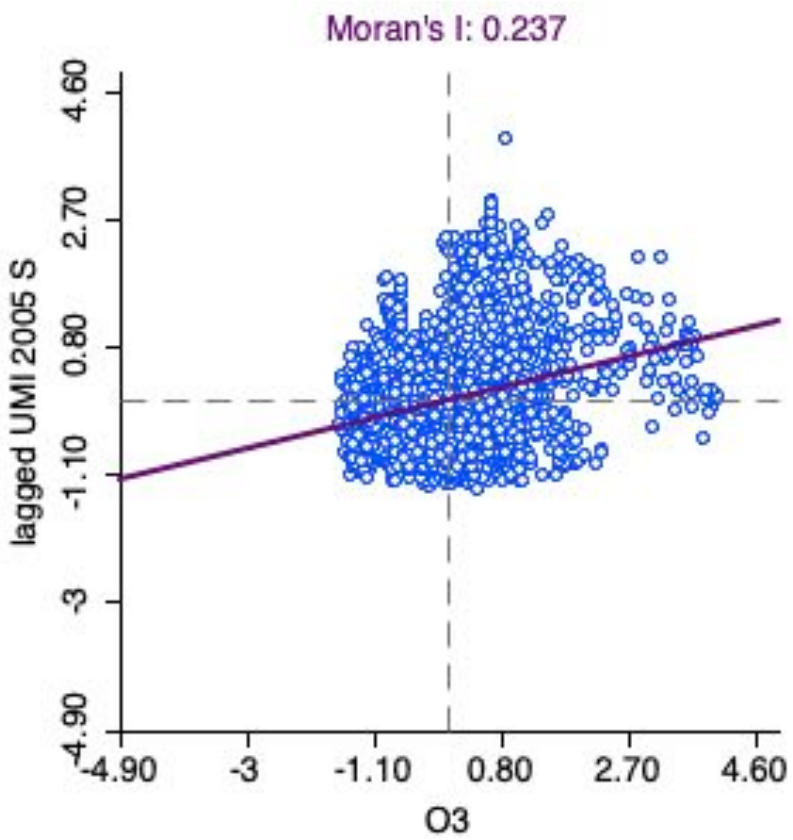

Figure 9.41 Bivariate Moran's I Scatter Plot for O_3 and Urban Marginalisation Index in 2005

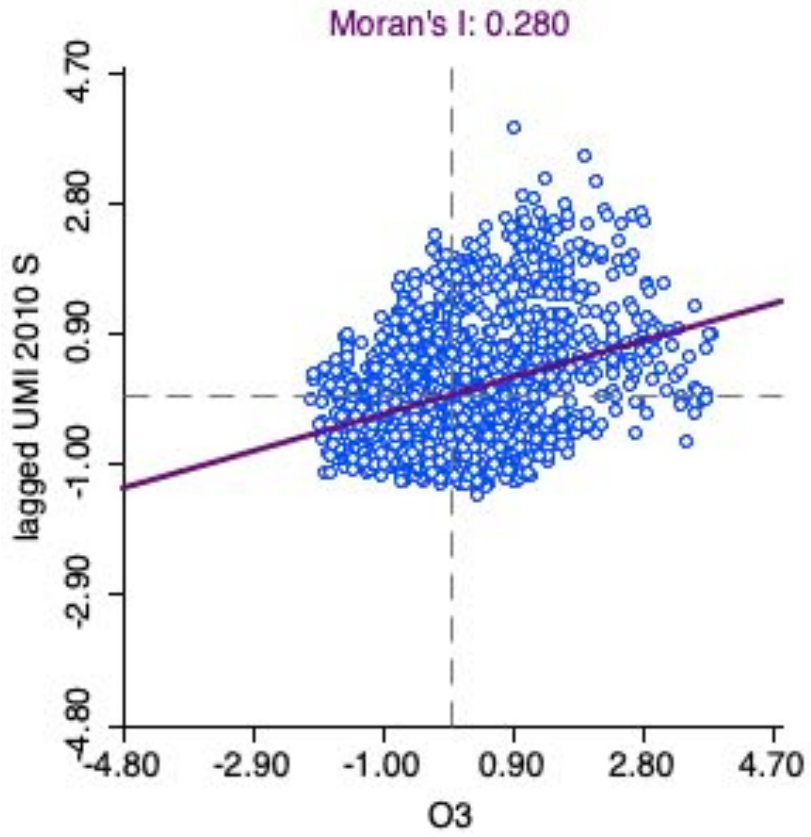

Figure 9.42 Bivariate Moran's I Scatter Plot for O_3 and Urban Marginalisation Index in 2010

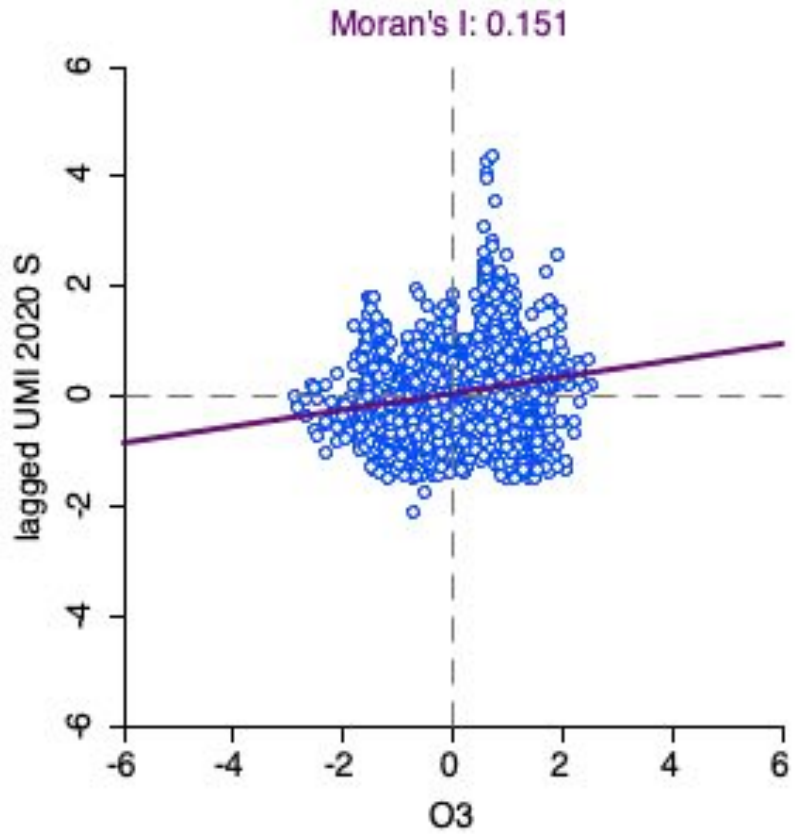

Figure 9.43 Bivariate Moran's I Scatter Plot for O_3 and Urban Marginalisation Index in 2020

Carbon Monoxide (CO)

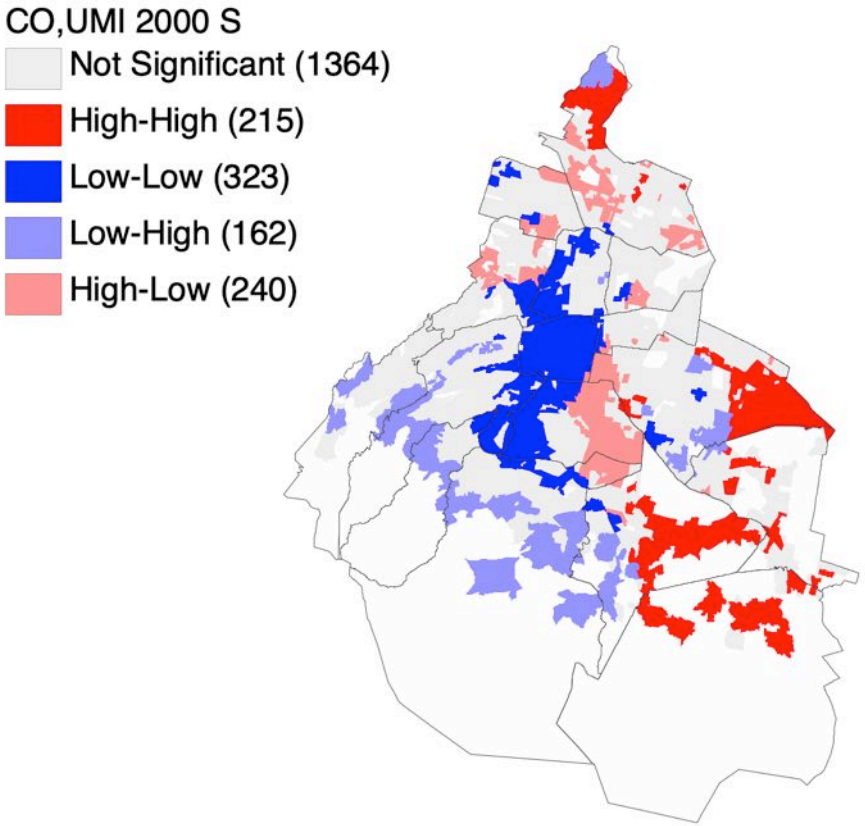

Figure 9.44 LISA Cluster Map for CO and Urban Marginalisation Index in 2000

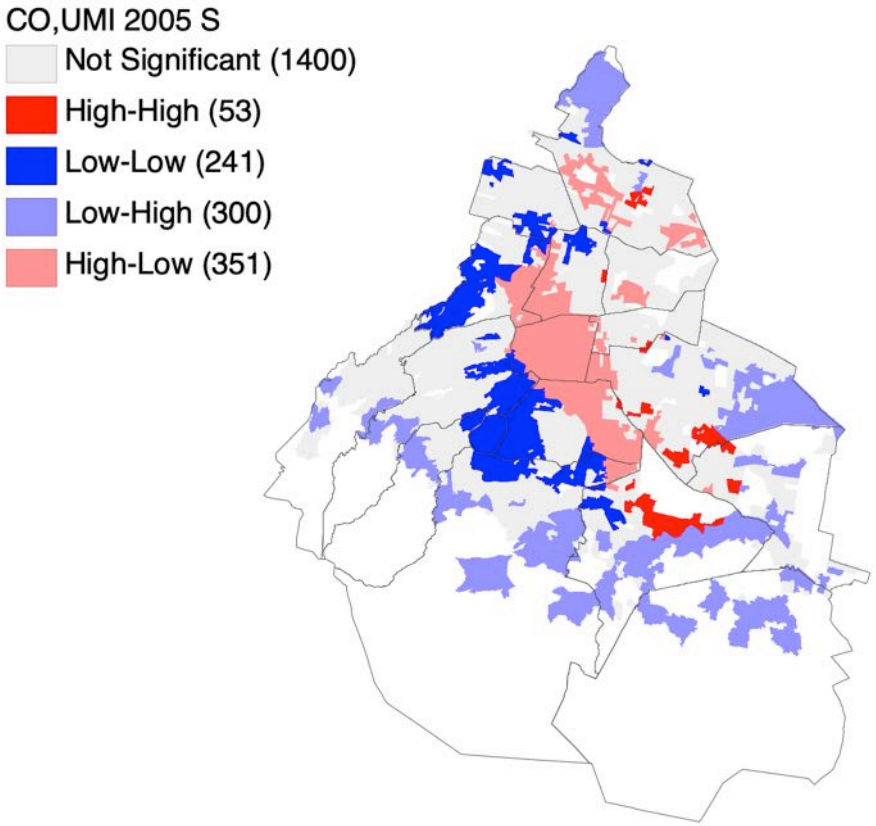

Figure 9.45 LISA Cluster Map for CO and Urban Marginalisation Index in 2005

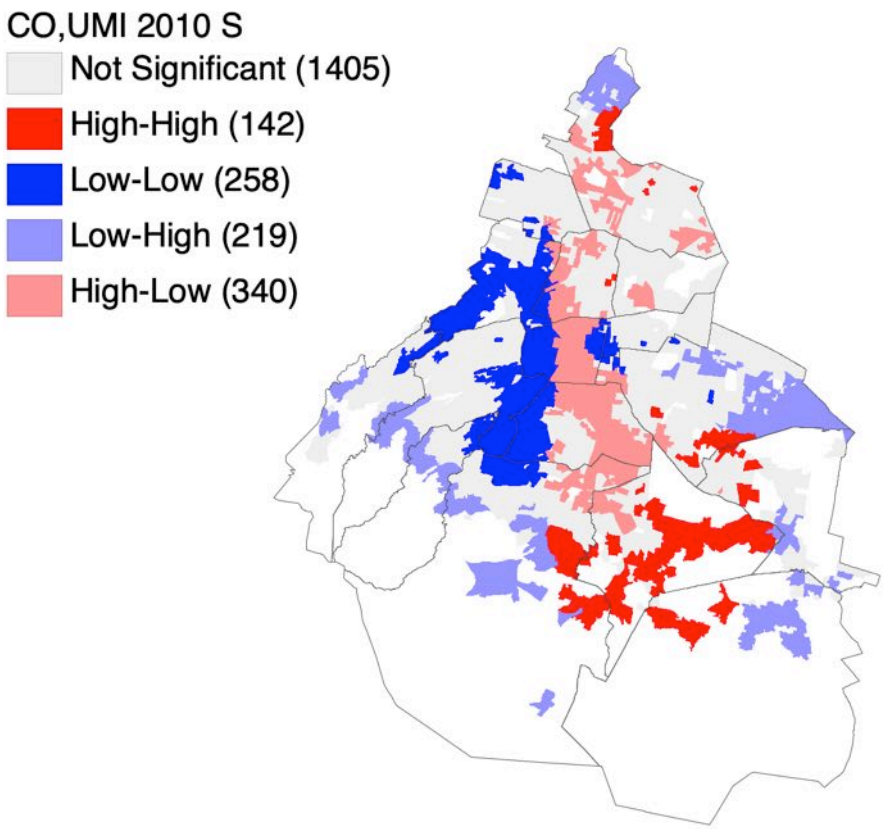

Figure 9.46 LISA Cluster Map for CO and Urban Marginalisation Index in 2010

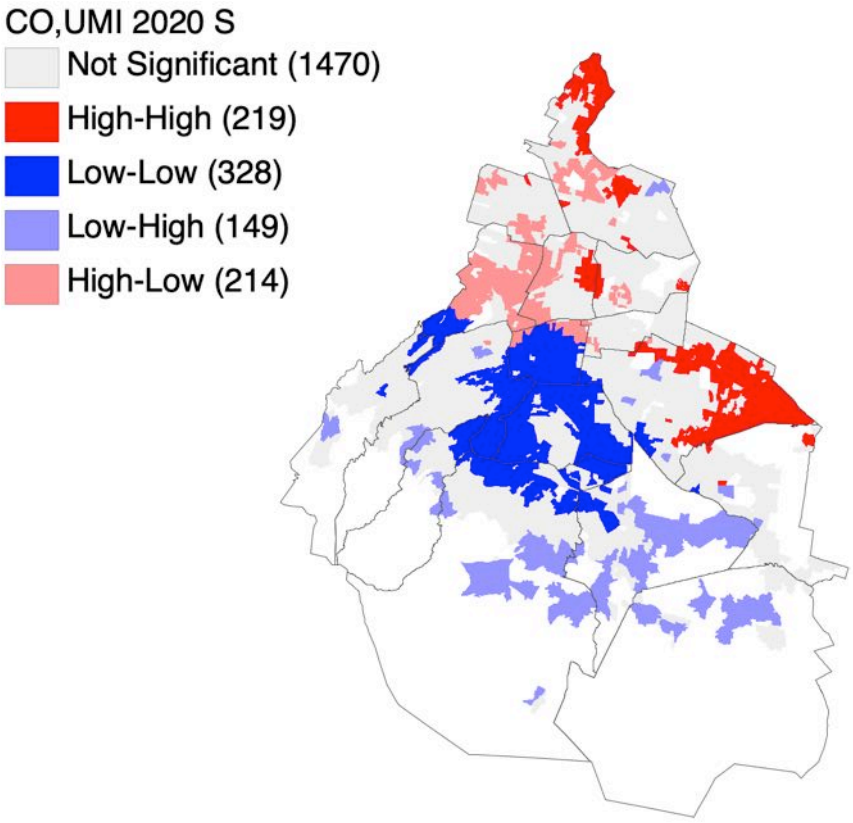

Figure 9.47 LISA Cluster Map for CO and Urban Marginalisation Index in 2020

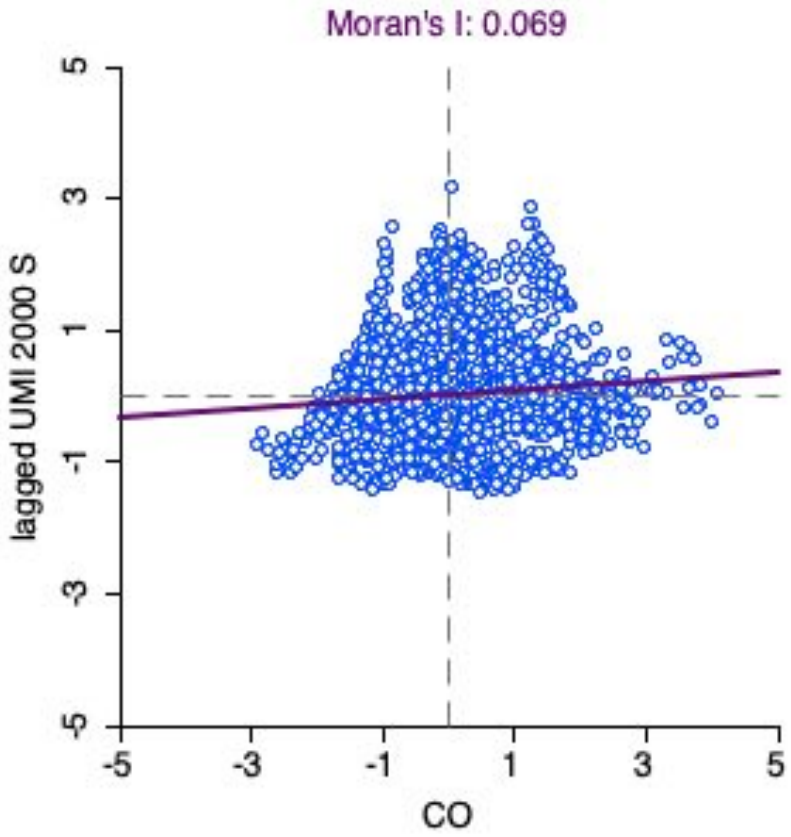

Figure 9.48 Bivariate Moran's I Scatter Plot for CO and Urban Marginalisation Index in 2000

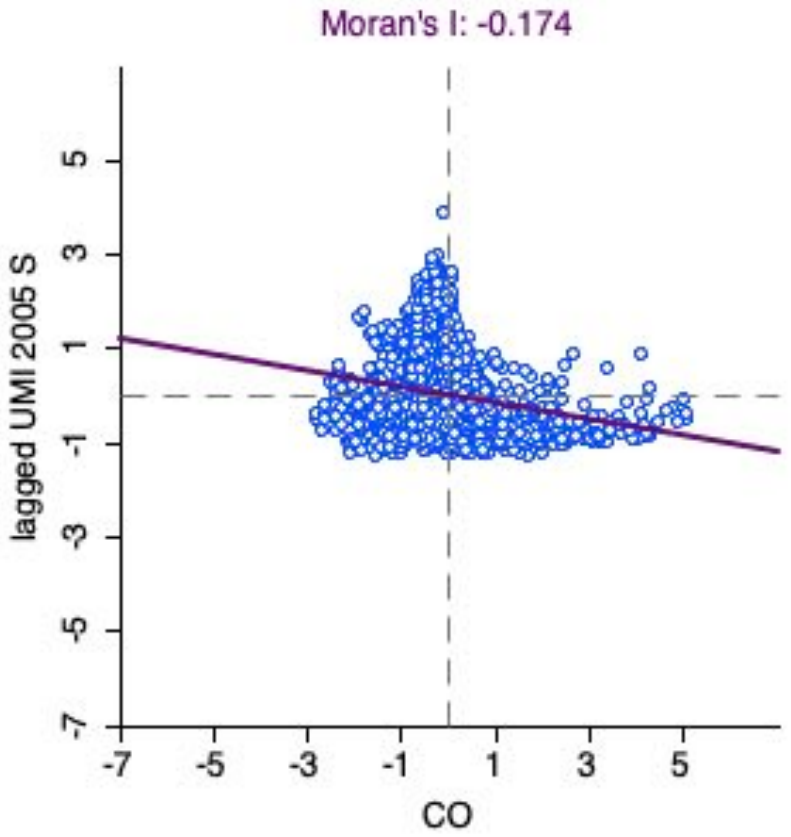

Figure 9.49 Bivariate Moran's I Scatter Plot for CO and Urban Marginalisation Index in 2005

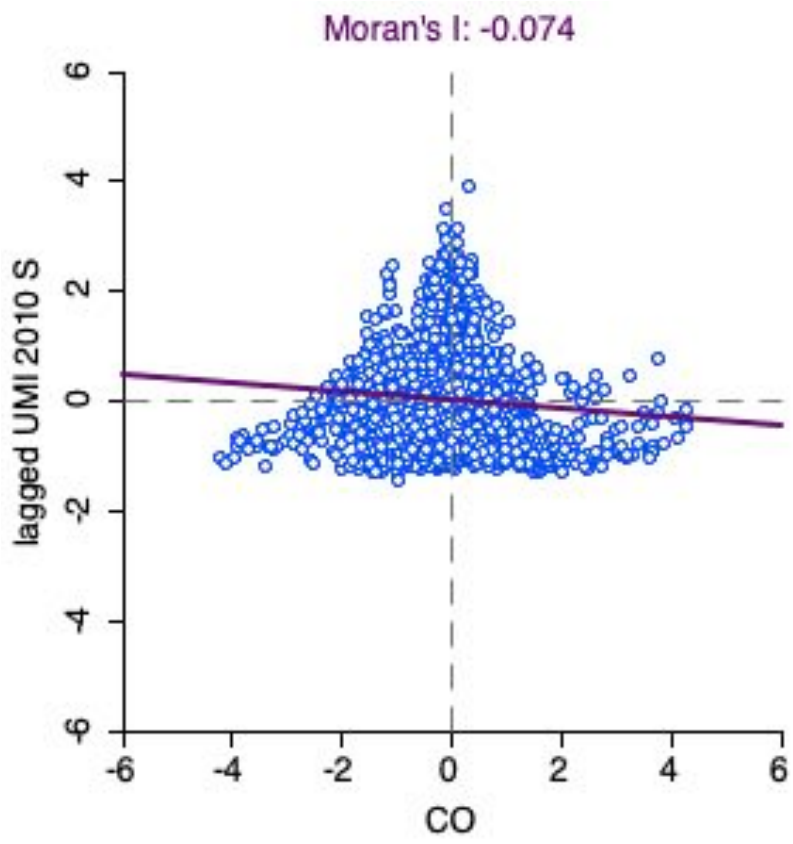

Figure 9.50 Bivariate Moran's I Scatter Plot for CO and Urban Marginalisation Index in 2010

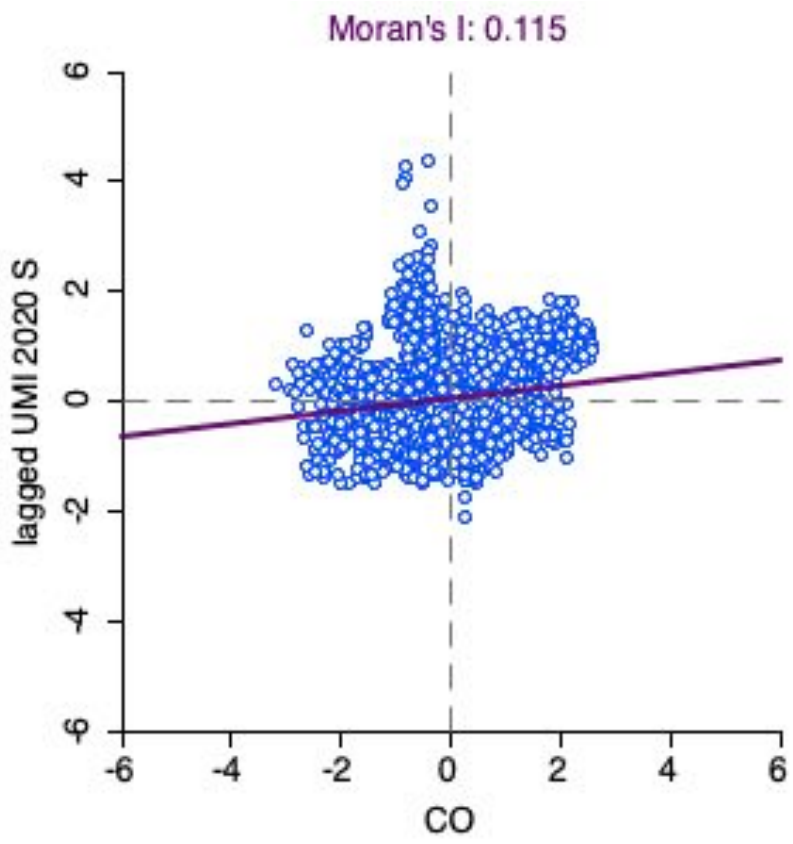

Figure 9.51 Bivariate Moran's I Scatter Plot for CO and Urban Marginalisation Index in 2020

Nitrogen Oxides (NOx)

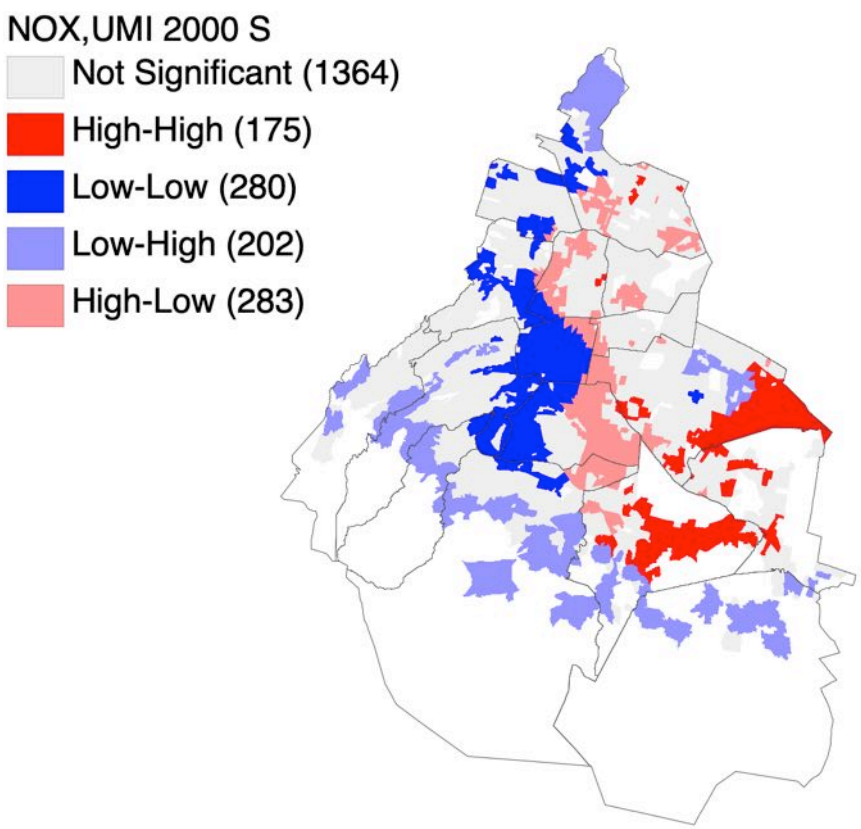

Figure 9.52 LISA Cluster Map for NOx and Urban Marginalisation Index in 2000

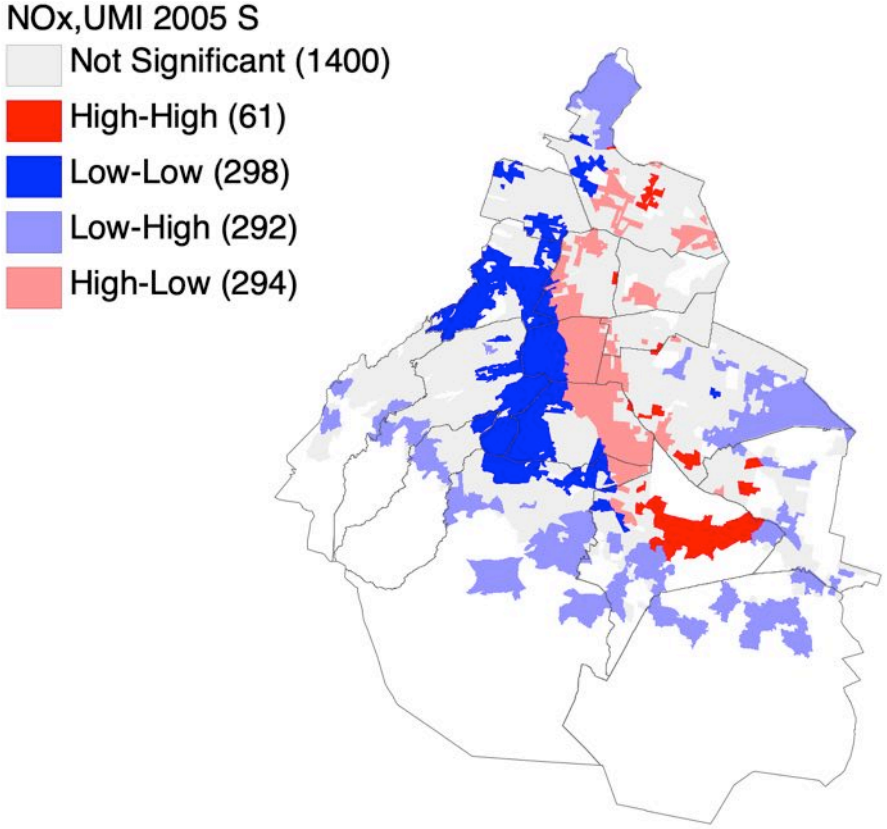

Figure 9.53 LISA Cluster Map for NOx and Urban Marginalisation Index in 2005

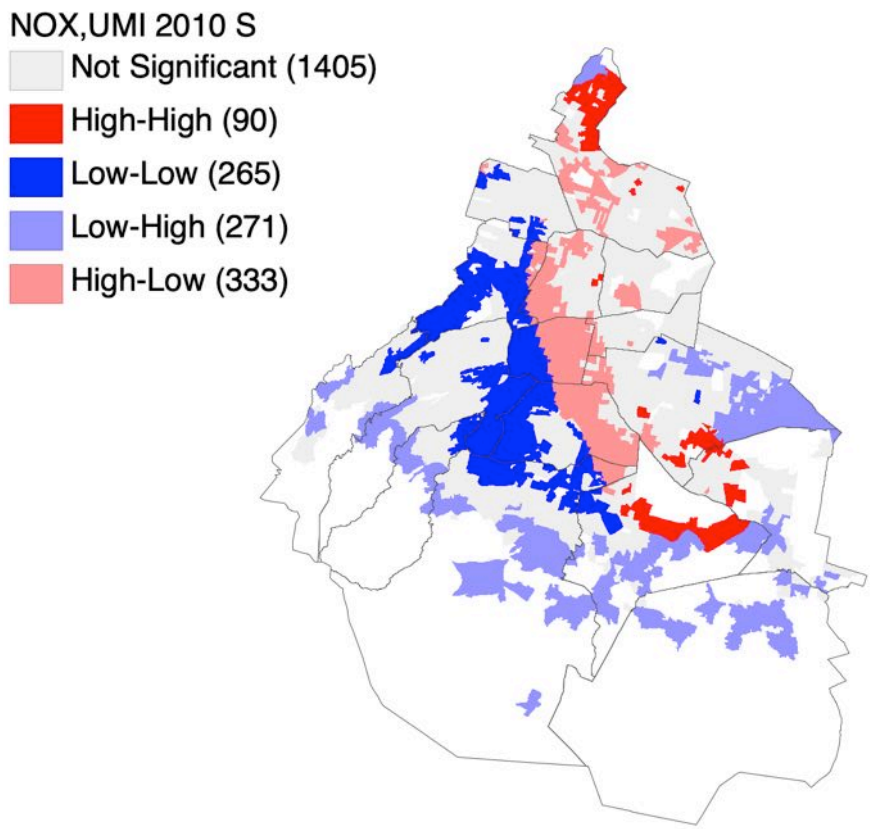

Figure 9.54 LISA Cluster Map for NOx and Urban Marginalisation Index in 2010

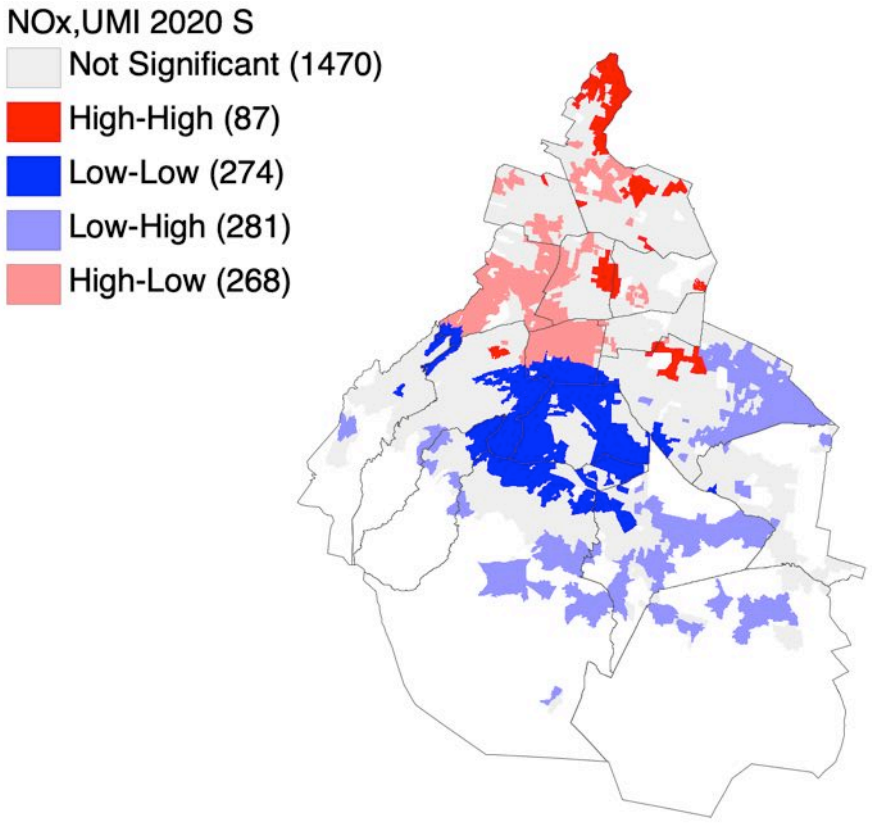

Figure 9.55 LISA Cluster Map for NOx and Urban Marginalisation Index in 2020

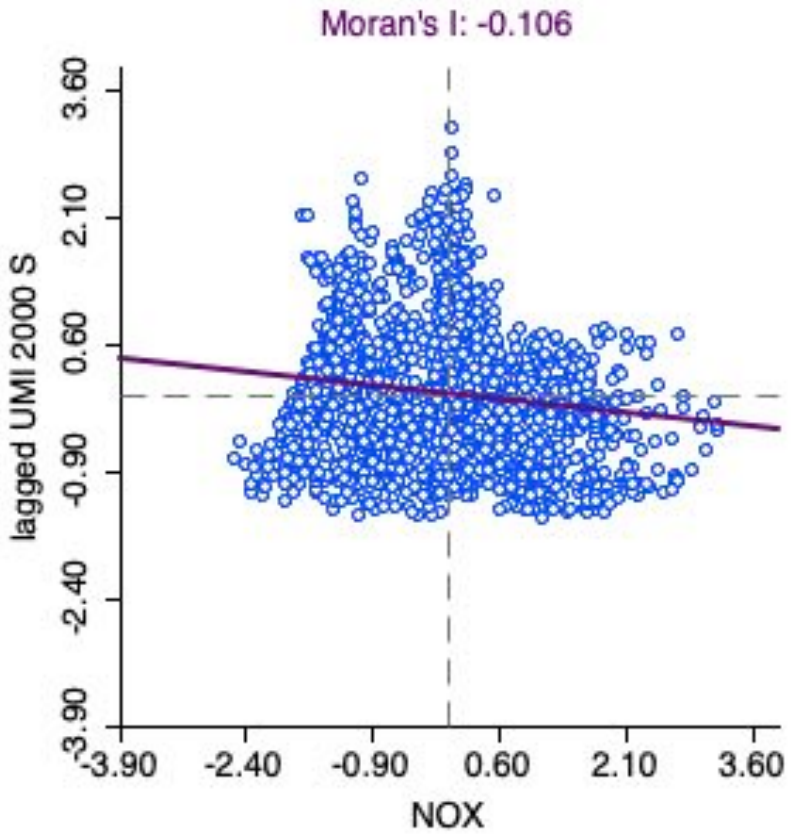

Figure 9.56 Bivariate Moran's I Scatter Plot for NOx and Urban Marginalisation Index in 2000

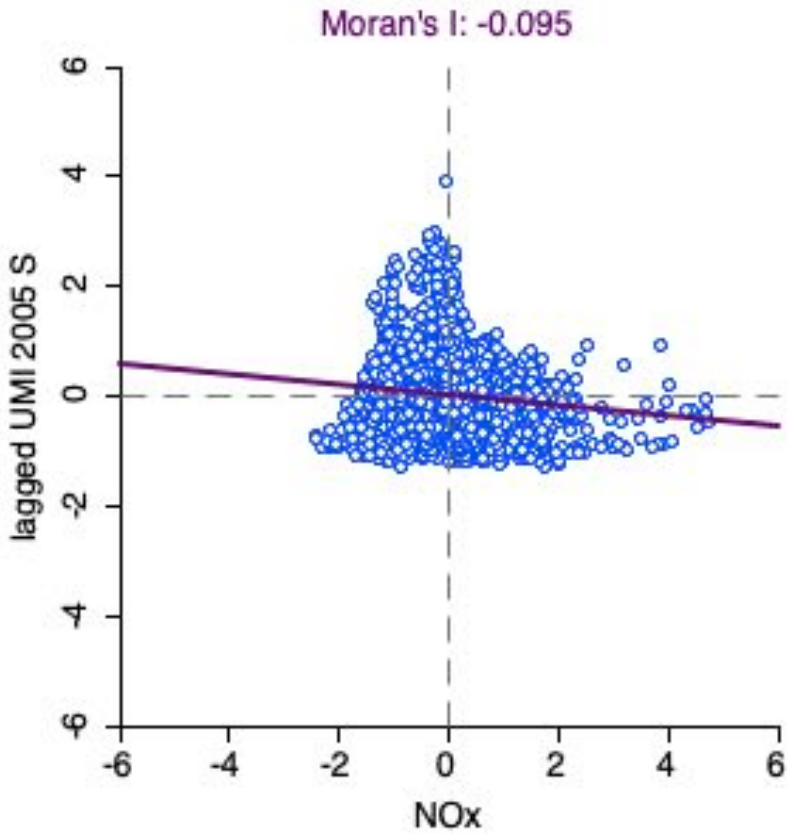

Figure 9.57 Bivariate Moran's I Scatter Plot for NOx and Urban Marginalisation Index in 2005

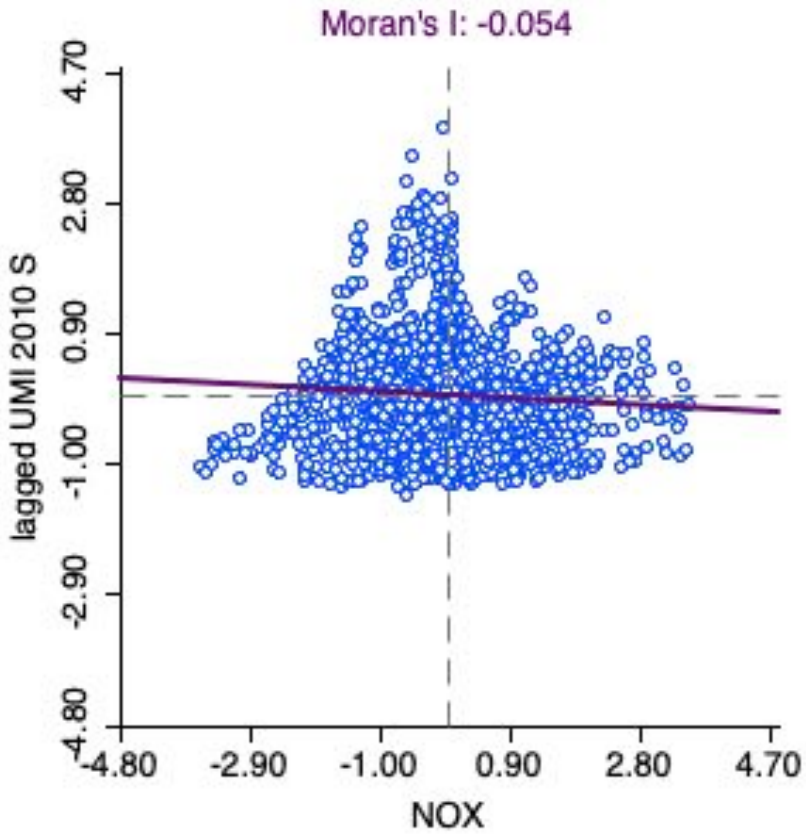

Figure 9.58 Bivariate Moran's I Scatter Plot for NOx and Urban Marginalisation Index in 2010

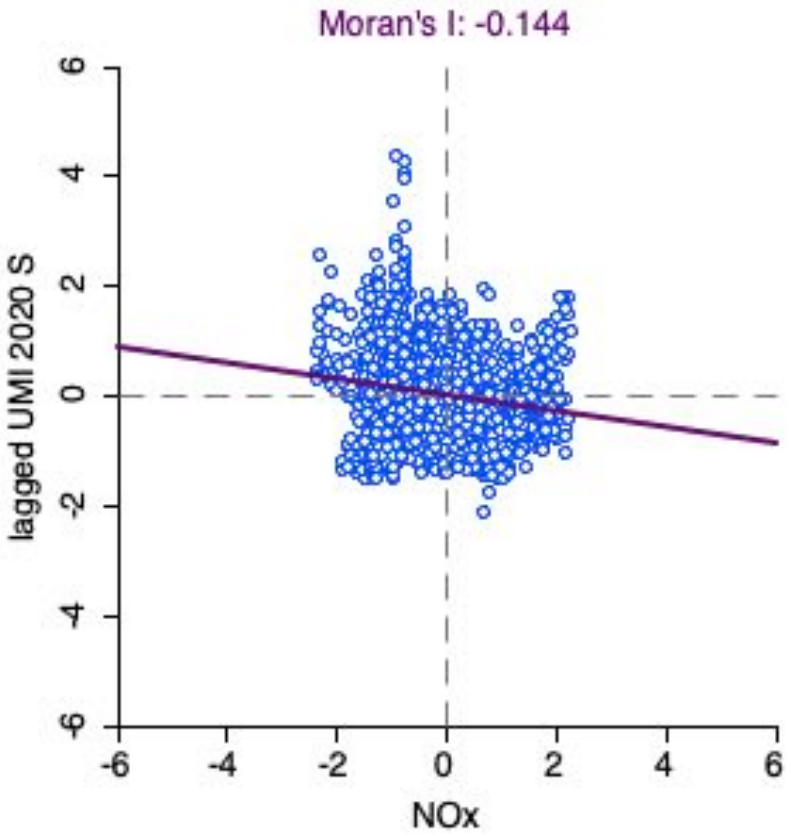

Figure 9.59 Bivariate Moran's I Scatter Plot for NOx and Urban Marginalisation Index in 2020

Sulphur Dioxide (SO_2)

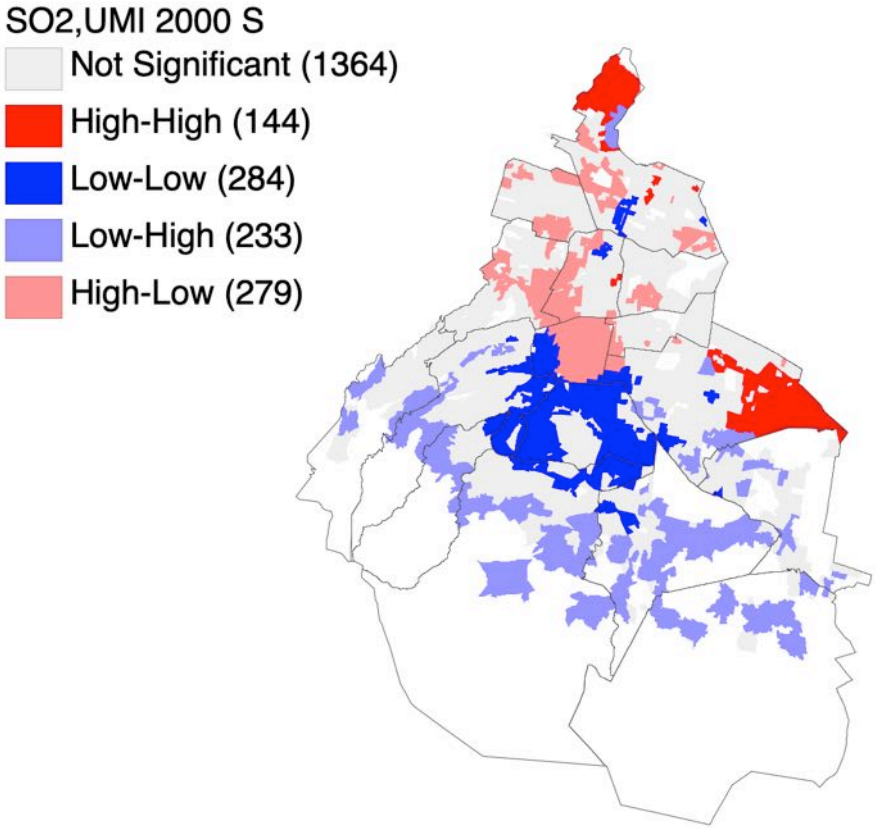

Figure 9.60 LISA Cluster Map for SO_2 and Urban Marginalisation Index in 2000

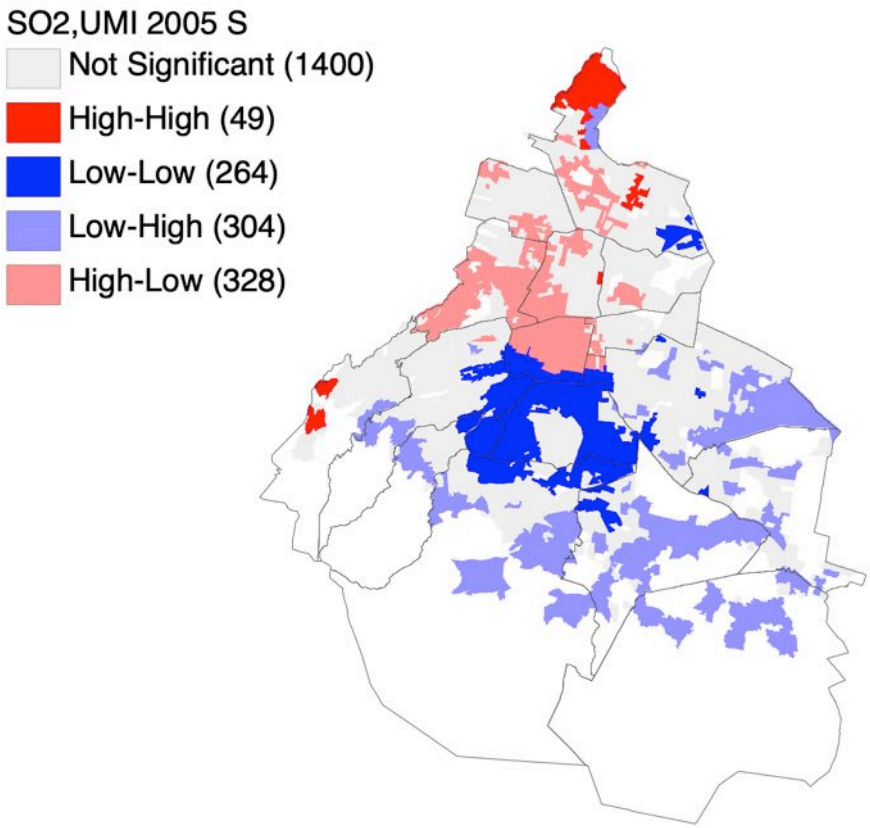

Figure 9.61 LISA Cluster Map for SO_2 and Urban Marginalisation Index in 2005

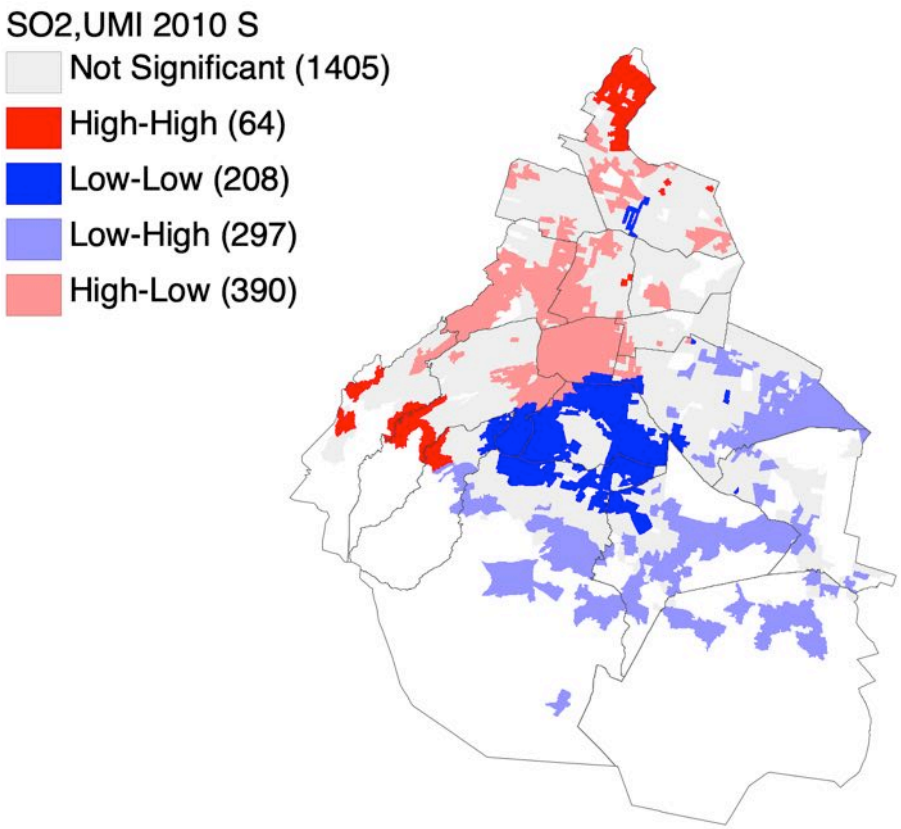

Figure 9.62 LISA Cluster Map for SO_2 and Urban Marginalisation Index in 2010

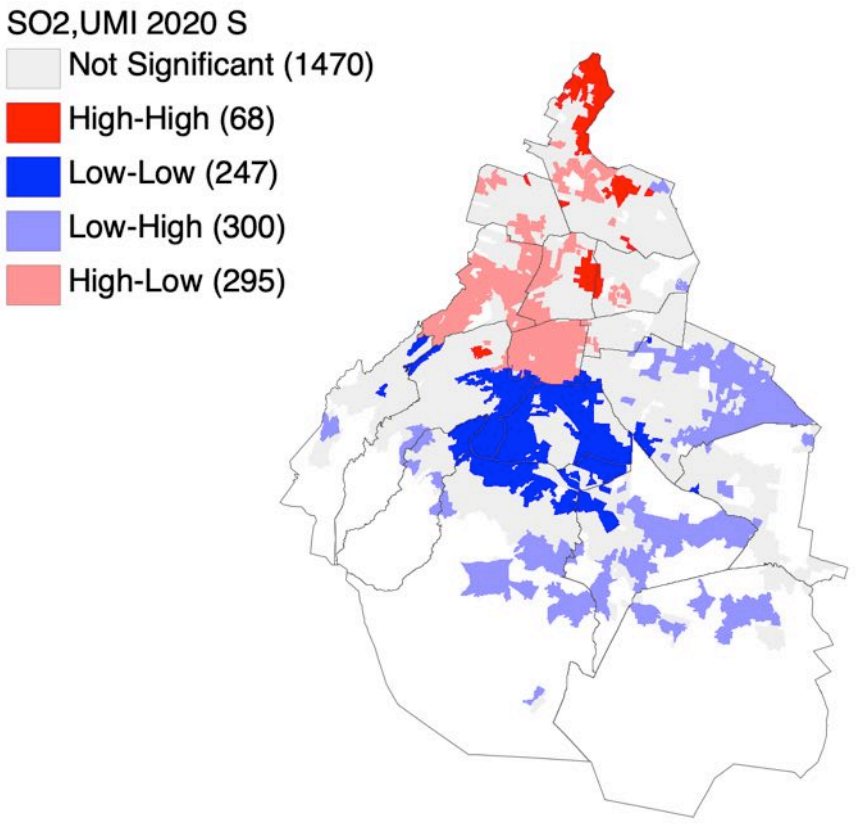

Figure 9.63 LISA Cluster Map for SO_2 and Urban Marginalisation Index in 2020

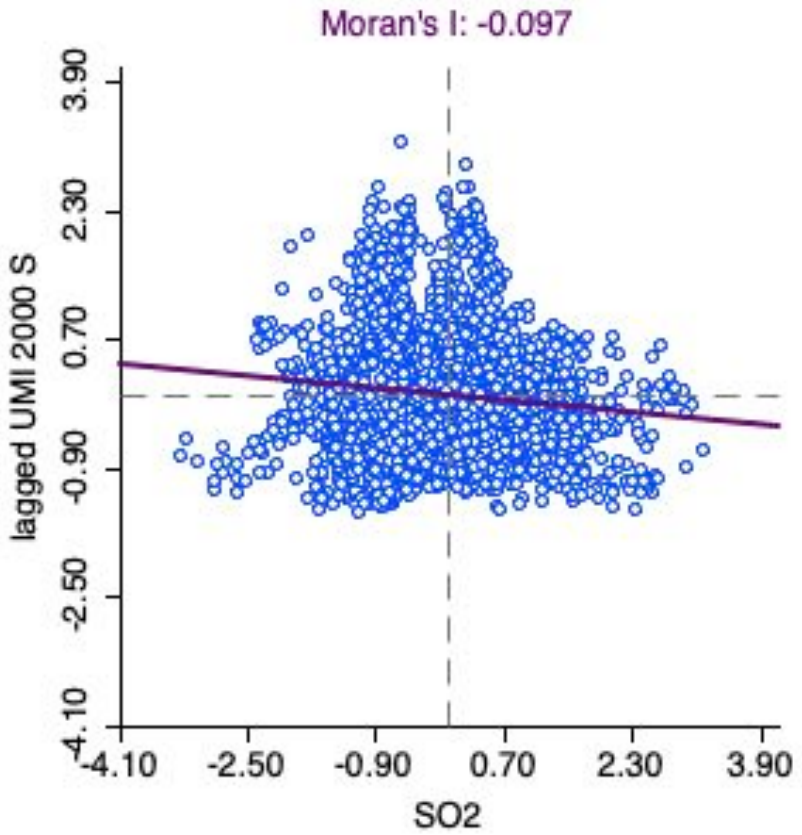

Figure 9.64 Bivariate Moran's I Scatter Plot for SO_2 and Urban Marginalisation Index in 2000

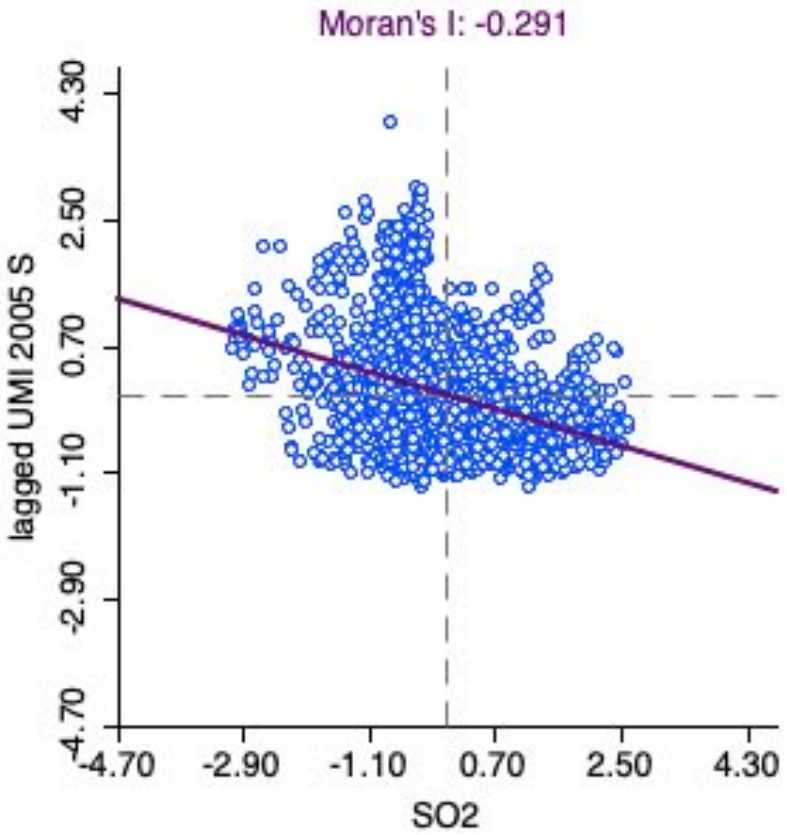

Figure 9.65 Bivariate Moran's I Scatter Plot for SO_2 and Urban Marginalisation Index in 2005

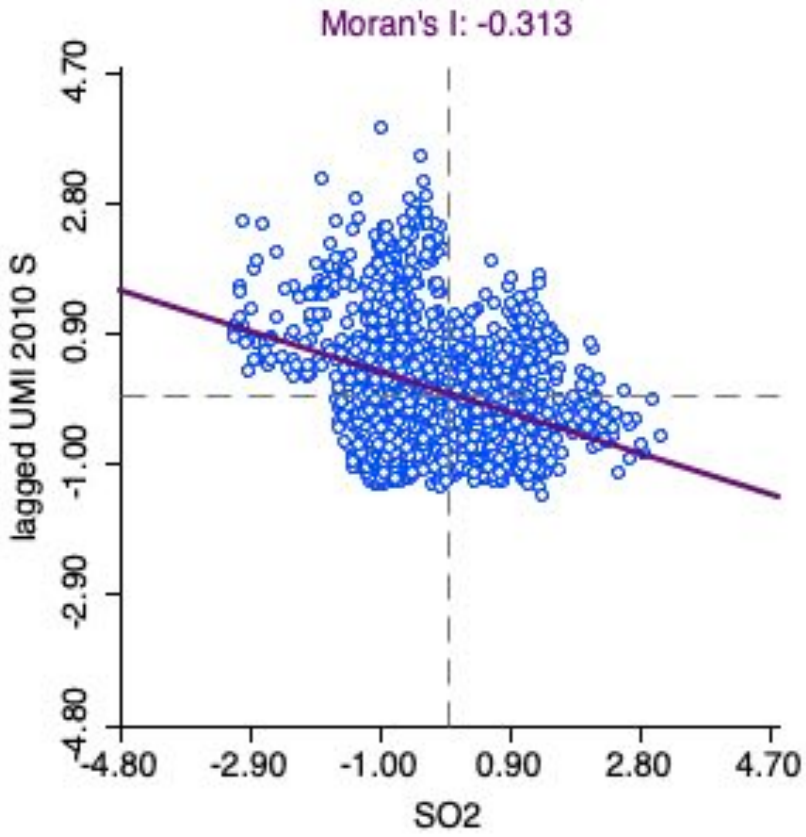

Figure 9.66 Bivariate Moran's I Scatter Plot for SO_2 and Urban Marginalisation Index in 2010

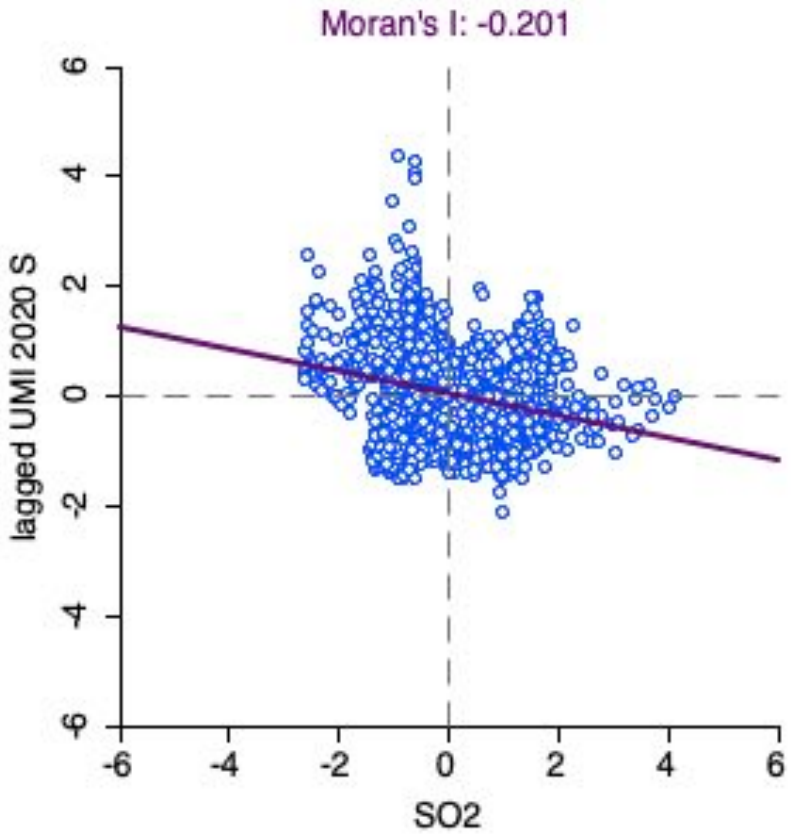

Figure 9.67 Bivariate Moran's I Scatter Plot for SO_2 and Urban Marginalisation Index in 2020

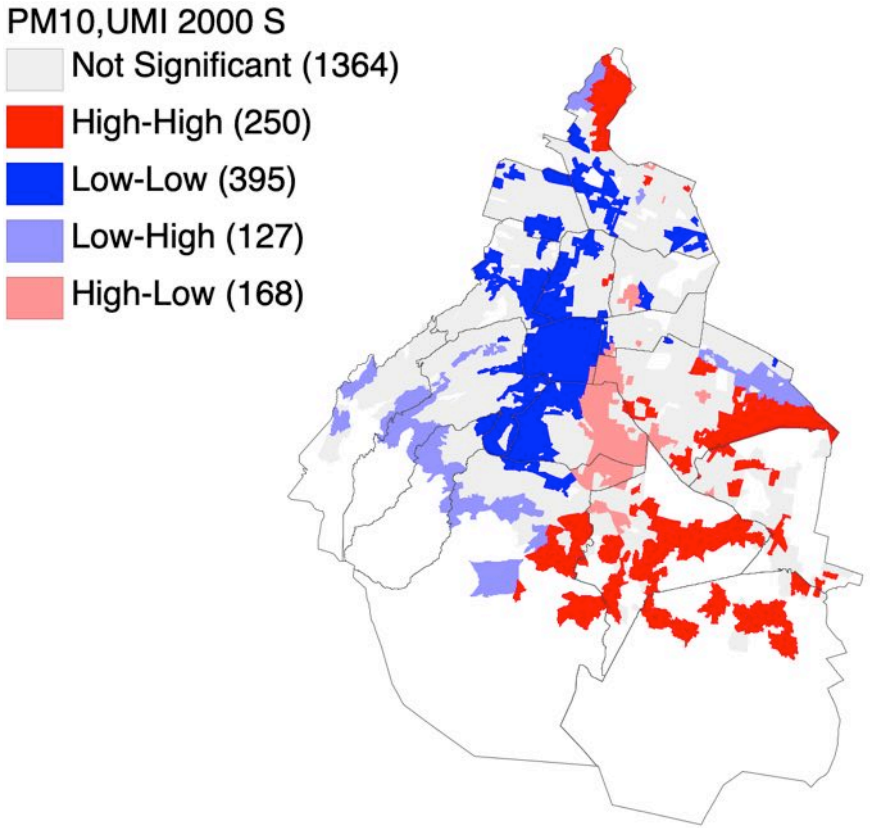

Figure 9.68 LISA Cluster Map for PM_{10} and Urban Marginalisation Index in 2000

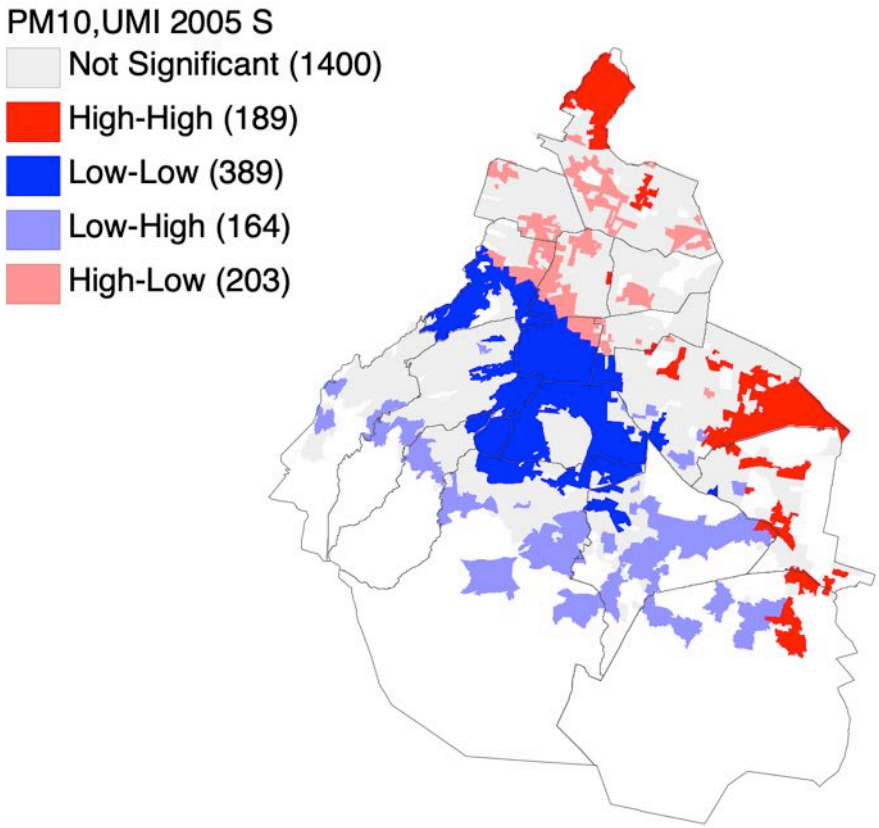

Figure 9.69 LISA Cluster Map for PM_{10} and Urban Marginalisation Index in 2005

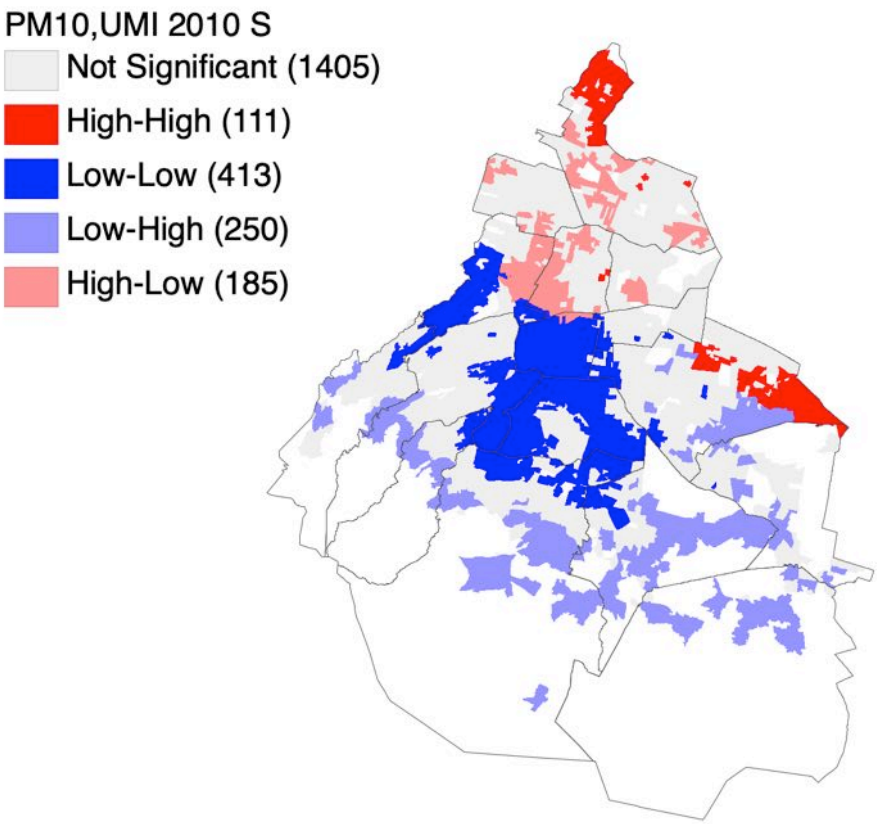

Figure 9.70 LISA Cluster Map for PM_{10} and Urban Marginalisation Index in 2010

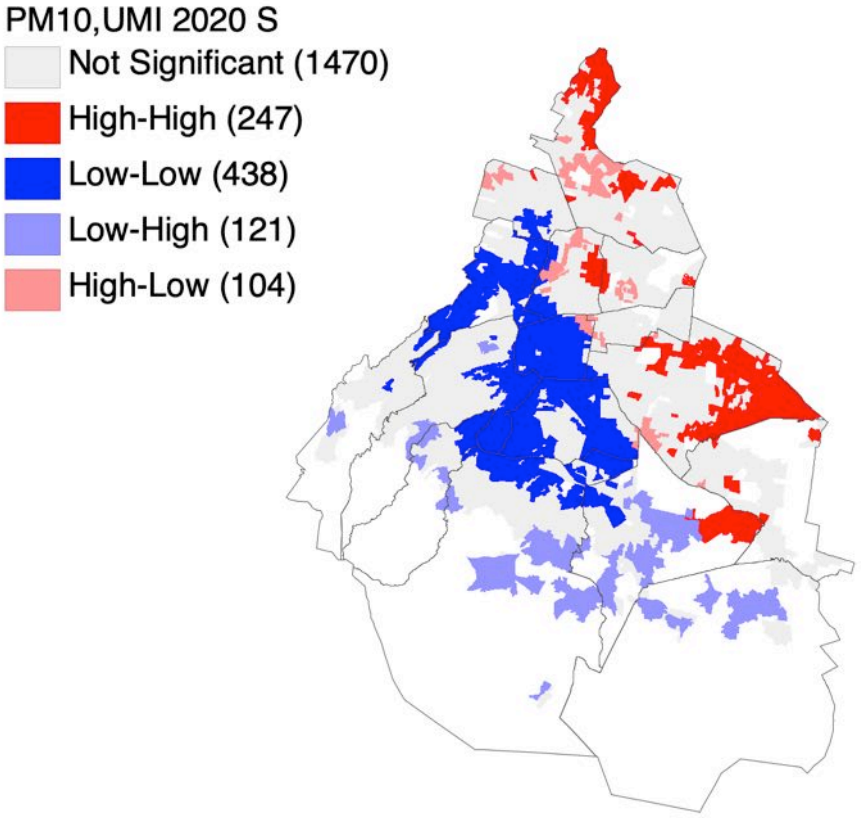

Figure 9.71 LISA Cluster Map for PM_{10} and Urban Marginalisation Index in 2020

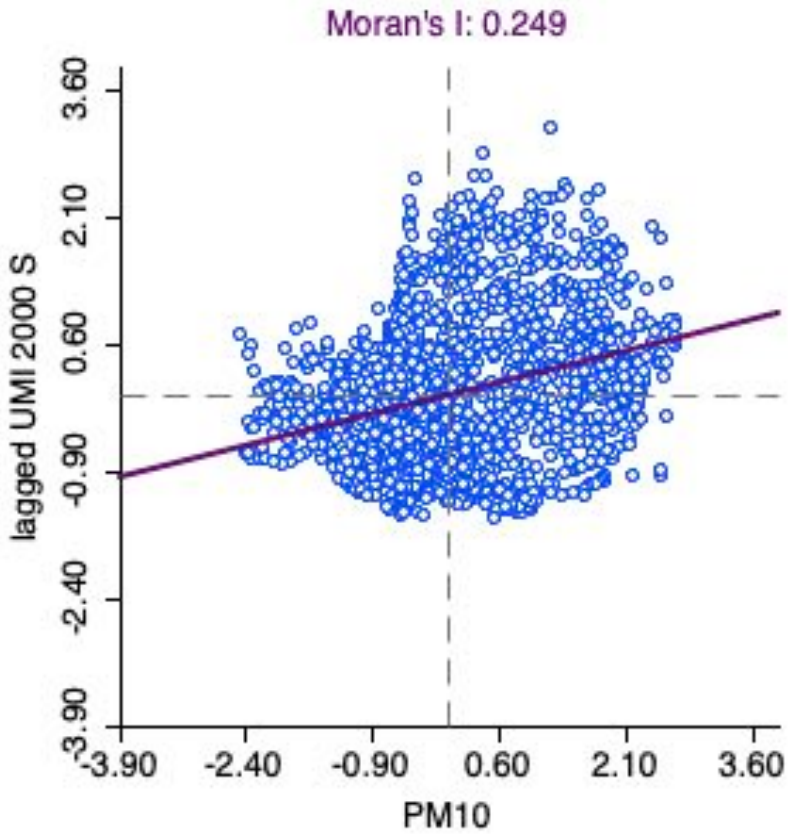

Figure 9.72 Bivariate Moran's I Scatter Plot for PM_{10} and Urban Marginalisation Index in 2000

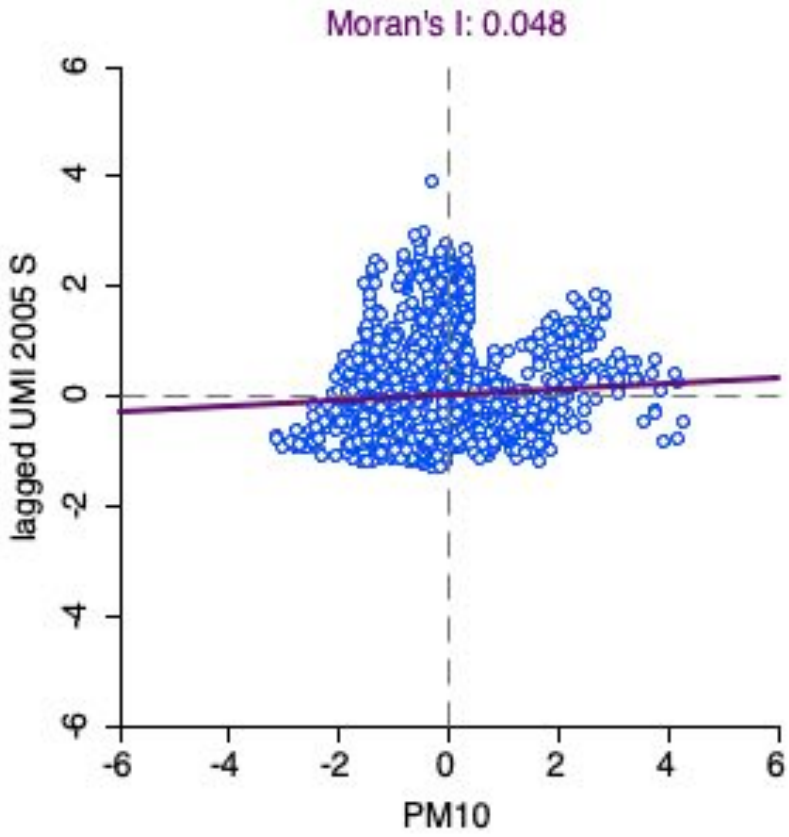

Figure 9.73 Bivariate Moran's I Scatter Plot for PM_{10} and Urban Marginalisation Index in 2005

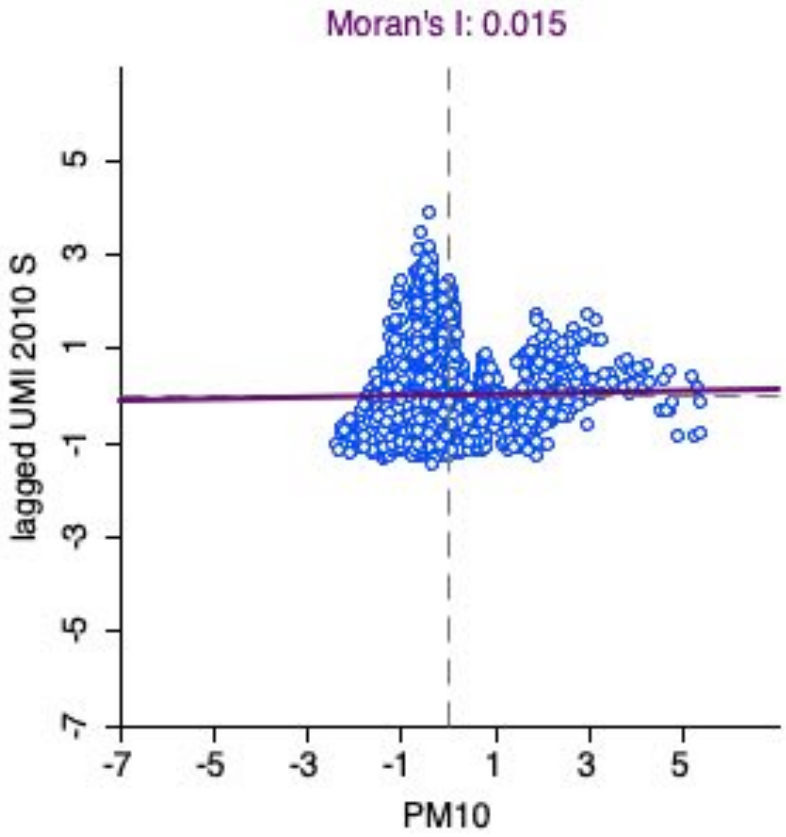

Figure 9.74 Bivariate Moran's I Scatter Plot for PM_{10} and Urban Marginalisation Index in 2010

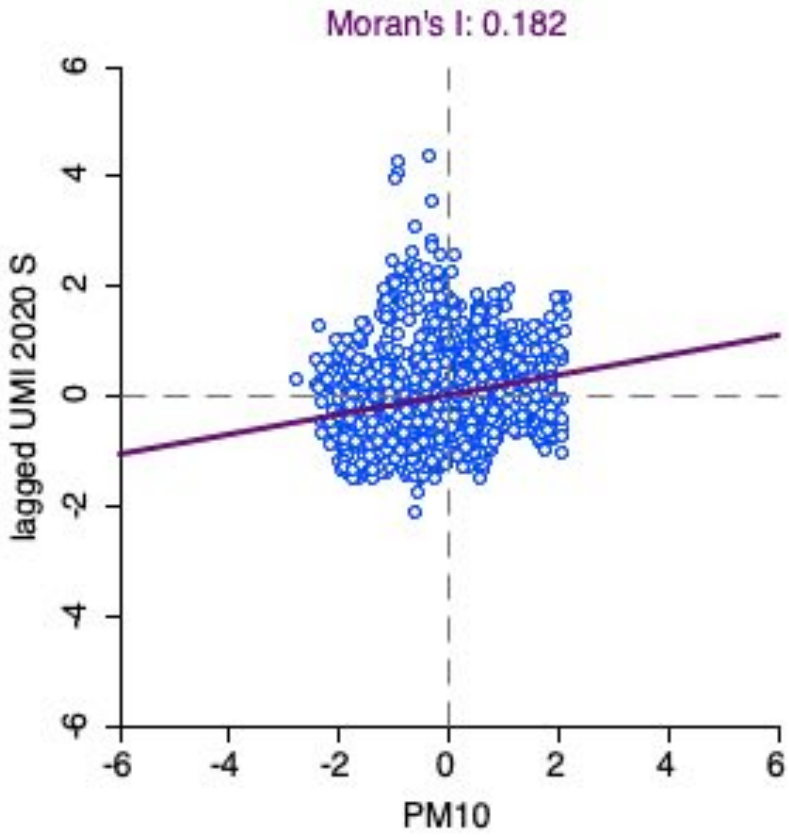

Figure 9.75 Bivariate Moran's I Scatter Plot for PM_{10} and Urban Marginalisation Index in 2020

Particulate Matter ($PM_{2.5}$)

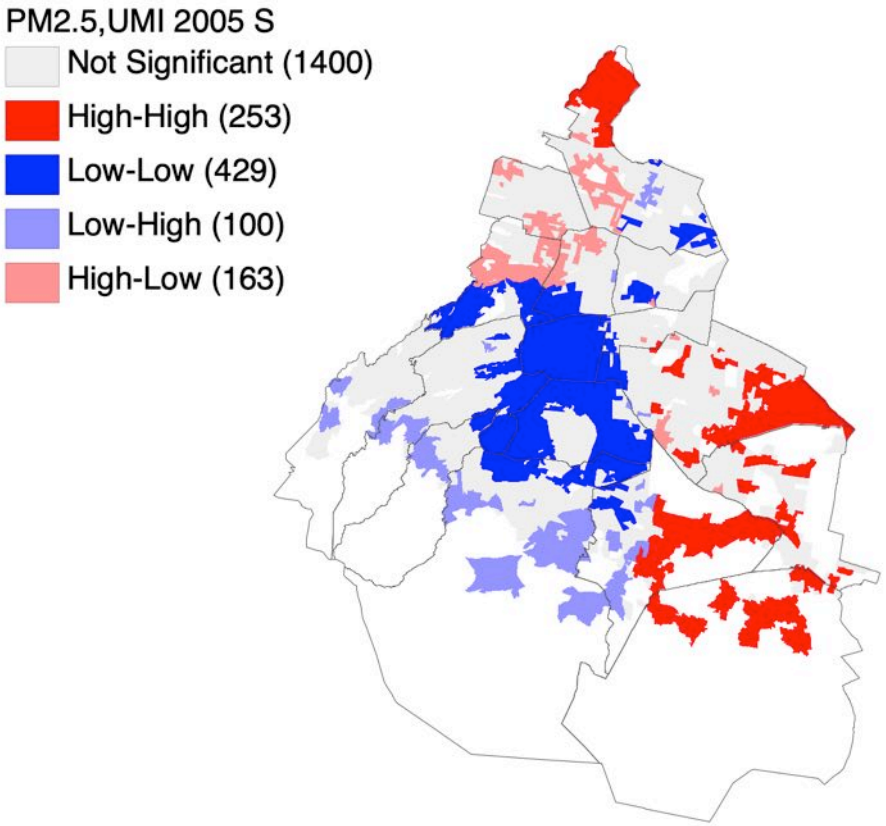

Figure 9.76 LISA Cluster Map for $PM_{2.5}$ and Urban Marginalisation Index in 2005

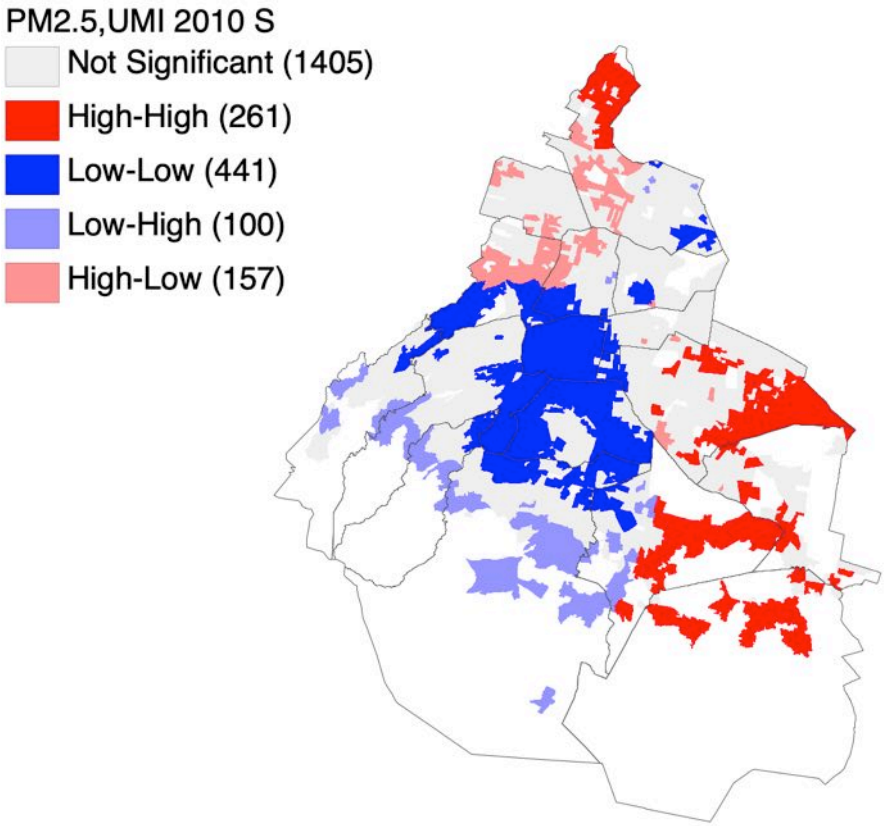

Figure 9.77 LISA Cluster Map for $PM_{2.5}$ and Urban Marginalisation Index in 2010

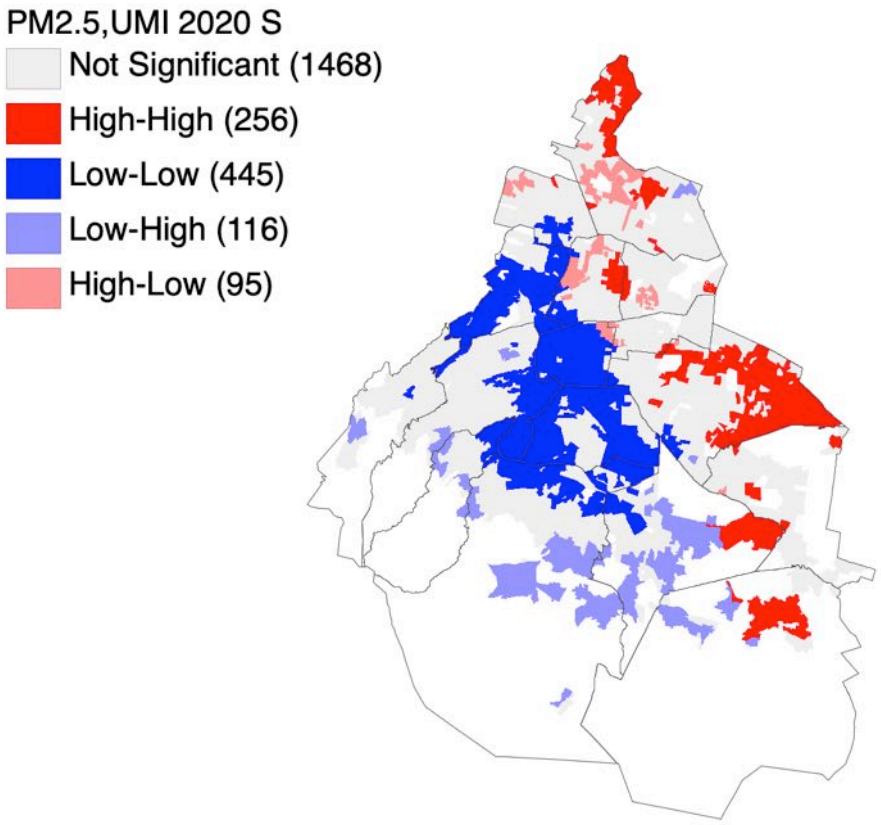

Figure 9.78 LISA Cluster Map for $PM_{2.5}$ and Urban Marginalisation Index in 2020

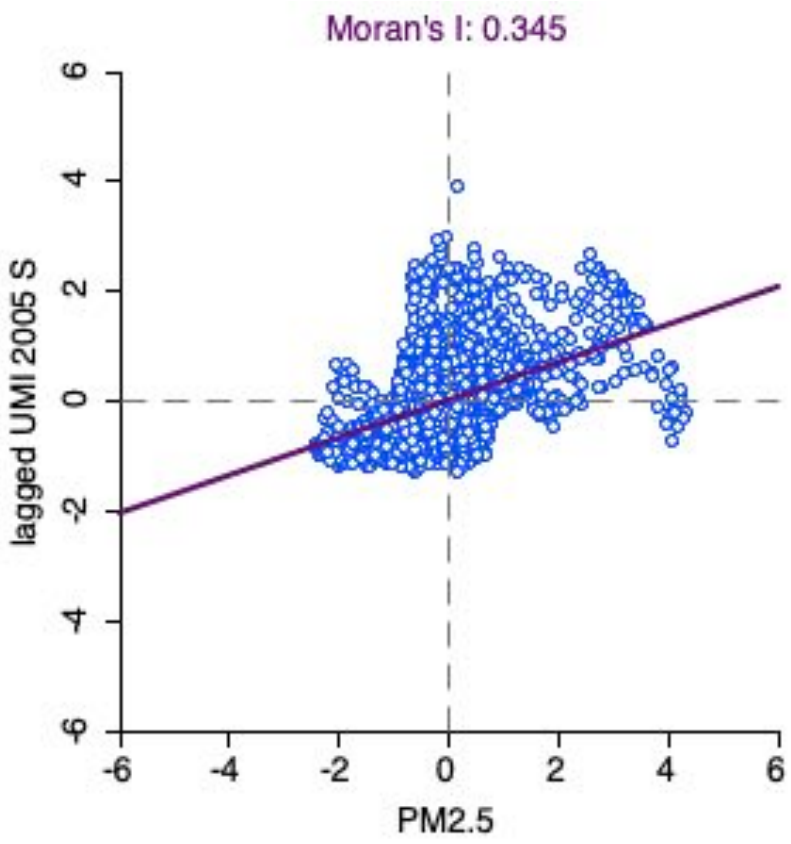

Figure 9.79 Bivariate Moran's I Scatter Plot for $PM_{2.5}$ and Urban Marginalisation Index in 2005

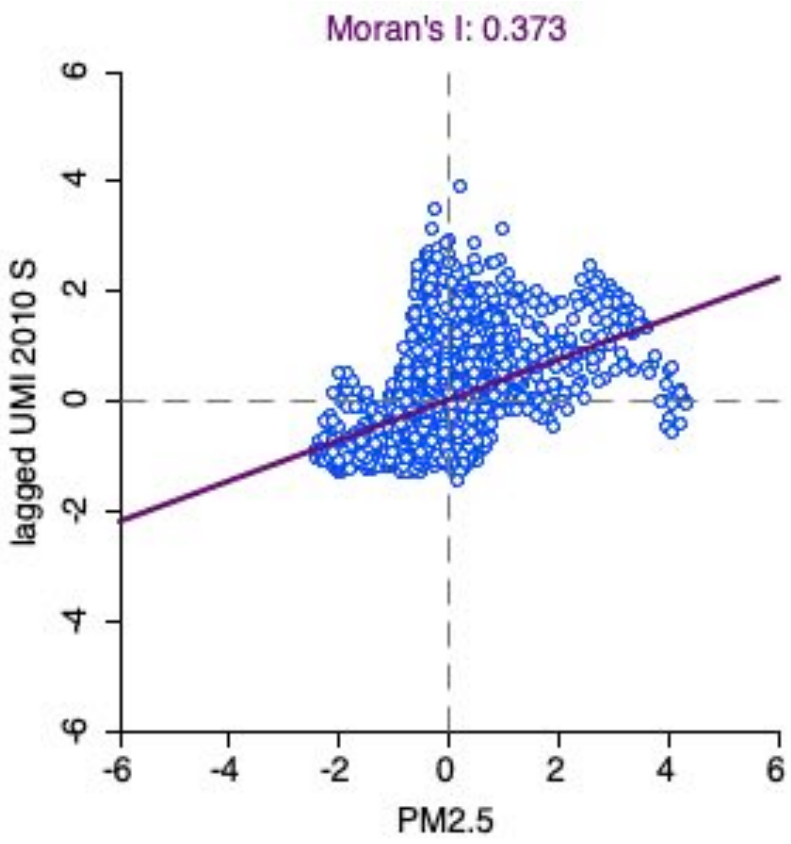

Figure 9.80 Figure 9.81 Bivariate Moran's I Scatter Plot for $PM_{2.5}$ and Urban Marginalisation Index in 2010

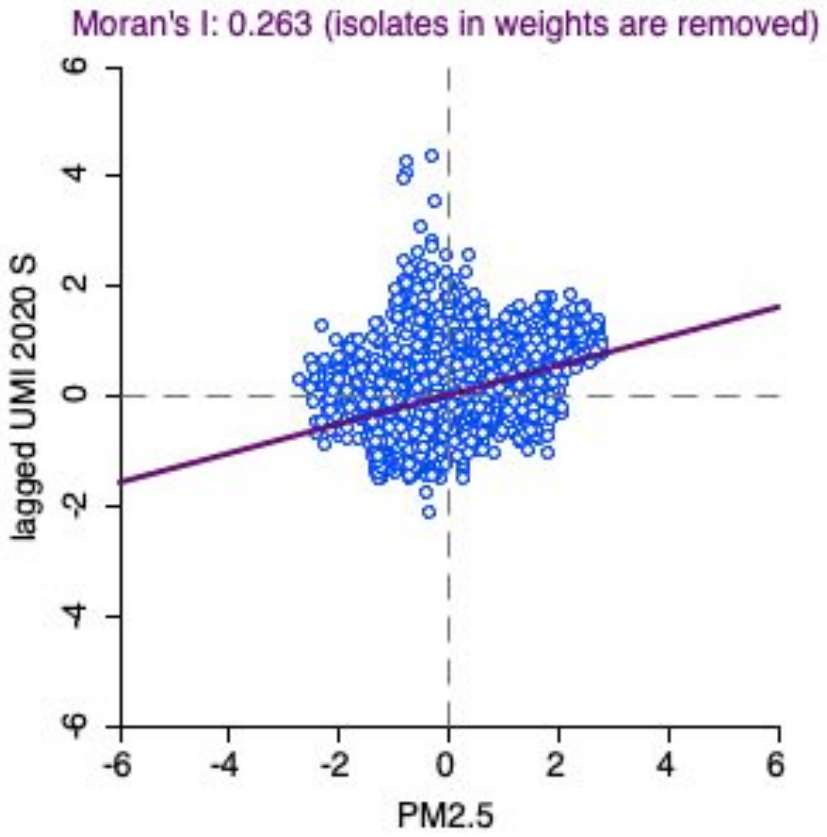

Figure 9.82 Bivariate Moran's I Scatter Plot for PM2.5 and Urban Marginalisation Index in 2020

Poverty Percentages

Ozone (O_3)

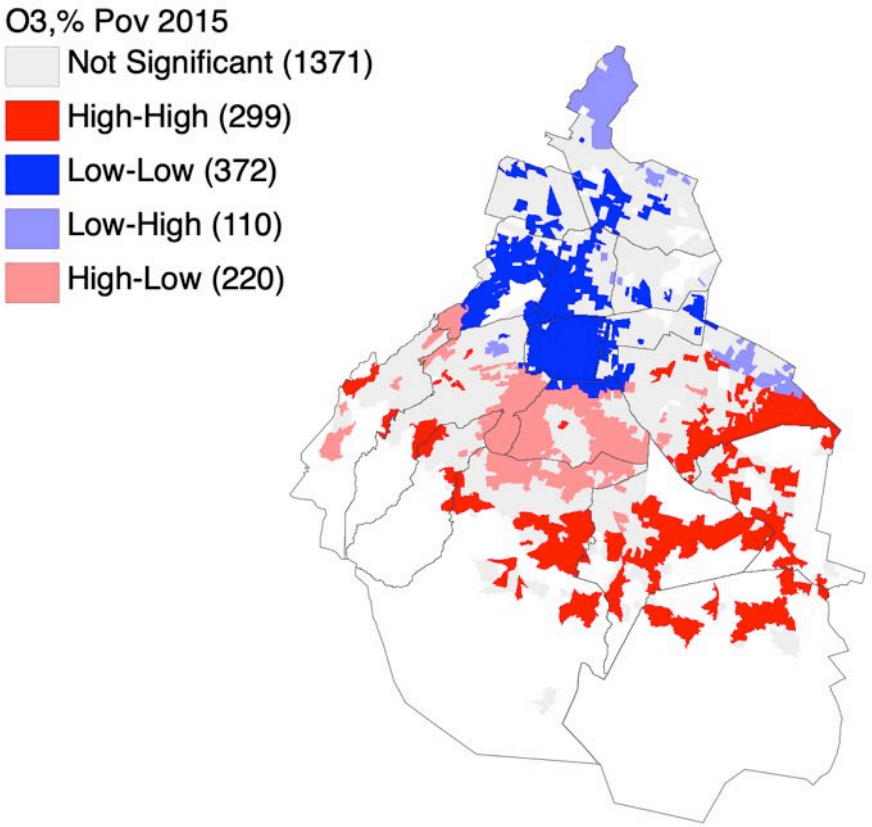

Figure 9.83 LISA Cluster Map for O_3 and Poverty Percentages in 2015

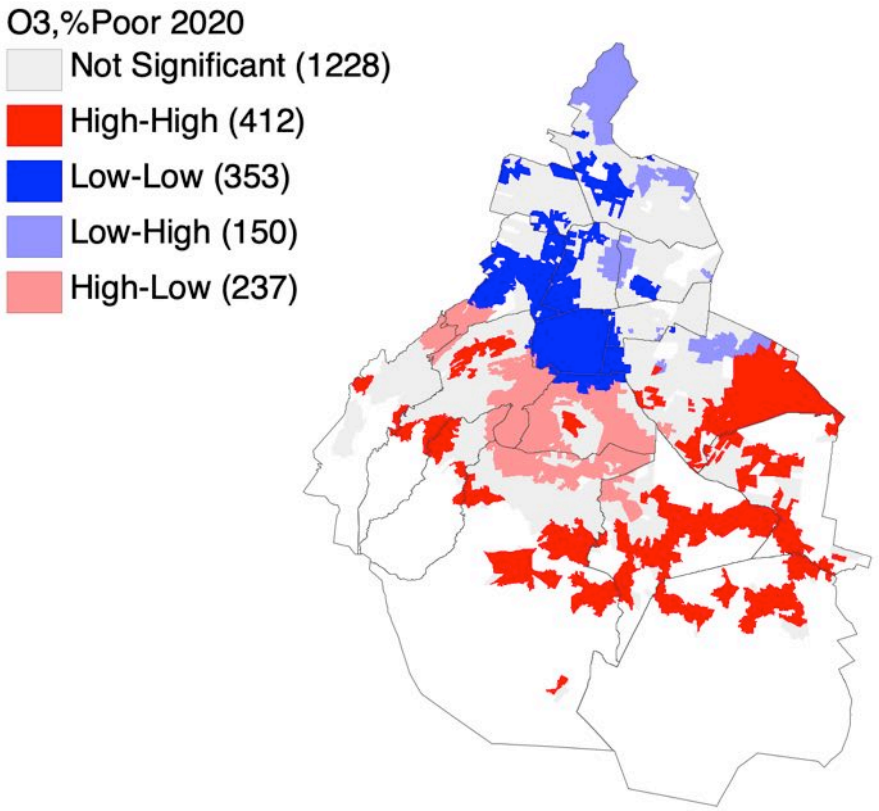

Figure 9.84 LISA Cluster Map for O3 and Poverty Percentages in 2020

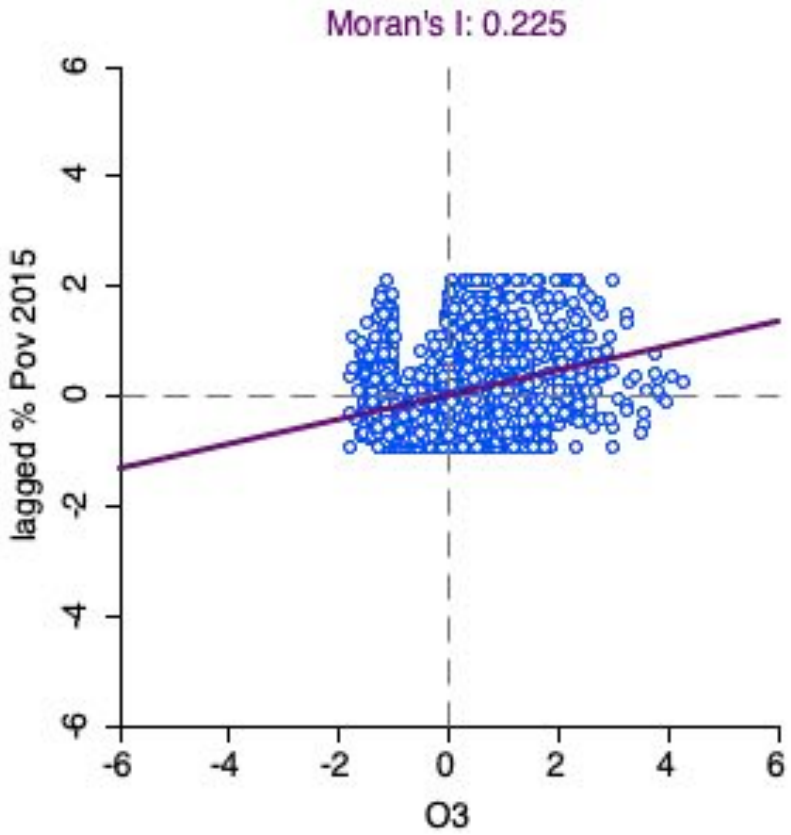

Figure 9.85 Bivariate Moran's I Scatter Plot for O_3 and Poverty Percentages in 2015

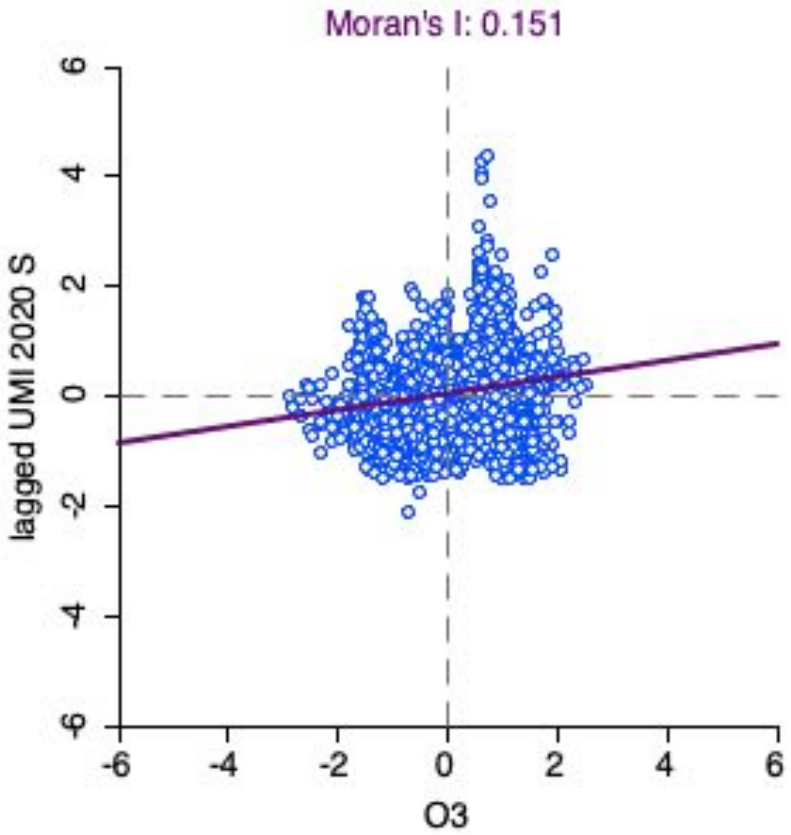

Figure 9.86 Bivariate Moran's I Scatter Plot for O3 and Poverty Percentages in 2020

Carbon Monoxide (CO)

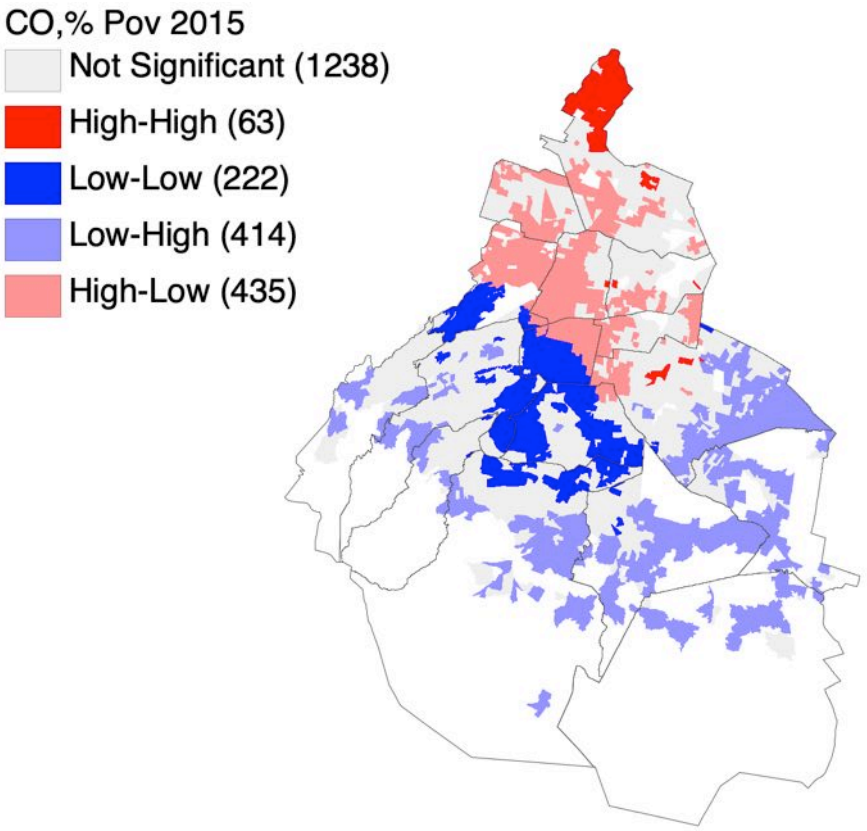

Figure 9.87 LISA Cluster Map for CO and Poverty Percentages in 2015

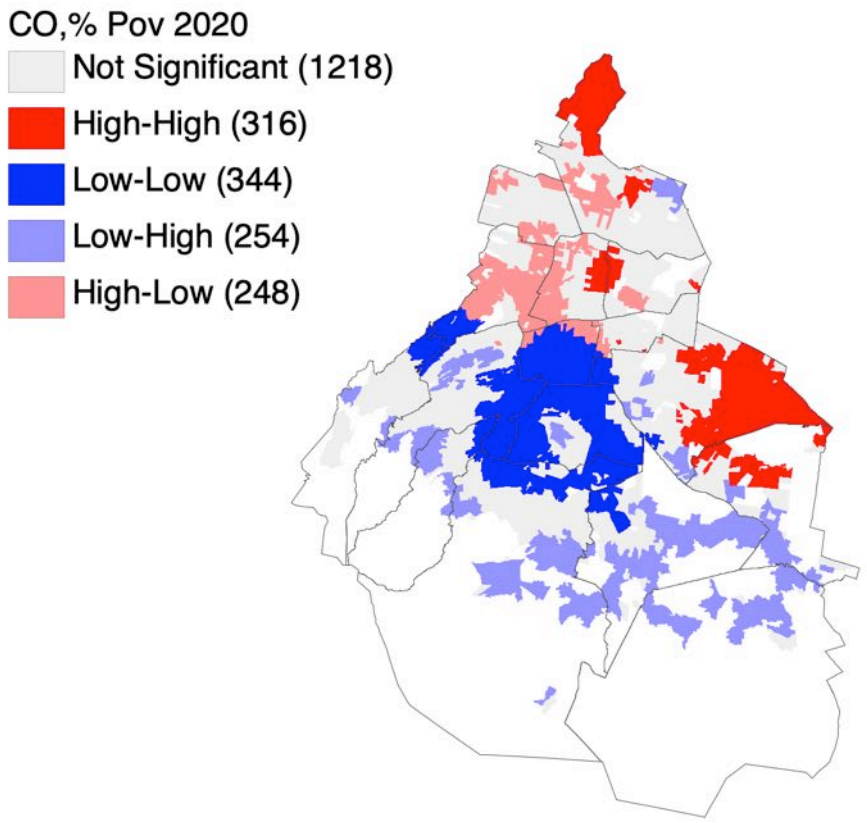

Figure 9.88 LISA Cluster Map for CO and Poverty Percentages in 2020

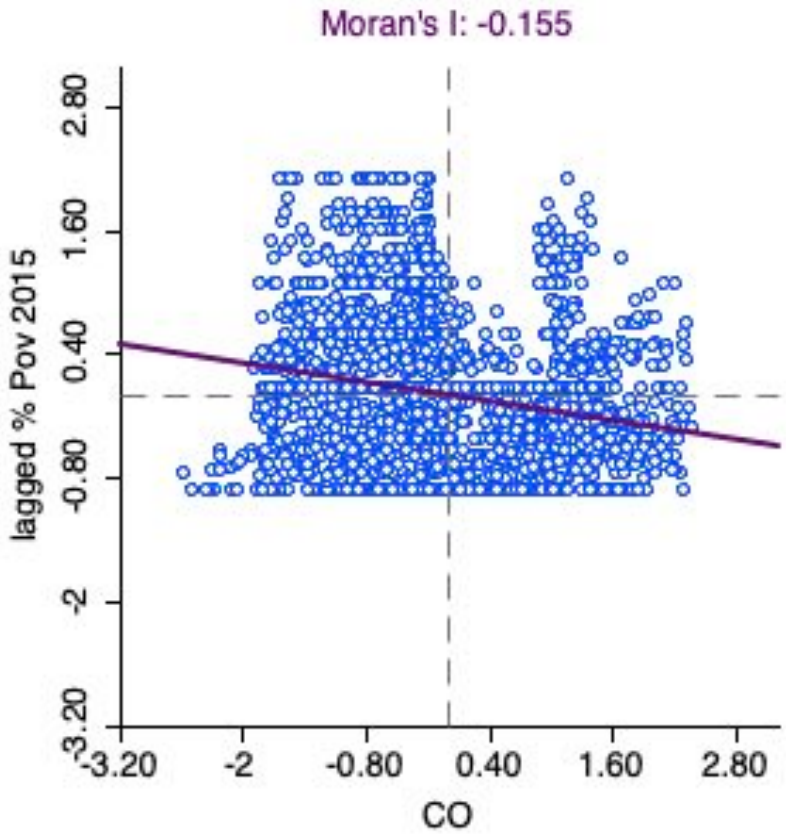

Figure 9.89 Bivariate Moran's I Scatter Plot for CO and Poverty Percentages in 2015

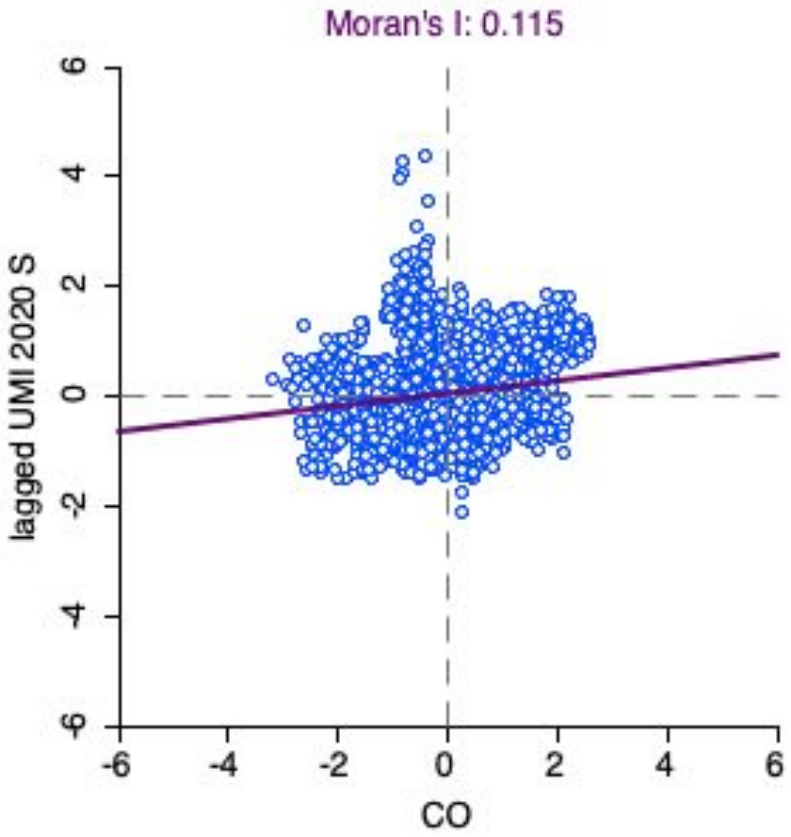

Figure 9.90 Bivariate Moran's I Scatter Plot for CO and Poverty Percentages in 2020

Nitrogen Oxides (NOx)

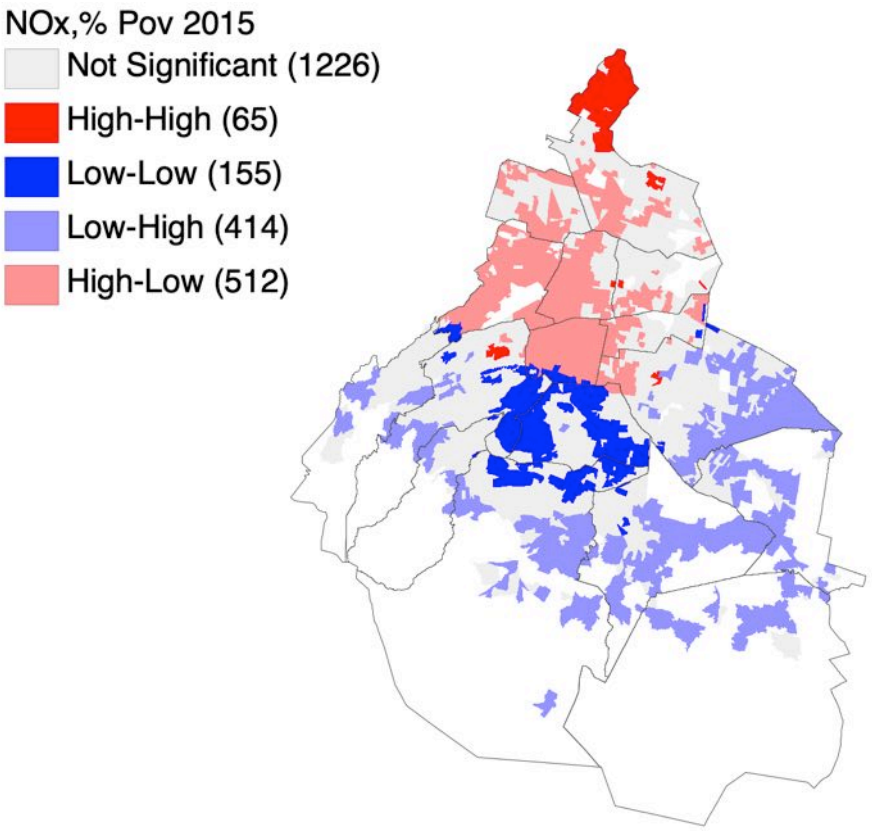

Figure 9.91 LISA Cluster Map for NOx and Poverty Percentages in 2015

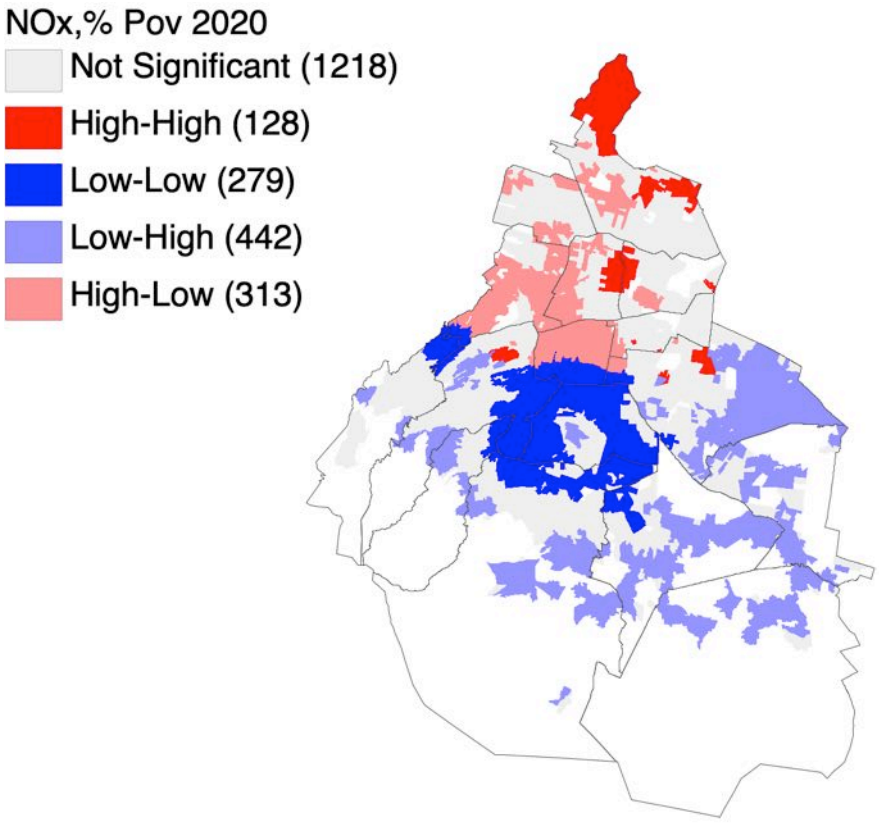

Figure 9.92 LISA Cluster Map for NOx and Poverty Percentages in 2020

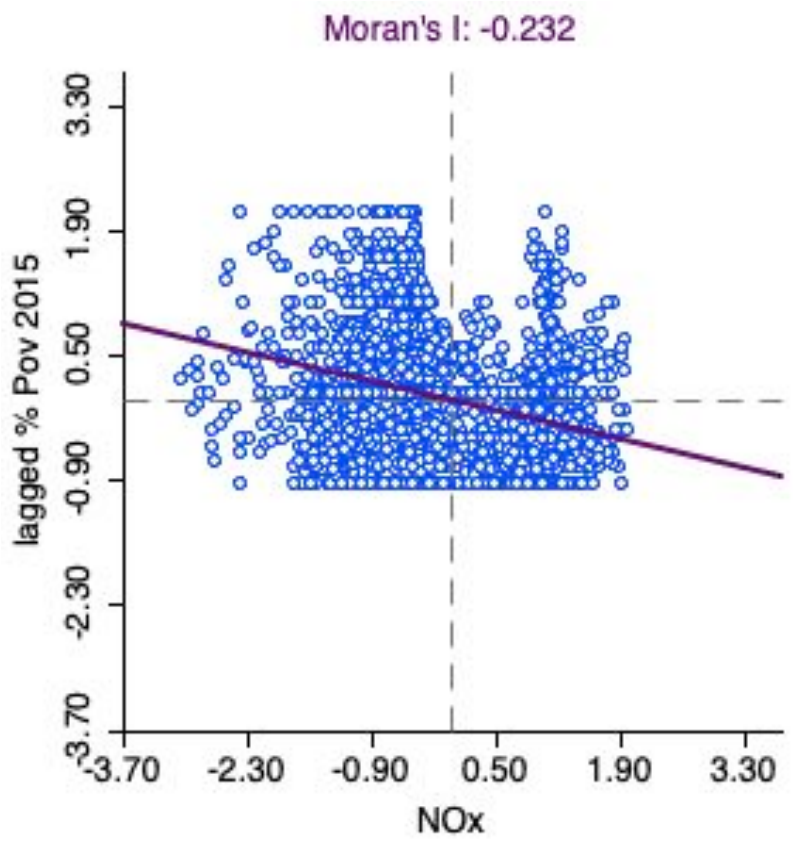

Figure 9.93 Bivariate Moran's I Scatter Plot for NOx and Poverty Percentages in 2015

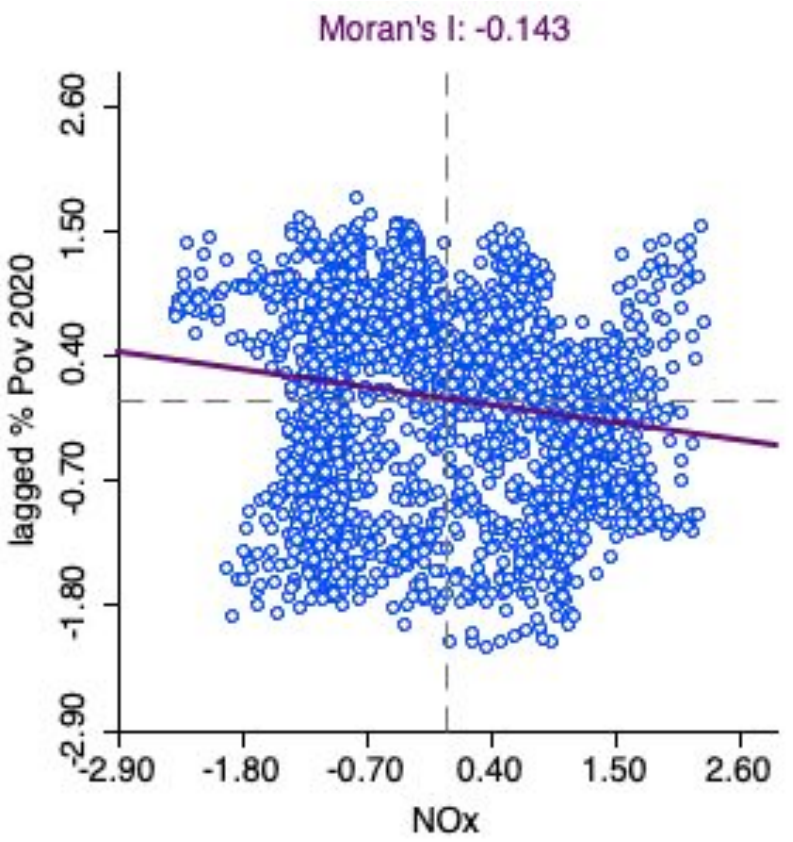

Figure 9.94 Bivariate Moran's I Scatter Plot for NOx and Poverty Percentages in 2020

Sulphur Dioxide (SO_2)

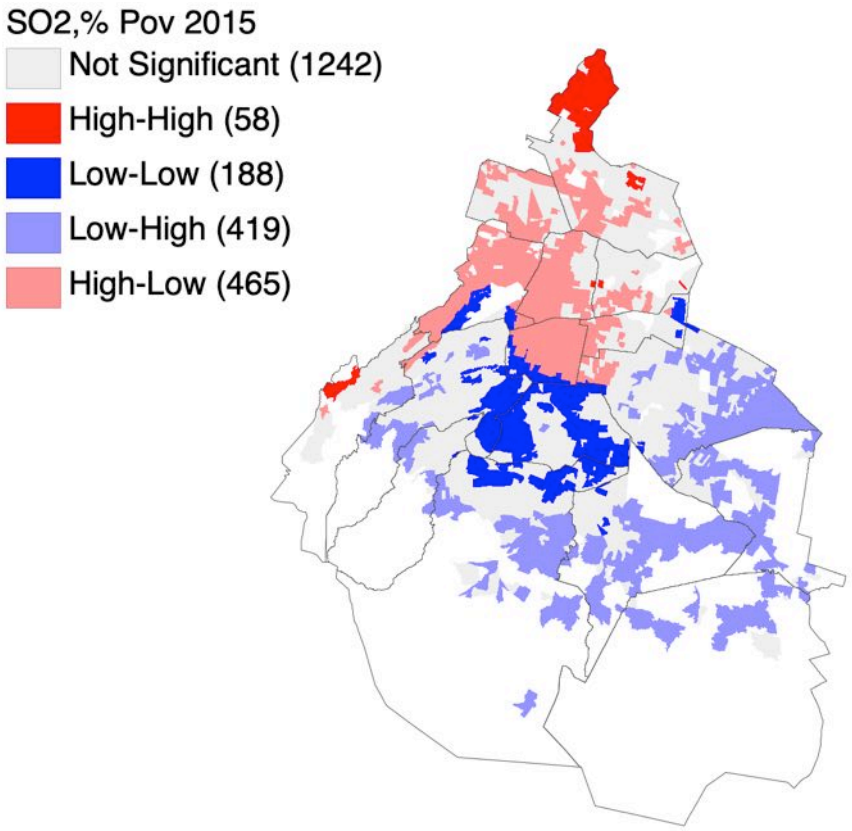

Figure 9.95 LISA Cluster Map for SO_2 and Poverty Percentages in 2015

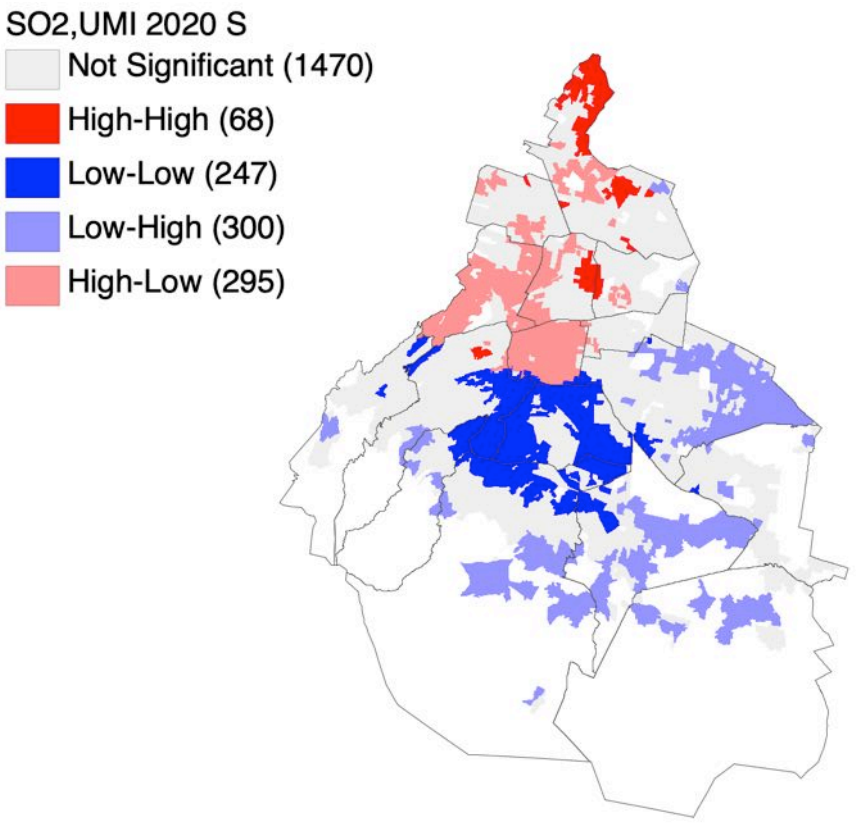

Figure 9.96 LISA Cluster Map for SO_2 and Poverty Percentages in 2020

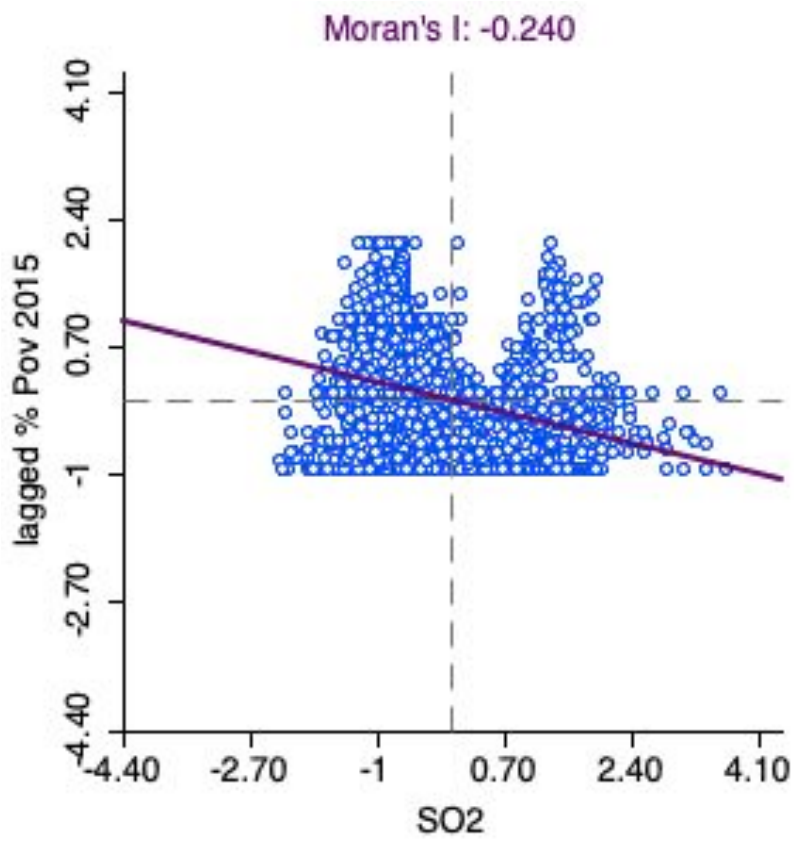

Figure 9.97 Bivariate Moran's I Scatter Plot for SO_2 and Poverty Percentages in 2015

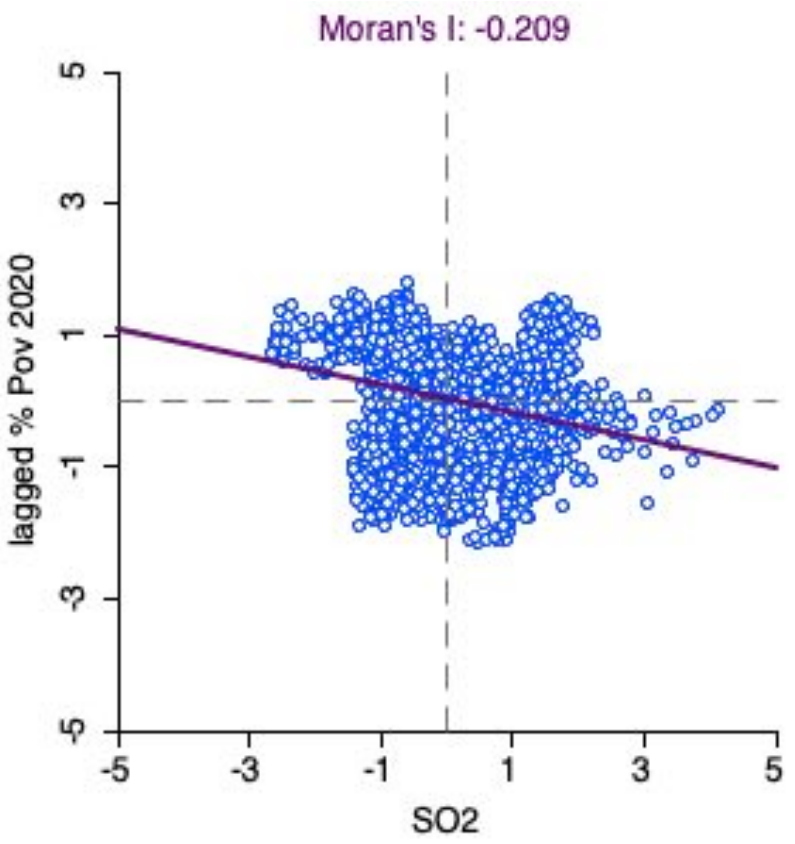

Figure 9.98 Bivariate Moran's I Scatter Plot for SO_2 and Poverty Percentages in 2020

Particulate Matter (PM_{10})

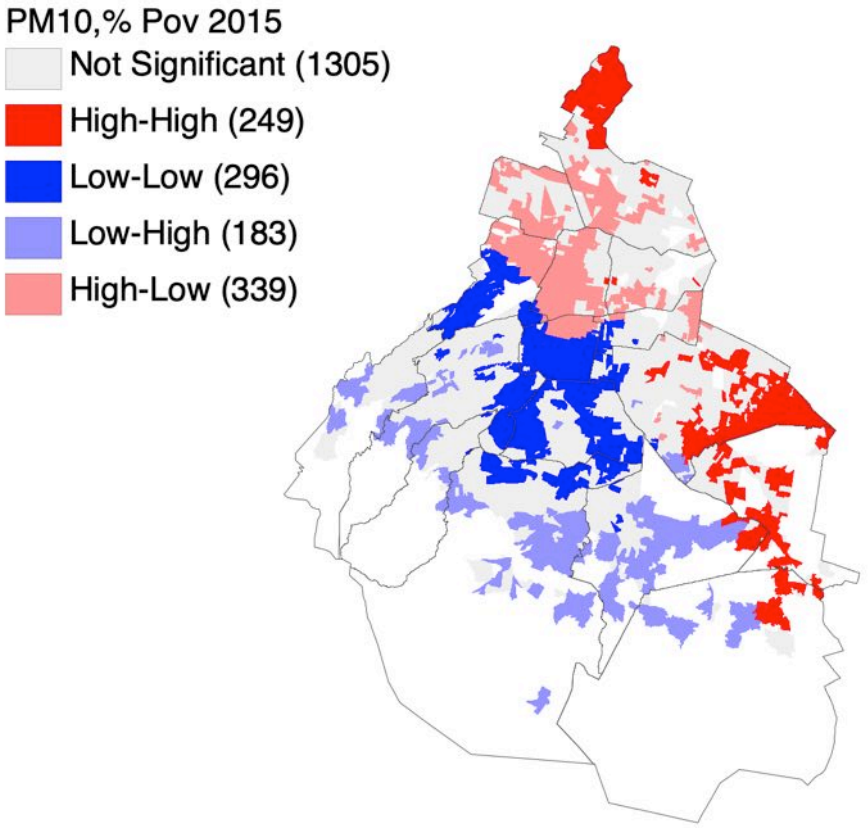

Figure 9.99 LISA Cluster Map for PM_{10} and Poverty Percentages in 2015

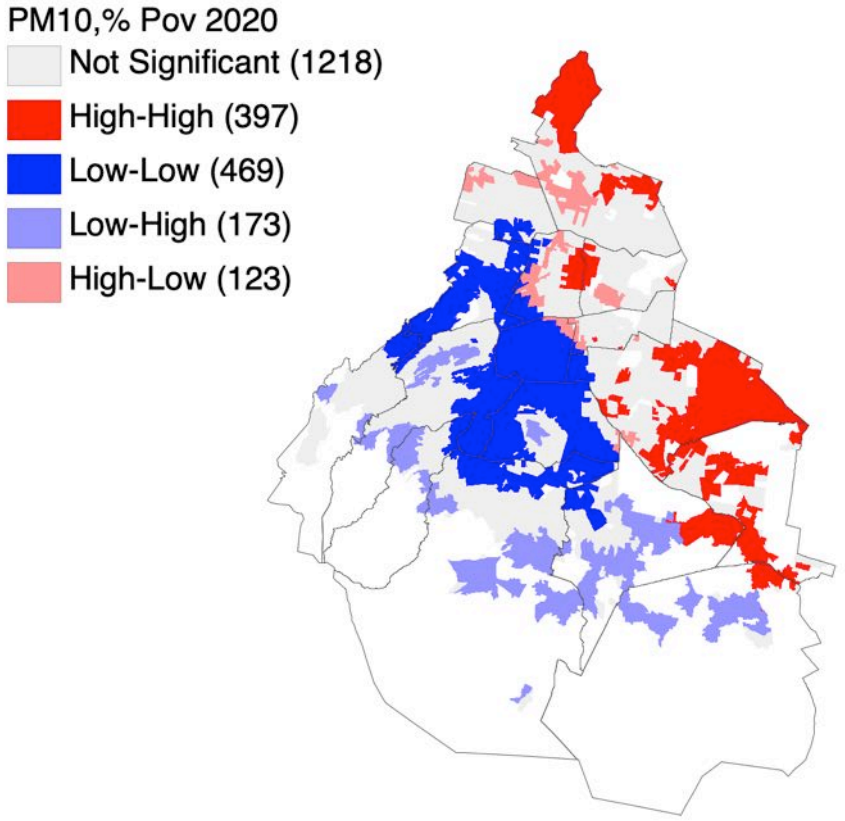

Figure 9.100 LISA Cluster Map for PM_{10} and Poverty Percentages in 2020

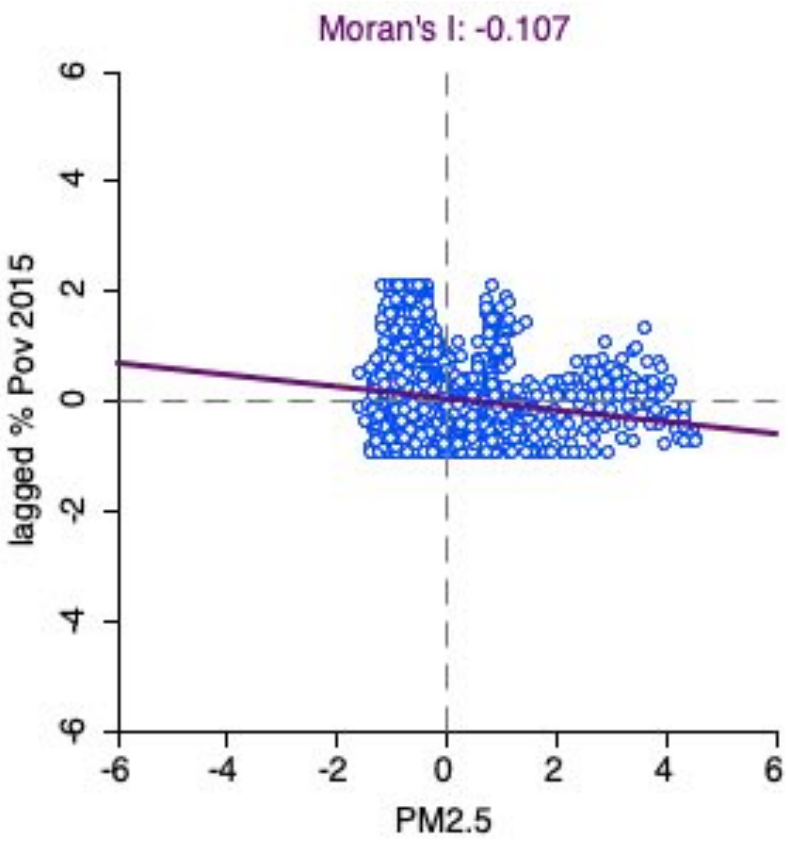

Figure 9.101 Bivariate Moran's I Scatter Plot for PM_{10} and Poverty Percentages in 2015

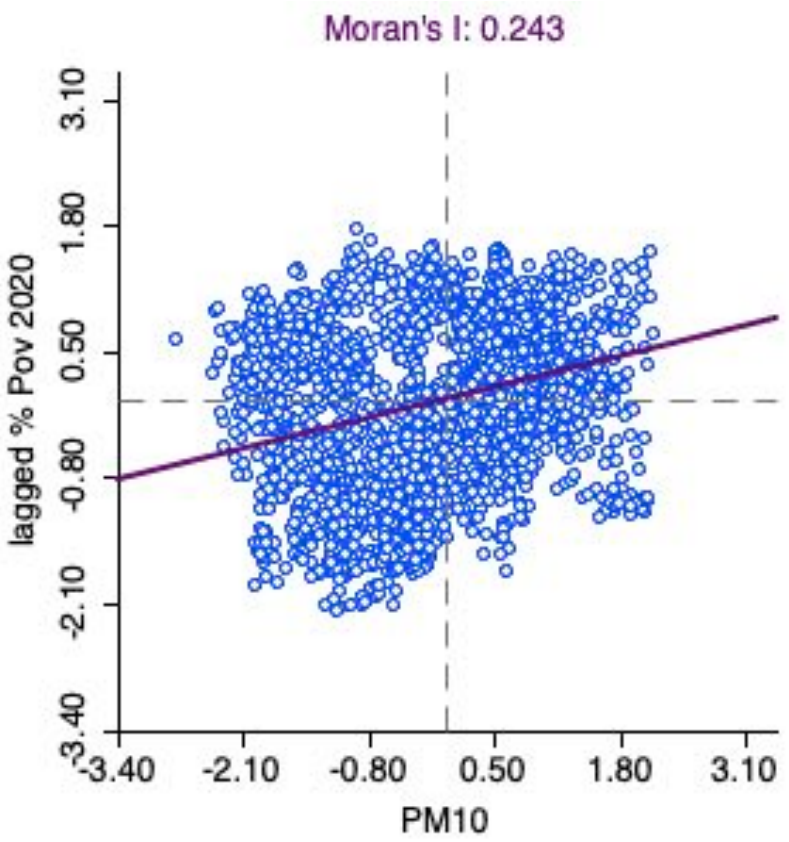

Figure 9.102 Bivariate Moran's I Scatter Plot for PM_{10} and Poverty Percentages in 2020

Particulate Matter ($PM_{2.5}$)

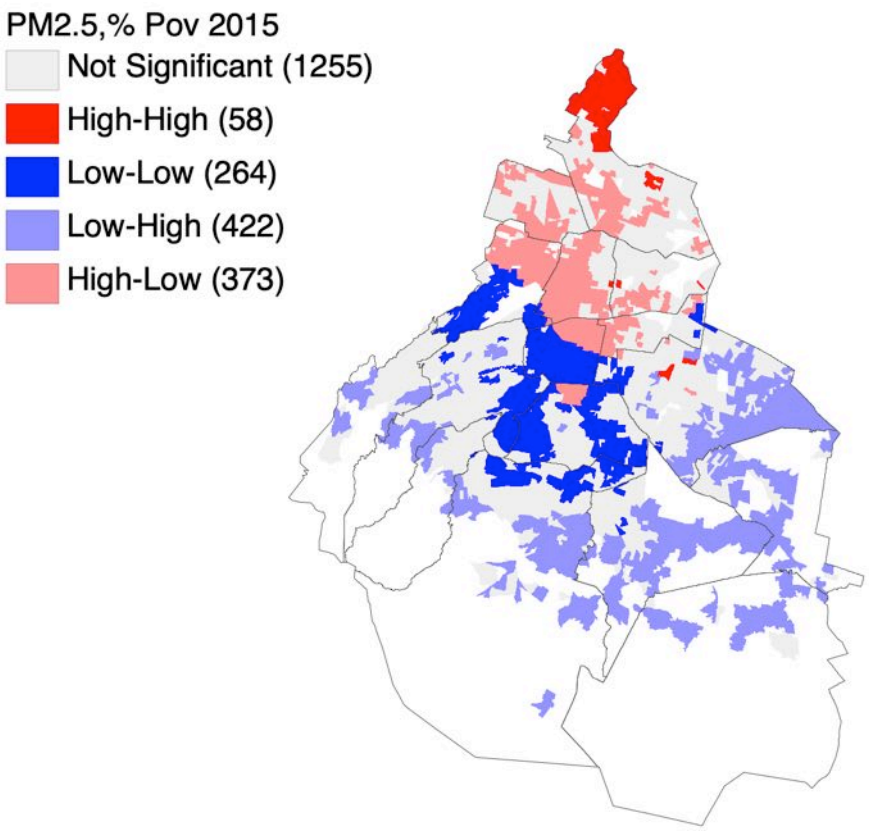

Figure 9.103 LISA Cluster Map for $PM_{2.5}$ and Poverty Percentages in 2015

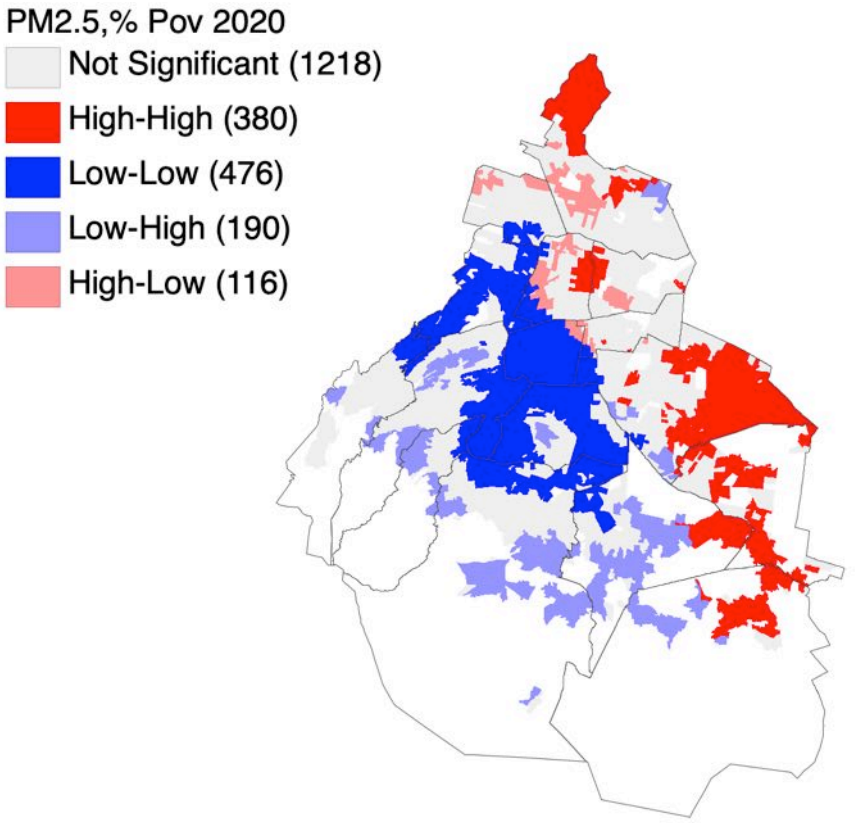

Figure 9.104 LISA Cluster Map for $PM_{2.5}$ and Poverty Percentages in 2020

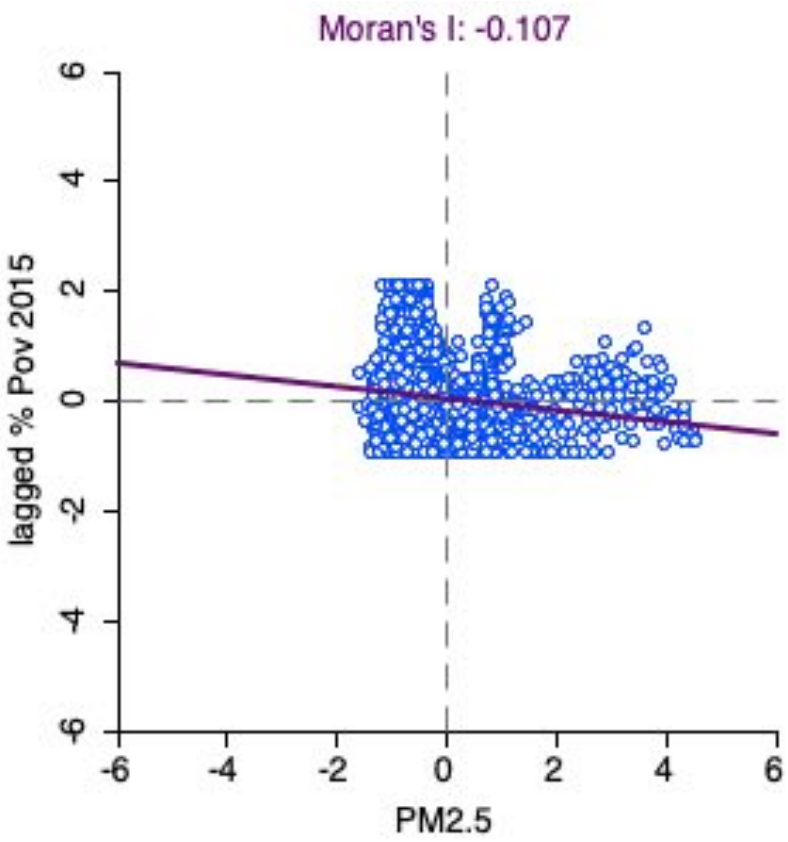

Figure 9.105 Bivariate Moran's I Scatter Plot for $PM_{2.5}$ and Poverty Percentages in 2015

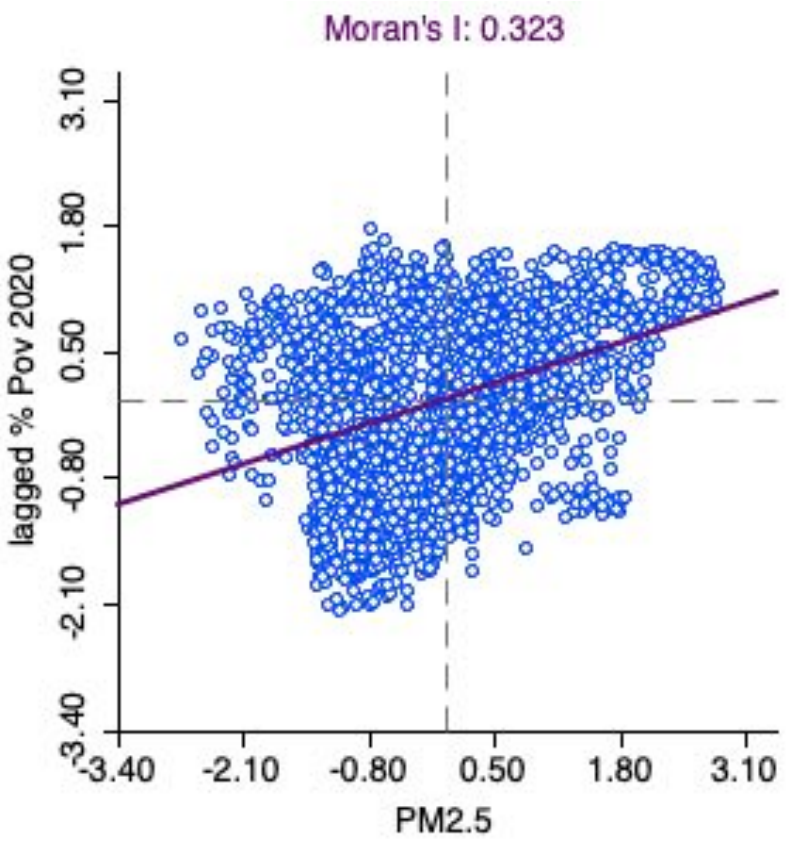

Figure 9.106 Bivariate Moran's I Scatter Plot for $PM_{2.5}$ and Poverty Percentages in 2020